Economic Geology, v. 103, pp. 1097–1134

Depositional Gaps in Abitibi Greenstone Belt Stratigraphy: A Key to Exploration for Syngenetic Mineralization

P. C. Thurston,†

Mineral Exploration Research Centre, Laurentian University, Sudbury, Ontario, Canada P3E 2C6

J. A. Ayer,

Ontario Geological Survey, Sudbury, Ontario, Canada P3E 6B5

J. Goutier,

Géologie Québec, Ministère des Ressources naturelles et de la Faune, Rouyn-Noranda, Quebec, Canada J9X 6R1

and M. A. Hamilton

Jack Satterly Geochronology Laboratory, Department of Geology, University of Toronto, Earth Sciences Centre, 22 Russell Street Toronto, Ontario, Canada M5S 3B1

Abstract

Models of greenstone belt development are crucial for exploration. Allochthonous models predict belts to be a collage of unrelated fragments, whereas autochthonous models allow for prediction of syngenetic mineral deposits within specific stratigraphic intervals. Superior province greenstone belts consist of mainly volcanic units unconformably overlain by largely sedimentary "Timiskaming-style" assemblages, and field and geochronological data indicate that the Abitibi greenstone belt developed autochthonously. We describe major revisions to stratigraphy of the Abitibi greenstone belt and the implications of an autochthonous development of the volcanic stratigraphy for exploration for syngenetic mineralization. The Abitibi greenstone belt is subdivided into seven discrete volcanic stratigraphic episodes on the basis of groupings of numerous U-Pb zircon ages of pre-2750, 2750 to 2735, 2734 to 2724, 2723 to 2720, 2719 to 2711, 2710 to 2704, and 2704 to 2695 Ma. We present revised lithotectonic and/or stratigraphic nomenclature using these time intervals, including (1) isotopic inheritance in younger episodes which indicates that the older episodes (2750–2735 and 2734–2724 Ma) had greater extent than is presently seen, (2) dikes feeding younger volcanic episodes (2706 Ma) cutting older volcanic units (2734–2724 Ma), and (3) 2710 to 2704 Ma mafic to ultramafic sills intruding the 2719 to 2711 Ma episode. Changes to the nomenclature include the identification of pre-2750 Ma volcanic episode (supracrustal fragments) in the northern and southern Abitibi greenstone belt and subdivision of the 2719 to 2711 Ma, 2710 to 2704 Ma, and 2704 to 2695 Ma episodes into lower and upper parts. We present the results of this lithostratigraphic subdivision as the first geochronologically constrained stratigraphic and/or lithotectonic map of the Abitibi greenstone belt.

Many of the volcanic episodes are intercalated with and capped by a relatively thin "sedimentary interface zone" dominated by chemical sedimentary rocks. Stratigraphic and geochronological analysis of these zones indicates discontinuous deposition with localized gaps of 2 to 27 m.y. between volcanic episodes. The zones consist of up to 200 m of iron formation, chert breccia, heterolithic debris flows of volcanic provenance, sandstone and/or argillite and conglomerate. Modeling of the time required for deposition of the volcanic units based on rates of magma production in modern arc and plume environments is on the order of 10^3 to 10^4 years, whereas the time interval between basalt-rhyolite cycles is 10^6 years. The sedimentary interface zones are therefore interpreted as condensed sections, zones with very low rates of sedimentation in a basinal setting, or zones with negligible rates of sedimentation marked by silicification of existing rock types. The sedimentary interface zones are therefore considered submarine correlative conformities, disconformities, or unconformities separating the equivalent of group level stratigraphic and lithotectonic units. The unconformity-bounded stratigraphic model provides a new regional to deposit-scale interpretive model for use in exploration for syngenetic mineralization.

Introduction

The Abitibi greenstone belt lies in the eastern part of the Wawa-Abitibi subprovince of the southern Superior province (Fig. 1). The belt has long been central to understanding greenstone belt mineral deposits (e.g., Goodwin, 1965). The Abitibi greenstone belt had had a total mineral production valued at ~$120 billion as of 2005, derived from world-class volcanogenic massive sulfide (VMS) deposits, such as in Rouyn-Noranda (Gibson and Watkinson, 1990) and at Kidd Creek (Bleeker et al., 1999), gold-rich VMS deposits, such as Laronde Penna (Dubé et al., 2007; Mercier-Langevin et al., 2007a, b), and epigenetic gold deposits, such as the Hollinger-McIntyre and Dome mines (Bateman et al., 2008), the Kirkland Lake "main break" deposits (Ispolatov et al., 2008), and the Sigma-Lamaque complex (Robert, 2003). The presence of this mineral wealth led to considerable amounts

† Corresponding author: e-mail, pthurston@laurentian.ca

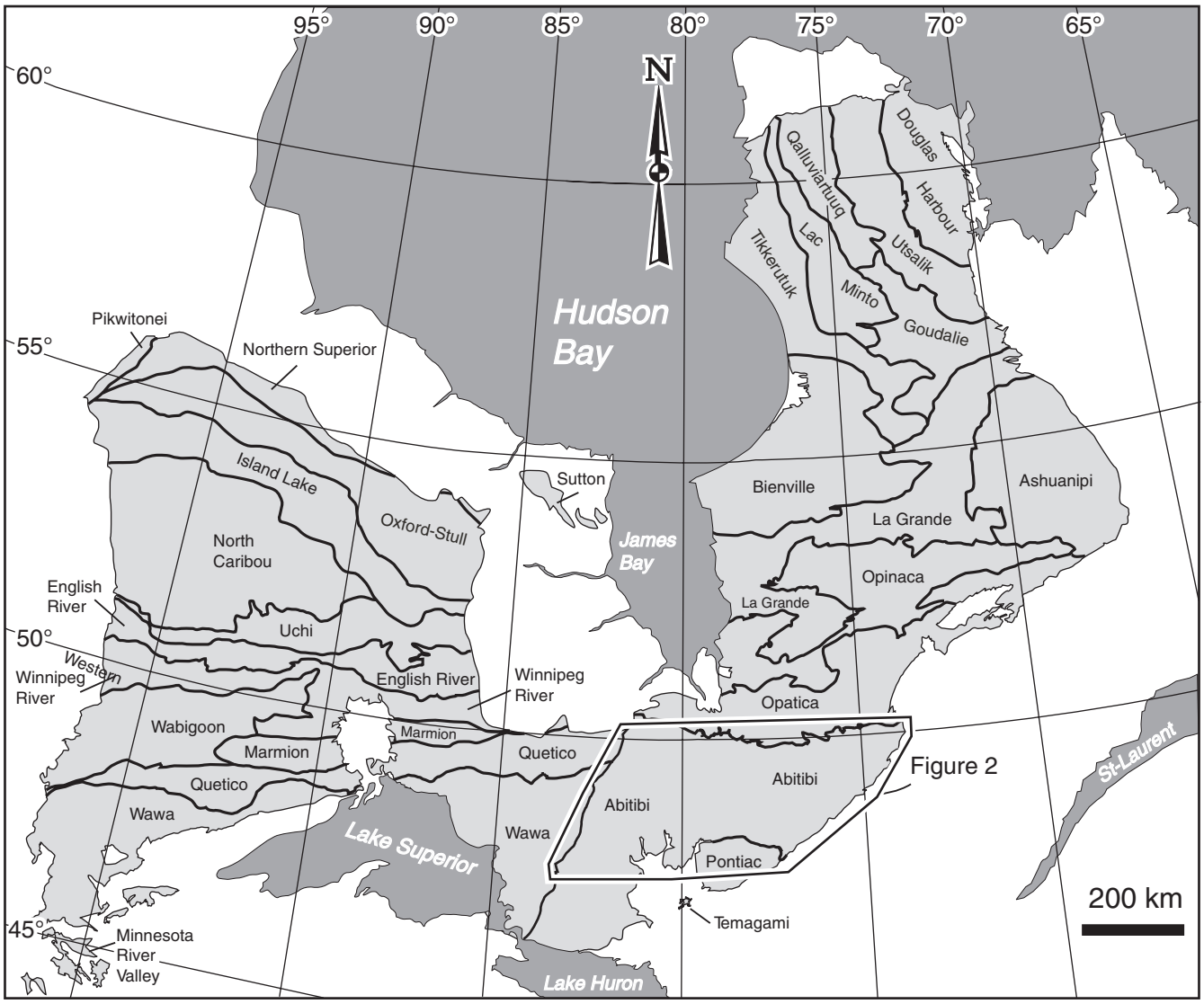

FIG. 1. Location of the Abitibi greenstone belt and Figure 2 within the Superior province. The boundaries and names of major units are from maps of Card (1990), Morey and Meints (2000), Thériault (2002), Ayer et al. (2006), Goutier et Melançon (2007) and Stott et al. (2007).

of mapping and geoscience research resulting in the Abitibi greenstone belt having been an important area for models of development and evolution of greenstone belts (Goodwin, 1979; Dimroth et al., 1982, 1983; Jensen and Langford, 1985; Jackson et al., 1994).

Mapping in the 1930s and 1940s (e.g., Gunning and Ambrose, 1939; Wilson, 1941) established that volcanic-dominated units are unconformably overlain by "Timiskaming"-type successor basins of metasedimentary and metavolcanic rocks (Gunning and Ambrose, 1939). By the 1980s, the Abitibi greenstone belt had been mapped at a large scale (e.g., Goodwin, 1979; MER-OGS, 1984; Jensen and Langford, 1985), but this mapping was complicated by the relatively late understanding of the komatiitic units as volcanic rocks (Pyke et al., 1973). Integration of komatiites into stratigraphic models (e.g., Jensen, 1985; Corfu et al., 1989), along with banded iron formation as major marker units, permitted establishment of belt-wide stratigraphy, based on principles of large-scale cyclical volcanism and a limited geochronological database (Goodwin, 1979; MER-OGS, 1984; Jensen, 1985).

In the late 1980s, increasing evidence for large-scale lateral tectonics throughout the Superior province (Percival and Williams, 1989; Williams et al., 1992) and geochemical evidence for arc-related petrogenesis of volcanic units (Sylvester et al., 1987) within greenstone belts led to the application of plate tectonic principles and the lithotectonic assemblage concept to the Ontario part of the Abitibi greenstone belt (Jackson and Fyon, 1991; Jackson et al., 1994). Heather (2001) and Ayer et al. (2002a) established that many previously defined assemblages were of similar age resulting in seven volcano-sedimentary assemblages in the Ontario part of the Abitibi greenstone belt, ranging from ~2750 to 2695 Ma (Table 1, Fig. 2). In Québec, however, stratigraphic terminology (Table 2) has been retained.

TABLE 1. Stratigraphy of the Southern Abitibi Geenstone Belt

Assemblage name and volcanic episode[1]	Thickness	Dominant rock types	Volcanic magma clan[2]
Timiskaming 2677–2670 Ma	Max. 2–3 km	Polymictic conglomerate and sandstone in subaerial alluvial fan, fluvial, and deltaic settings, alkaline volcanic rocks in Kirkland Lake area	Alkaline to calc-alkaline
Porcupine 2690–2685 Ma	Max. 2–3 km	Local basal felsic pyroclastic rocks of the Krist Formation (Timmins area) overlain by turbiditic sediments (argillite to wacke)	Calc-alkaline
Upper Blake River 2701–2695 Ma	1–7 km	Mafic to felsic volcanic units with volcaniclastic components	Tholeiitic to calc-alkaline
Lower Blake River 2704–2701 Ma	~10 km	Minor clastic metasediments overlain by high Mg and Fe tholeiites with minor tholeiitic andesite, dacite, and rhyolite forming upper 5%	Tholeiite similar to mid-ocean ridges
Upper Tisdale 2706–2704 Ma	~5 km	Intermediate to felsic amygdaloidal flows heterolithic debris flows, and volcaniclastic units	Calc-alkaline
Lower Tisdale 2710–2706 Ma	~5–10 km (poorly constrained)	Mafic volcanic rocks with localized ultramafic, intermediate to felsic volcanics and iron formation	Tholeiites with slight depletion of LREE, HFSE, Nb, and Ti; komatiites AUK[3]; rhyolites variably tholeiitic to calc-alkaline
Upper Kidd-Munro 2717–2711 Ma	~5 km in Munro Township	Mafic volcanic rocks with localized ultramafic and felsic volcanics and graphitic metasediments	MORB-like tholeiitic mafic and felsic volcanics with minor ADK[3] and AUK[3] komatiites
Lower Kidd-Munro 2719–2717 Ma	~5 km in Rand Township	Intermediate-felsic calc-alkaline rocks	Calc-alkaline
Stoughton-Roquemaure 2723–2720 Ma	Max. 12 km SE of Lake Abitibi batholith	Tholeiitic basalts with komatiites and local felsic volcanic rocks	MORB-like tholeiite with komatiite (ADK-AUK[3])
Deloro 2734–2724 Ma	~5 km	Mafic to felsic calc-alkaline volcanic rocks with local tholeiitic mafic volcanic units and an iron formation cap	Calc-alkaline with minor tholeiites
Pacaud 2750–2735 Ma	5 km in Shining Tree area	Ultramafic, mafic, and felsic volcanic, with minor iron formation	AEK[3] Komatiites, high Fe and high Mg tholeiites and calc-alkalic
Pre-2750 Ma 2766 ± 1.1 Ma (un-named unit, Temagami area)	~5 km	Intermediate to felsic pyroclastic rocks capped by iron formation	Calc-alkaline

[1] Based on age ranges in Ayer et al. (2005) and modified with new ages (see in the text)
[2] Magma clan information based on Ayer et al. (2002) and references therein
[3] Komatiite types as reviewed in Sproule et al. (2005): ADK = alumina-depleted komatiite, AUK = alumina-undepleted komatiite, AEK = alumina-enriched komatiite

The southern part of the Abitibi greenstone belt was originally estimated to represent a composite stratigraphic thickness of 45 km or more (Ayres and Thurston, 1985, and references therein). This is difficult to reconcile with geothermal gradients of about 25° to 30°C/km and subgreenschist metamorphic facies over large parts of the belt. This conundrum raised the question as to whether the greenstone belt had undergone large-scale, volcanism-related subsidence (e.g., Hargraves, 1976), thrust-based condensation of stratigraphy, or whether the stratigraphy represents a series of off-lapping lenses to resolve the disparity of apparent stratigraphic thickness versus low metamorphic grade. In essence, one of the central questions is whether the postulated stratigraphy and stratigraphic thickness of the Abitibi greenstone belt (Ayer et al., 2002a) is belt-wide or represents off-lapping units similar to the Pilbara craton (Van Kranendonk et al., 2002, 2007) and whether deposition was continuous over a 50-m.y. period or episodic. These are critical distinctions for mineral exploration in that identifiable hiatuses in deposition are important loci for syngenetic mineralization.

The synthesis of Ayer et al. (2002a) indicated that six of seven of the volcanic assemblages (Fig. 2) displayed local to regional-scale stratigraphic gaps but did not describe their character or cause. Heather (2001) postulated that one such gap between the ~2735 Ma Marion Group and the 2705 Ma Trail Breaker Group represents an unconformity (Fig. 3) in the Swayze greenstone belt, a western extension of the Abitibi greenstone belt. Heather (2001) asserted that this unconformity was regional in scale. However, documentation of the unconformity was general and details of its regional importance were not fully developed. As well, these authors did not fully explore the metallogenic and tectonic consequences of an unconformity-bounded stratigraphic model for the Abitibi greenstone belt.

Our purpose in this contribution is to identify stratigraphic and/or lithotectonic packages, based on similarities of age

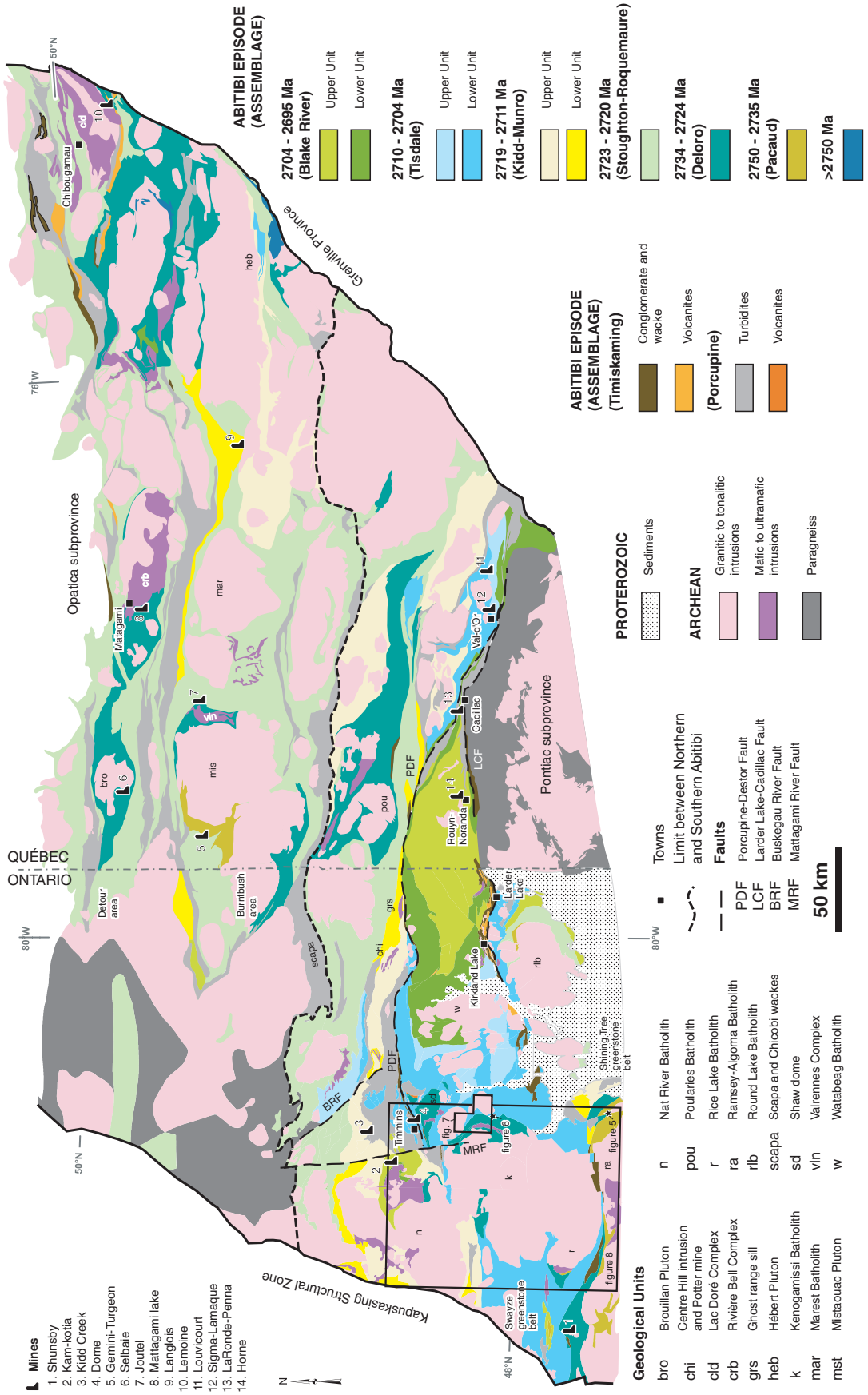

FIG. 2. Stratigraphic map of the Abitibi greenstone belt. The geology of the southern Abitibi greenstone belt is based on Ayer et al. (2005) and the Québec portion on Goutier and Melançon (2007). Abbreviations and acronyms used on the map are listed.

TABLE 2. Ages of Individual Stratigraphic Units in Québec Within the Age Ranges Used Herein

Volcanic episode	Unit	Age	Magma clan[1]	Reference
2704–2695 Ma	Reneault-Dufresnoy Fm Blake River Group	2698-2696 Ma	TH-CA, flows and pyroclastics	Mortensen (1993a); Lafrance et al. (2005)
	Bousquet Formation Blake River Group	2699-2698 Ma	TR-CA flows and pyroclastics	Mercier-Langevin et al. (2007a); Lafrance et al. (2005)
	Noranda Formation Blake River Group	2698-2696 Ma	TR flows	David et al. (2006); David et al. (2007)
	Rouyn-Pelletier Formation Blake River Group	2701 ± 2 Ma	TH flows	Lafrance et al. (2005)
	Duprat-Montbray Formation	2702-2697 Ma	TH-TR flows	Mortensen (1993a); David et al. (2006)
	Héva Formation	2702 ± 1 Ma	TH basalt and andesite	Pilote et al. (2000)
	Villebon Group	2703 ± 1 Ma	TH-TR flows,	Moorhead et al. (2000b)
2710–2704 Ma	Val-d'Or Formation	2705-2704 Ma	TR-CA flows, pyroclastics	Wong et al. (1991); Pilote et al. (2000); Moorhead et al. (2000a); Scott et al. (2002)
	Figuery Formation (Mine Abcourt)	2706 ± 1 Ma	TH flows	David et al. (2007)
	Urban Formation	2707 ± 3 Ma	CA felsic tuff and glomeroporphyric basalt	Bandyayera et al. (2004)
2717–2711 Ma	La Motte-Vassan Formation	2714 ± 2 Ma	Felsic tuff between komatiitic flows	Pilote et al. (2000)
	Lac Arthur Group	2714 ± 3 Ma	TR felsic and andesitic flows	Labbé (1999)
	Quévillon Group	2716 ± 1 Ma	TR felsic flows	David et al. (2007)
	Windfall Member Macho Formation	2717 ± 1 Ma	TR-CA felsic flows	Bandyayera et al. (2003)
2719–2717 Ma	Lanaudière Formation	2718 ± 2 Ma	TH rhyolite, andesite, basalt and komatiitic basalt	Zhang et al. (1993); Goutier (1997)
	Mine Langlois (unnamed unit)	2718 ± 2 Ma	CA mafic to intermediate lapilli tuff	Davis et al. (2005)
2723–2720 Ma	Dussieux Formation	2720 ± 1 Ma	TR to CA pyroclastics and flows	Davis et al. (2005)
	Estrades unit	2720 ± 3 Ma	TH felsic flows	David et al. (2007)
	Collines de Cartwright Group	2721 ± 3 Ma	Andésite, basalt and komatiite	Legault et al. (2002)
	Vanier-Dalet-Poirier Group	2722 ± 2 Ma	Synvolcanic intrusion	Gaboury and Daigneault (1999)
	Beaupré Formation	2722 ± 3 Ma	Sodic rhyolite	Zhang et al. (1993); Lafrance (2003)
	Manthet Group (Detour Lake Mine)	2722 +3/-2 Ma	Feldspar porphyry dike	Marmont and Corfu (1989)
	Lac Watson Group (North limb)	2723 ± 1 Ma	TH felsic flows	Mortensen (1993b); Goutier et al. (2004)
2734–2724 Ma	Lac Watson Group (South limb)	2725 ± 2 Ma	TH felsic flows	Mortensen (1993b)
	Rivière Bell Complex	2725 ± 2 Ma	Gabbroic Complex	Mortensen (1993b)
	Mistaouac Pluton	2726 ± 2 Ma	Tonalite	Davis et al. (2000)
	Chanceux Formation	2727 ± 1 Ma	CA felsic pyroclastics	Bandyayera et al. (2004)
	Lac Doré Complex	2727 ± 1 Ma 2728 ± 1 Ma	Gabbroic and anorthositic complex	Mortensen (1993b)
	Valrennes Complex	2728 ± 1 Ma	Gabbroic complex	Legault et al. (2002)
	Poirier Member, Joutel Formation	2728 ± 2 Ma	TR felsics flows	Mortensen (1993b); Legault et al. (2002)
	Normétal Group	2728 ± 1 Ma	TR-TH volcanics	Mortensen (1993a); Lafrance (2003)
	Brouillan-Fénelon Group	2726 ± 3 Ma 2729 ± 3 Ma	TR felsic flows	Barrie and Krogh (1996)
	Waconichi Formation (Mine Lemoine area)	2728 ± 1 Ma 2730 ± 2 Ma	TH felsic flows and porphyry intrusion	Mortensen (1993b)
	Mine Hunter Group	2732-2725 Ma	CA felsic flows, pyroclastics, iron formation and gabbro	Mueller and Mortensen (2002); Mortensen (1993a)
2750–2735 Ma	Gemini-Turgeon rhyolite	2736 ± 1 Ma	CA flows, pyroclastics	Davis et al. (2005)
Pre-2750 Ma	des Vents Member	2788-2757 Ma	CA flows, pyroclastics	Mortensen (1993b)
	Fecteau Formation	2791 ± 1 Ma	CA flows, pyroclastics	Bandyayera et al. (2004)

[1] Magma clan based on Barrett and MacLean (1994): KM = komatiitic, MgO >9%; TH = tholeiitic, Zr/Y <4.5; TR = transitional, Zr/Y = 4.5–7; CA = Calc-alkaline, Zr/Y >7

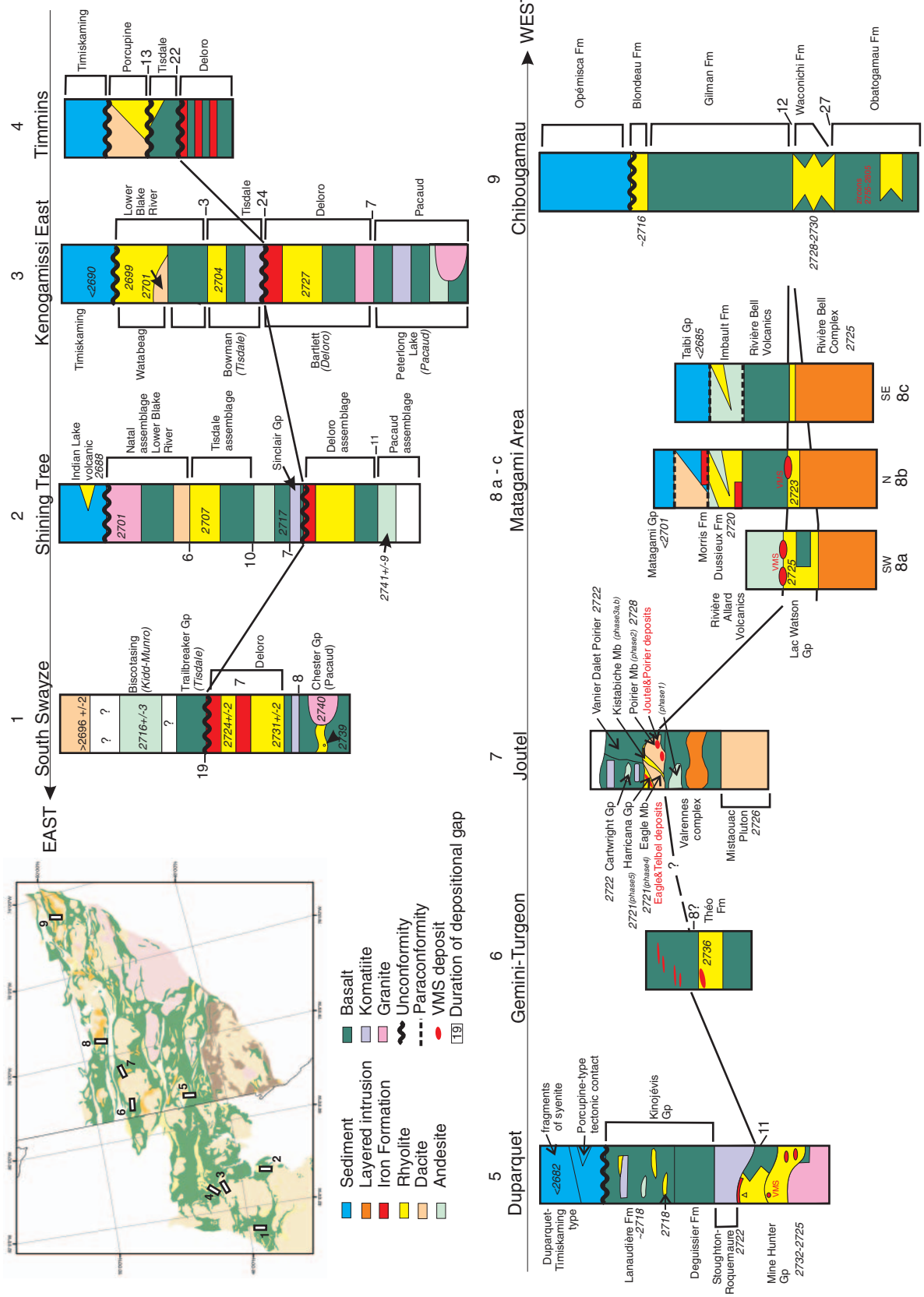

FIG. 3. Stratigraphic columns from selected locations across the Abitibi greenstone belt showing proposed correlation of various 2734 to 2724 Ma units and their relationship to VMS mineralization and iron formation. Numbers placed at the upper contacts of selected individual episodes represent the duration of depositional gaps in millions of years based on U-Pb zircon dates of nearby units.

intervals, stratigraphy, and geochemistry, utilizing previous syntheses of the southern Abitibi greenstone belt (e.g., Davis et al., 2000; Heather, 2001; Ayer et al., 2002a) and a new synthesis of the entire Abitibi greenstone belt (Ayer et al., 2005; Goutier and Melançon, 2007). We use the stratigraphic and/or lithotectonic succession to define major structures and provide a guide to identification and tracing of volcanic hiatuses and thus syngenetic mineralized environments. And, we use the stratigraphic and/or lithotectonic patterns and estimates of the rates of igneous processes to understand the genesis of the sedimentary interface zones spatially associated with the depositional gaps and their relationship to development of syngenetic mineralization.

Abitibi Greenstone Belt Stratigraphy and Depositional Gaps

The stratigraphy of the Abitibi greenstone belt at a large scale is seen as laterally continuous mafic and felsic volcanic units unconformably overlain by successor basins. However, in detail mafic and felsic volcanic units lack laterally persistent marker horizons. Detailed mapping and petrographic, facies, and geochemical data indicate that many mafic volcanic units of the Abitibi greenstone belt represent individual overlapping shield volcanoes (e.g., Goodwin, 1979; Dimroth et al., 1982, 1983). Felsic volcanic units form lenses with limited lateral persistence (MER-OGS, 1984), commonly subdivided on the basis of eruption mechanisms (Mueller and Donaldson, 1992a), geochemistry (Ayer et al., 2002a), and stratigraphy (Scott et al., 2002). The only units with significant lateral persistence are the clastic and chemical sedimentary units at the top of mafic to felsic volcanic units (e.g., Ayer et al., 2005; Goutier and Melançon, 2007). Therefore, the laterally extensive sedimentary units are used herein to define stratigraphic gaps important in identifying horizons of importance for deposition of syngenetic mineralization.

Tables 1 and 2 list volcanic units ranging in age from 2750 to 2695 Ma throughout the Abitibi greenstone belt, with some minor older volcanic units (e.g., Bandyayera et al., 2004). The stratigraphy of the belt is autochthonous, based on (1) the lateral persistence of first-order lithologic and lithotectonic and/or stratigraphic units throughout the belt (MER-OGS, 1984, Heather, 2001; Ayer et al., 2005; Goutier and Melançon, 2007; Fig. 2); (2) the presence of major folds with upward younging and upward structural facing at Chibougamau (Pilote, 2006) and between the Porcupine-Destor fault and the Larder Lake-Cadillac fault in Québec and Ontario; (3) the presence of crustal sections with outward-younging stratigraphy that are cored by batholiths, centered on the Chibougamau area (Pilote, 2006), the Mistaouac pluton (Fig. 2), the Poularies pluton (Mueller and Mortensen, 2002), the Round Lake batholith (Ayer et al., 2002a), and the Kenogamissi batholith (Ayer et al., 2002a); and (4) the presence of crosscutting, in situ geologic relationships between rock packages such as feeder dikes (Heather, 2001). The continuously upward-younging stratigraphic succession is also supported by the lack of evidence for any large-scale thrusting, based on (1) detailed reflection seismic sections (Snyder and Reed, 2005, Snyder et al., 2008), (2) the small number of out-of-sequence rock units (i.e., older over younger: Ayer et al., 2005), and (3) other structural studies summarized by Benn and Peschler (2005).

Given the apparently continuous nature of deposition of the volcanic rocks in the Abitibi greenstone belt, it is striking to observe that there are depositional gaps in representative stratigraphic sections across the Abitibi greenstone belt (Figs. 2, 3). These include: (1) the central part of the Swayze area, southwest of Timmins, where Heather (2001) and van Breemen et al. (2006) noted a depositional gap between the 2735 +6/-4 Ma Marion Group and the 2705 ± 2 Ma Trailbreaker Group (see also Heather et al., 1995); (2) south of Timmins, where rocks of the 2730 to 2724 Ma Deloro assemblage are overlain by the 2710 to 2704 Ma Tisdale assemblage (Ayer et al., 2002a); (3) the Shining Tree area, south of Timmins, where the 2750 to 2735 Ma Pacaud assemblage is overlain by the 2730 to 2724 Ma Deloro assemblage (Ayer et al., 2002a); (4) the Matagami area, where rocks of the 2725 to 2723 Ma Lac Watson Group are overlain by rocks of the 2720 ± 1 Ma Dussieux Formation (Goutier et al., 2004); and (5) the Chibougamau area, where ca. 2730 Ma rocks of cycle 1 are overlain by 2718 ± 2 Ma volcanic rocks of cycle 2 (Mortensen, 1993b; Pilote, 2006).

In light of these age gaps and a lack of evidence for large-scale thrusting, we review possible models to explain the presence of these depositional gaps in the Abitibi greenstone belt and their relationship to syngenetic mineralization.

Terminology

Given the fact that a formal Abitibi-wide stratigraphic terminology does not exist, in this contribution we utilize the term "episode" to denote a geochronologically defined depositional interval. The time intervals of these episodes are based on about 450 highly precise U-Pb zircon ages in Ontario and Québec. This has allowed creation of the first, geochronologically constrained Abitibi-wide stratigraphy. Volcanism was not continuous within a given episode. However, the number and distribution of the U-Pb ages has constrained the duration of volcanism within these episodes. On a local basis within the Abitibi greenstone belt, the stratigraphy and the geochronological data have permitted identification of depositional gaps which are described below. Within these episodes we use the existing terminology for easier comparison with the literature. Thus, we refer to lithotectonic assemblages in Ontario (Ayer et al., 2002a, 2005) and the local formalized stratigraphic terminology for units in Québec (Goutier and Melançon, 2007). The accepted formation names in Québec are French which are not translated into English to ease access to the literature and to preserve the nomenclature. Correlation of these two systems of nomenclature is ongoing between the two geological surveys and is beyond the scope of this paper. As the fundamental control on syngenetic mineralization is stratigraphic, with VMS mineralization having formed locally during many of the major volcanic episodes, we examine implications of the model for syngenetic mineralization but also consider belt-scale structural geology, isotopic inheritance, petrogenesis, regional correlation, and recognition of the successor basins. We use the term "sedimentary interface zone," noted above, to describe laterally persistent 1- to 350-m-thick units of chemical and minor clastic sedimentary rocks that are intercalated within and cap units deposited during a number of the volcanic episodes within the Abitibi greenstone belt.

Geographic townships are used to aid the reader in locating features and detailed map areas. A map of the townships is provided in Appendix 1.

Large-Scale Geologic Setting of the Abitibi Greenstone Belt

Subdivisions of the Abitibi greenstone belt

Previously the Abitibi greenstone belt has been subdivided into northern and southern parts on stratigraphic and structural criteria (e.g., Dimroth et al., 1982; Ludden et al., 1986; Chown et al., 1992). New U-Pb zircon ages and recent mapping by the Ontario Geological Survey and Géologie Québec clearly show similarity in timing of volcanic episodes and ages of plutonic activity between the northern and southern Abitibi greenstone belt as indicated in Figure 2 and summarized below. Therefore, the geographic limit between the northern and southern parts of the Abitibi greenstone belt has no tectonic significance but is herein provided (Fig. 2) merely for reader convenience and is similar to the limits between the internal and external zones of Dimroth et al. (1982) and that between the Central granite-gneiss and Southern volcanic zones of Ludden et al. (1986). The boundary passes south of the wackes of the Chicobi and Scapa Groups with a maximum depositional age of 2698.8 ± 2.4 Ma (Ayer et al., 1998, 2002b).

Distribution of rock types

The Abitibi greenstone belt is composed of east-trending synclines of largely volcanic rocks and intervening domes cored by synvolcanic and/or syntectonic plutonic rocks (gabbro-diorite, tonalite, and granite) alternating with east-trending bands of turbiditic wackes (MER-OGS, 1984; Ayer et al., 2002a; Daigneault et al., 2004; Goutier and Melançon, 2007). Most of the volcanic and sedimentary strata dip vertically and are generally separated by abrupt, east-trending faults with variable dip. Some of these faults, such as the Porcupine-Destor fault, display evidence for overprinting deformation events including early thrusting, later strike-slip and extension events (Goutier, 1997; Benn and Peschler, 2005, Bateman et al., 2008). Two ages of unconformable successor basins occur—early, widely distributed "Porcupine-style" basins of fine-grained clastic rocks, followed by "Timiskaming-style" basins of coarser clastic and minor volcanic rocks which are largely proximal to major strike-slip faults (Porcupine-Destor, Larder-Cadillac, and similar faults in the northern Abitibi greenstone belt; Ayer et al., 2002a; Goutier and Melançon, 2007). In addition, the Abitibi greenstone belt is cut by numerous late-tectonic plutons from syenite and gabbro to granite with lesser dikes of lamprophyre and carbonatite.

Stratigraphy of the Abitibi Greenstone Belt

Stratigraphic analysis of Archean greenstone belts is bedevilled by problems of variable primary distribution of volcanic rocks and the vagaries of subsequent preservation resulting from multiple orogenies. Most of the crustal sections in the Abitibi greenstone belt (enumerated previously) preserve rocks of the 2734 to 2724 Ma volcanic episodes on the margins of the batholiths and to a lesser extent rocks of pre-2734 Ma episodes. However, relatively widespread ca. 2750 Ma inherited zircons found in younger volcanic rocks of the southern Abitibi greenstone belt (Ayer et al., 2005) suggest that ca. 2750 Ma rocks may have been widespread and largely assimilated by granitoid magmatism during gravity-driven inversion of Archean crust (cf. Bleeker, 2002; Van Kranendonk et al., 2004, Ketchum et al., 2008), simple stoping and assimilation during synvolcanic tilting of strata (e.g., Finamore (Hocker) et al., 2008), or detachment folding resulting in emplacement of older rocks in the midcrust, as represented by the Opatica subprovince (Benn and Peschler, 2005).

Details of Abitibi greenstone belt stratigraphy have been presented in several publications (e.g., MER-OGS, 1984; Ayer et al., 2002a, 2005; Goutier and Melançon, 2007). We intend to minimize stratigraphic and lithologic details herein and to concentrate on stratigraphic development revealed by new mapping and geochronology (Ayer et al., 2005), the stratigraphic relationships between rock packages, as shown in Figure 2, and the implications of these relationships for regional metallogeny.

In contrast to Ayer et al. (2002a), in which the nature of the basal contacts of lithotectonic assemblages was emphasized, we describe relationships at the top of assemblages, to aid in documenting depositional gaps related to the succession in question. Sedimentary interface zones are placed with the underlying volcanic rock packages based on petrographic and geochronologic evidence such as the presence of rhyolitic ash and detrital zircons from immediately underlying units (cf. Ayer et al., 2002, 2005; Hickman and Van Kranendonk, 2004). Tables 1 and 2 summarize the major stratigraphic features of the volcanic episodes in the southern and northern Abitibi greenstone belt. In the following descriptions, we emphasize the distribution of units produced during specific volcanic episodes and the contact relationships and character of the sedimentary interface zones capping most of the volcanic rock packages. Whereas previous mapping simply noted that sedimentary interface zone was iron formation, more recent mapping has disclosed details such as of clastic and/or pyroclastic units, chert breccia, and conglomerate which bear on the origin of the sedimentary interface zone (e.g., Ayer et al., 2005; Goutier, 2006; Pilote, 2006).

Pre-2750 Ma volcanic unit

Three pre-2750 Ma volcanic units have been identified, situated on the margins of batholiths. These are (1) the 2791 ± 1 Ma Fecteau Formation, southwest of Chibougamau (Bandyayera et al., 2004), (2) the ~2759 Ma Des Vents Member in the Chibougamau greenstone belt (Mortensen, 1993b), and (3) a 2766.9 ± 1.1 Ma basalt to rhyolite succession on the north edge of the Temagami greenstone belt (Ayer et al., 2006). The importance of these older episodes is that they are locally preserved on margins of batholiths on the eastern and western margins of the Abitibi greenstone belt. The Fecteau Formation (basalt and minor rhyolite capped by iron formation) is the oldest assemblage in the northern Abitibi greenstone belt (Bandyayera et al., 2004). It forms an isolated, east-trending fragment near the south flank of the Hébert pluton (Bandyayera et al., 2004). Its contact with the 2727 ± 1 Ma Chanceux Formation tholeiitic basalts is a thrust (Bandyayera et al., 2004). The ~2759 Ma Des Vents Member is an isolated felsic center in the Chibougamau greenstone belt, which

contains 2805 Ma xenocrysts (Mortensen, 1993b). The 2767 Ma mafic to felsic volcanic unit at Temagami (south of the area shown in Fig. 2) is capped by iron formation. The presence of rare ca 2860 Ma xenocrysts in volcanic units of the Kidd-Munro assemblage (Ayer et al., 2005) and in synvolcanic phases of the Rice Lake batholith (the southwest lobe of the Kenogamissi batholith), clearly suggests the localized presence of ~2.8 Ga basement in the westernmost part of the Abitibi greenstone belt (Ketchum et al., 2008).

2750 to 2735 Ma volcanic episode (Pacaud assemblage)

In the southern Abitibi greenstone belt, the Pacaud assemblage is the oldest supracrustal unit of substantial lateral extent, with dated rhyolites having a range of ages from 2747 to 2736 Ma (Ayer et al., 2002a; van Breemen et al., 2006). It occurs on the flanks of the Round Lake, Kenogamissi, and Ramsey-Algoma batholiths, with a basal intrusive contact with granitoid units. The relationship of 2750 to 2735 Ma units of the southern Abitibi greenstone belt to the pre-2750 Ma units of the northern Abitibi greenstone belt (Mortensen, 1993a; Bandyayera et al., 2004) is unknown. Synvolcanic, 2747 to 2740 Ma tonalite-trondhjemite-granodiorite magmatism has been dated in both the Rice Lake batholith (i.e., southwestern lobe of the Kenogamissi batholith) and the Round Lake batholith (Ketchum et al., 2008).

The age of the Pacaud assemblage compared to the overlying Deloro assemblage in the southern Abitibi greenstone belt in Ontario suggests a local age gap or depositional hiatus of 2 to 5 m.y. between the two assemblages. The thickest remnant of the Pacaud assemblage occurs in the Shining Tree area where it is represented largely by tholeiitic mafic volcanic rocks with lesser komatiite and calc-alkaline intermediate to felsic volcanic rocks. In the southern Swayze greenstone belt, there is a depositional gap of ~8 m.y. between the 2739 ± 1 Ma Chester Group and the 2731 ± 2 Ma Marion Group (van Breemen et al., 2006).

Previously, the Obatogamau Formation in the northern Abitibi greenstone belt (Chibougamau area) was considered to be ~2760 Ma (Mortensen, 1993a). This age is now assigned strictly to the Des Vents Member below the 2730 Ma Obatogamau Formation (Chown et al., 1992). Rocks clearly belonging to the 2750 to 2735 Ma volcanic episode in the northern Abitibi greenstone belt are the felsic volcanic rocks at Gemini-Turgeon and the subjacent basalts (2736 ± 1 Ma: Davis et al., 2005) on the eastern flank of the Mistaouac pluton (Fig. 2). This unit is capped by an undated sedimentary interface zone consisting of clastic sedimentary rocks and VMS mineralization.

2734 to 2724 episode (Deloro assemblage)

In the southern Abitibi greenstone belt, units of the 2730 to 2724 Ma Deloro assemblage (Ayer et al., 2005) occur as homoclinal panels underlain by the Pacaud assemblage on the northeastern flank of the Round Lake batholith, the southwestern and eastern flanks of the Kenogamissi batholiths, and on the northern flank of the Ramsey-Algoma batholith in the Shining Tree and Swayze areas (Fig. 2). The Deloro assemblage also occurs in the core of the Shaw dome south of Timmins and in north and east Timmins, north of the Porcupine Destor fault. A small remnant of the Deloro assemblage also occurs in a local-scale thrust enclosed by the Tisdale assemblage on the southeastern flank of the Shaw dome.

In Québec, volcanic units with ages in the range of 2734 to 2724 Ma range (Fig. 2) are on the margins of large synvolcanic and syntectonic plutons. These include the Mine Hunter Group (English terminology = Hunter Mine Group) on the margin of the Poularies pluton, near the Ontario-Québec border (Mortensen, 1993b; Mueller and Mortensen, 2002), the Poirier Member of the Joutel Formation and Valrennes Complex on the margin of the Mistaouac pluton in the Joutel area (Mortensen, 1993b; Davis et al., 2000; Legault et al., 2002); the Brouillan-Fénelon Group on the flank of the Brouillan pluton in the area of the Selbaie mines (Barrie and Krogh, 1996), the Waconichi Formation and the Lac Doré Complex in the Chibougamau area (Mortensen, 1993b); the Chanceux Formation (Lac Hébert area, Bandyayera et al., 2004) and the Lac Watson Group and the Rivière Bell Complex in the Matagami area (Mortensen, 1993a).

The Deloro assemblage and the Mine Hunter Group are composed of calc-alkaline flows and pyroclastic rocks (Ayer et al., 2002a; Mueller and Mortensen, 2002) and are variably overlain by rocks of the Tisdale, Kidd-Munro, and Stoughton-Roquemaure assemblages (Fig. 2). The Deloro assemblage is capped by a sedimentary interface zone consisting of a regionally extensive unit of iron formation and related hydrothermal breccias (Fig. 4A), iron formation conglomerate (Fig. 4B), fluidized iron formation (Fig. 4C), and debris flows. These sedimentary interface zone units occur within the Swayze greenstone belt (Heather, 2001), the Shining Tree greenstone belt (Johns and Amelin, 1998; Leblanc et al., 2000), and south of Timmins, on the flanks of the Shaw and Bartlett domes (Ayer et al., 2004a). In the Swayze greenstone belt (Heather, 2001) and the Shaw dome (Hall and Houlé, 2003), iron formations occur at differing stratigraphic levels, the uppermost of which is brecciated at both locations. In the Shining Tree greenstone belt, the top of the Deloro assemblage is marked by a sedimentary interface zone with proximal carbonate and oxide facies iron formation (Figs. 4A, 5) and chert breccia grading laterally to "thinly laminated, contorted, brecciated black to grey chert and red chert" (Johns and Amelin, 1998). The brecciated nature of the unit suggests similarities to units in several locations at the top of the Deloro assemblage described below. Tentative correlations between areas based on this marker unit are shown in Figure 3.

Depositional gaps at the top of the 2734 to 2724 Ma volcanic episode range from 7 to 24 m.y. as shown in Figure 3. An age gap or depositional hiatus of lesser duration than that occurring between the 2730 to 2724 Ma Deloro assemblage and the overlying 2710 to 2704 Ma Tisdale assemblage in Ontario exists in Québec at the top of 2734 to 2724 Ma volcanic episode. For example, iron formation breccia occurs in the Lac Sauvage iron formation capping the Waconichi Formation in the Chibougamau area (Henry and Allard, 1979). Typically, these units are overlain by volcanic rocks dated at 2722 to 2720 Ma such as the Eagle Member at Joutel (Legault et al., 2002). This leads us to suppose that there is a time gap of 2 to 6 m.y. at the top of 2734 to 2724 Ma volcanic episode in the northern Abitibi greenstone belt. The duration of this time gap may also vary from place to place, because the ages of volcanic centers become younger toward Matagami during

FIG. 4. A. Carbonate facies iron formation and chert breccia capping the Deloro assemblage in Macmurchy Township in the Shining Tree greenstone belt south of Timmins. The GPS unit used as a scale is 15 cm long. B. Fractured chert fragments within iron formation clasts in a unit of heterolithic conglomerate toward the top of the 2734 to 2724 Ma iron formation unit in Deloro Township. The notebook is 19 cm long. C. Fluidized chert breccia capping the iron formation unit at the top of the Deloro assemblage in English Township south of Timmins. The notebook is 19 cm. long. D. Banded cherty iron formation at the contact between the Kidd-Munro and the Tisdale assemblage in Carscallen Township at the Wire Gold exploration pits. Note the decreasing thickness of magnetite-rich laminae and increasing proportion of chert toward the stratigraphic top (right of photo). The sledge is 1 m long.

2734 to 2724 Ma volcanism (Mortensen, 1993a; Goutier and Melançon, 2007). However, this observation is generally based on only one to a few dated units in each felsic center.

Another significant difference in the northern Abitibi greenstone belt is that the 2734 to 2724 Ma units are generally dominated by tholeiitic rocks rather than calc-alkaline. The tholeiitic Lac Watson Group in the Matagami area (2725–2723 Ma: Mortensen, 1993a) is approximately correlative with the Deloro assemblage, based on lithologic similarities and the error in the age data cited. It is overlain by the Rivière Bell volcanic rocks which are considered coeval with the 2725 $^{+3}_{-2}$ Ma Rivière Bell Complex (Mortensen, 1993b), but the latter must be younger than 2723 Ma because the Lac Watson Group lies above a 2723 ± 1 Ma rhyolite (Mortensen, 1993b; Goutier et al., 2004). In this region, we interpret a time gap between the Rivière Bell volcanic rocks (largely mafic flows) and the intermediate to felsic volcanic rocks of the 2720 ± 1 Ma Dussieux Formation (Goutier et al., 2004; Davis et al., 2005), which are correlative with the Stoughton-Roquemaure assemblage in the southern Abitibi greenstone belt. The contact between the Rivière Bell volcanic rocks and the Dussieux Formation is a sedimentary interface zone consisting of a 1-m-thick unit of carbonatized oxide and sulfide facies iron formation and heterolithic conglomerates (Goutier et al., 2004) that resemble the iron formation conglomerates at the top of the Deloro assemblage in the Timmins area.

The Mine Hunter Group does not exhibit a clear unconformity with overlying units of the Stoughton-Roquemaure Group. Possible evidence for a depositional gap consists of the presence of bands of oxide facies iron formation and iron formation breccias containing chert fragments between flows and volcaniclastic units within the upper part of the Mine

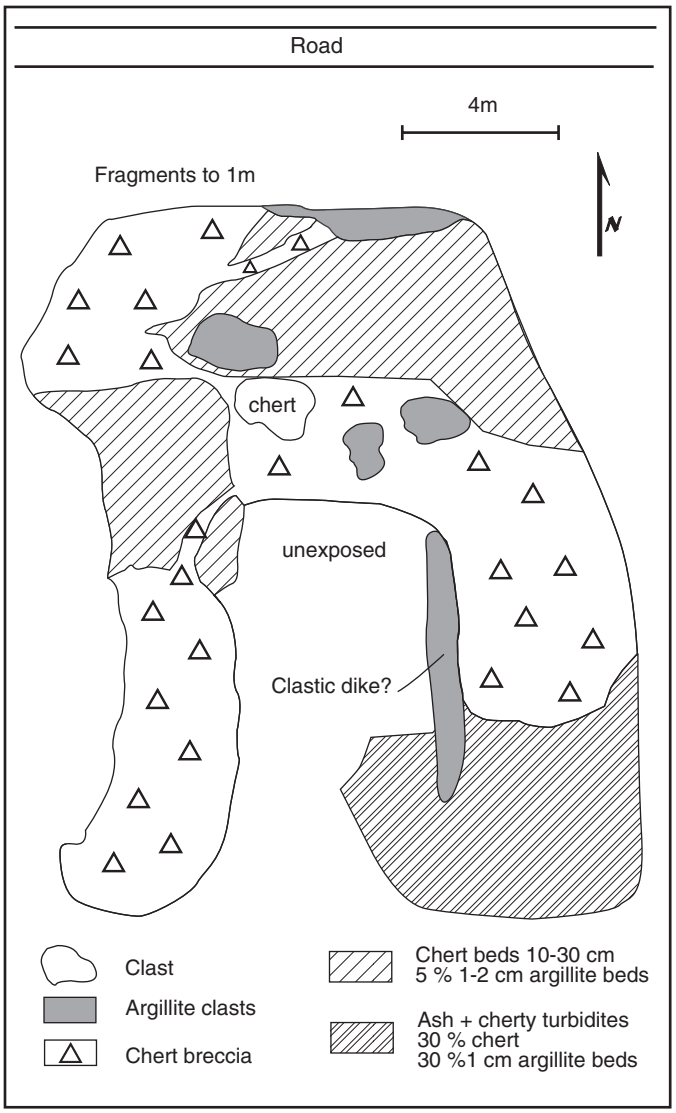

FIG. 5. Outcrop sketch map of the relationships between hydrothermal breccia with angular chert fragments in an iron carbonate matrix which cuts bedded sulfidic argillite, oxide facies relict ash turbidites, and chert beds at the top of the 2734 to 2724 Ma Deloro assemblage in the Shining Tree greenstone belt.

Hunter Group (Eakins, 1972; Chown et al., 2000; Goutier, 2000; Mueller and Mortensen, 2002).

Locations of the iron formation breccia and the character of related units capping the 2734 to 2724 Ma volcanic rocks are shown in Figure 2 and Table 3. Iron formation associated with the 2734 to 2724 Ma period of deposition is of two types: classic banded iron formation at lower stratigraphic levels within the Deloro assemblage (Ayer et al., 2005), and lean cherty iron formation at the top of the Deloro assemblage south of Timmins (Table 3). The former consists of alternating bands of white and red to orange chert and bands of magnetite-hematite and lesser beds of fine rhyolitic tuff. The latter consists of alternations of white chert and laminae of argillite with magnetite and subordinate pyrite. The distinctive iron formation breccia units at the top of the 2734 to 2724 Ma Deloro assemblage in the southern Abitibi greenstone belt (Fig. 4C) form part of a stratigraphic package found along the Deloro-Tisdale assemblage contact in the Shaw dome area and in the English Township area south of Timmins. The unit as a whole (Fig. 6) consists of finely laminated, chert-rich iron formation (BIF) succeeded upward by a heterolithic, unbedded, ungraded tuff breccia debris flow unit and matrix-supported, unbedded, ungraded iron formation breccia (Fig. 6) with medium-bedded, graded wacke beds at the top that have iron silicate mineralogy, and occasional chert clasts. The upper limit of the wacke unit is truncated by erosional features and is overlain by a debris flow unit. The lateral equivalents of this package, about 4 km to the north, include 15-cm- to 2-m-hick heterolithic volcaniclastic debris flows capped by centimeter-scale, finely laminated pyritic, argillaceous turbidites. Along strike facies relationships in the sedimentary interface zone iron formations south of Timmins are shown in Figure 7. Facies relationships for iron formation in the 2734 to 2724 Ma episode surrounding the Kenogamissi batholith are shown in Figure 8 and discussed further below.

2723 to 2720 Ma volcanic episode (Stoughton-Roquemaure assemblage)

Voluminous volcanism in the Abitibi greenstone belt occurred during this time interval, represented by deposition of the Stoughton-Roquemaure assemblage in Ontario and

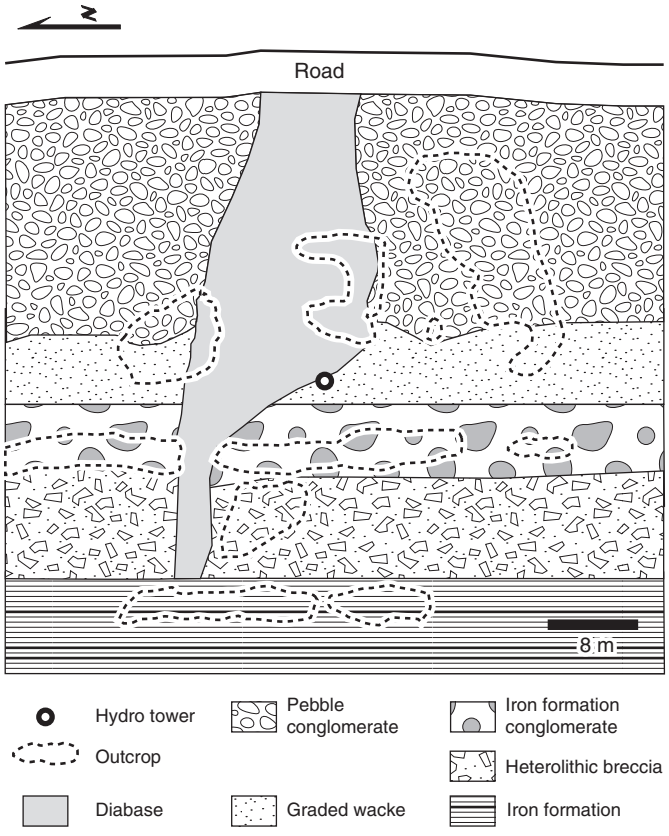

FIG. 6. Outcrop sketch map of sedimentary interface zone units at occurrence 5 (Table 3) with basal iron formation overlain by heterolithic, unbedded, ungraded dacitic tuff breccia debris flow, iron formation conglomerate, graded wacke and pebble conglomerate with an erosional channel at the top filled with a rhyolitic debris flow. The tower symbol refers to a hydroelectric transmission line tower.

TABLE 3. Iron Formation and Iron Formation Breccia Occurrences in the Deloro Assemblage and Broadly Correlative Units

General location	Detailed location	Description	Reference
1. Shaw dome N. flank	Shaw and Deloro Townships	"Dismembered chert" in a matrix of mafic to intermediate volcanic rock	Hall and Houlé (2003)
2. Shaw dome N. flank	Whitney Township	Banded iron formation, 1 m arkose, iron formation conglomerate with clasts to 60 cm in ferruginous chert matrix, capped with BIF	Ayer et al. (2004)
3. Shaw dome N. flank	Deloro Township	Banded iron formation succeeded by 2.5-m-thick iron formation clast bearing conglomerate with clasts to 15–20 cm overlain by 2724 Ma feldspar phyric lapilli tuff	Ayer et al. (2004, 2005)
4. Kenogamissi batholith E. flank	Bartlett Township	Feldspathic arkose beds 30–90 cm thick with 1- to 5-cm-thick graphitic, pyritic argillite tops	Ayer et al. (2005); Houlé (2006); Houlé and Solgadi (2007); Houlé et al. (2008b)
5. Kenogamissi batholith E. flank	English Township	Lean oxide-facies banded iron formation overlain by heterolithic pyroclastic breccia debris flows, heterolithic conglomerate containing dismembered chert clasts in a weakly cemented matrix of recrystallized chert, biotite, and feldspar; overlain by pebble conglomerates and wackes with chert clasts capped by an erosional channel	Ayer et al. (2005)
6. Kenogamissi batholith E. flank	McArthur Township	1. Basal 0.5–5 m oxide-facies iron formation with felsic tuff and jasper interbands 2. 5- to 40-m-thick chert-oxide iron formation with minor sulfide facies units 3. Upper 1- to 3-m graphitic and sulfidic argillite with minor chert at the contact with the overlying 2710–2704 Ma episode komatiites	Ayer et al. (2004); Houlé (2006); Houlé and Solgadi (2007); Houlé et al. (2008b)
7. Ramsey-Algoma batholith NE flank (Shining Tree)	Macmurchy Township and Churchill Township (central part)	Thinly laminated brecciated red chert (Macmurchy Township); thinly laminated contorted, brecciated black to gray and red chert	Johns and Amelin (1998); Leblanc et al. (2000)
8. Kenogamissi batholith W. flank	Marion Township, Woman River antiform	Banded chert intercalated with chert breccia units of tabular to rectangular chert casts in matrix of hematite and/or Fe carbonate	Goodwin (1965); Heather (2001)
9. Kenogamissi batholith W. flank	Kenogaming Township	Nat River iron formation contains horizons of chert breccia intercalated with banded cherty iron formation	Milne (1972)
10. Kenogamissi batholith W. Flank	Carscallen Township	Deloro assemblage pillowed basalts are overlain by 4.5 m of BIF and 4 m iron formation conglomerate and sandstone succeeded by 7 m of carbonatized komatiite flow of the Kidd-Munro assemblage	Hall and Smith (2002)
11. Mistaouac pluton NE flank (Joutel region)	South of Joutel	Heterolithic massive unbedded ungraded felsic tuff breccia with spatially associated ferruginous carbonate unit, brecciated graphitic argilllite	Hofmann and Masson. (1994); Legault et al. (2002)
12. Olga Pluton N flank (Matagami area)	Lac Olga region	Iron formation overlain by intermediate lapilli tuff heterolithic conglomerate with clasts in carbonate matrix	Goutier et al. (2004)

more extensive correlative units in the northern Abitibi greenstone belt (Fig. 2: Ayer et al., 2005; Goutier and Melançon, 2007). The time interval is characterized by broad regions of tholeiitic basalts, komatiitic basalts, and komatiites, as well as several relatively minor felsic volcanic centers. In the southern Abitibi greenstone belt, rocks of this age range are represented by the Stoughton-Roquemaure assemblage on the northeastern flank of the Round Lake batholith and an east-west–trending unit centered on Lake Abitibi, as well as the Deguisier Formation of the Kinojévis Group north of the Porcupine-Destor fault (Rouyn-Noranda area; Goutier, 1997).

Correlative units in the northern Abitibi greenstone belt include the Rivière Bell Volcanics (<2723 ± 1 Ma: Mortensen, 1993b) in the region of Matagami, the Vanier-Dalet-Poirier Group between the Mistaouac and Marest plutons dated at 2722 ± 2 Ma (Gaboury and Daigneault, 1999), the Eagle Member near Joutel dated at 2721 ± 2 Ma (Legault et al., 2002), and the Manthet Group at the contact of the Abitibi greenstone belt with rocks of the Opatica subprovince (2722^{+3}_{-2} Ma: Marmont and Corfu, 1989). The felsic centers of this age are the Beaupré sodic rhyolite, dated at 2722 ± 3 Ma (Zhang et al., 1993; Lafrance, 2003), and the 2720 ± 1 Ma Dussieux Formation (Goutier et al., 2004; Davis et al., 2005). Chert fragment conglomerate similar to that found south of Timmins above the Deloro assemblage caps the Dussieux Formation in the Matagami area (Goutier, 2006). Four recently dated volcanic units within the central Burntbush and Detour greenstone belts range in age from 2722.0 ± 3.2 to 2718.3 ± 3.5 Ma (Ayer et al., 2007), demonstrating that this

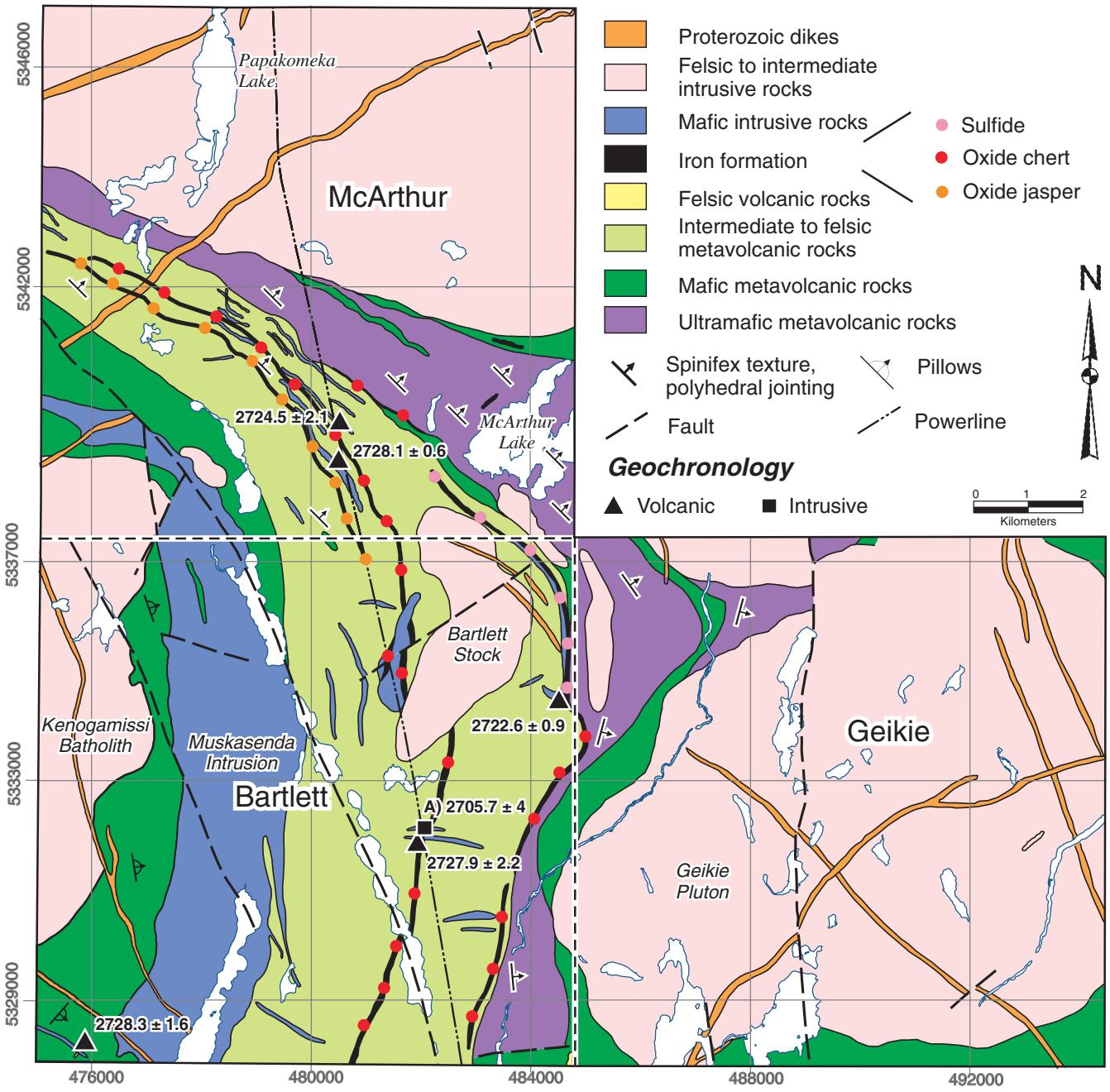

FIG. 7. Variations in iron formation facies in the sedimentary interface zone capping the 2734 to 2724 Ma volcanic episode in McArthur, Bartlett, and English Townships south of Timmins. The figure demonstrates that oxide and sulfide facies are dominant in this part of the strike extent of the "sedimentary interface zone". Modified from Houlé (2006), Houlé and Soldagi (2007), and Houlé et al. (2008b).

volcanic episode also has widespread distribution in the northern Abitibi of Ontario (Fig. 2).

South of Kirkland Lake, the 2723 to 2720 Ma Stoughton-Roquemaure assemblage is underlain by the 2750 to 2735 Ma Pacaud assemblage, thus representing a substantial depositional gap of about 13 m.y. (Ayer et al., 2005). Although the contact between the two assemblages is highly strained (Jackson and Harrap, 1989), age data indicating inheritance with Stoughton-Roquemaure-aged zircons in the overlying assemblages is consistent with an autochthonous primary relationship (Ayer et al., 2005). The upper part of the Stoughton-Roquemaure assemblage in this area (formerly the Catherine Group), which includes iron formation (Jackson and Fyon, 1991), is overlain by felsic volcanic rocks of the Skead Group (part of the Upper Blake River assemblage) with ages of 2701 ± 3 Ma, but also containing 2720 Ma xenocrystic zircons (Corfu, 1993), indicating a depositional gap of ~ 20 m.y. In Québec rocks of the 2723 to 2720 Ma volcanic episode are overlain by rocks of the upper part of the 2719 to 2711 Ma episode. Thus, there are likely substantial

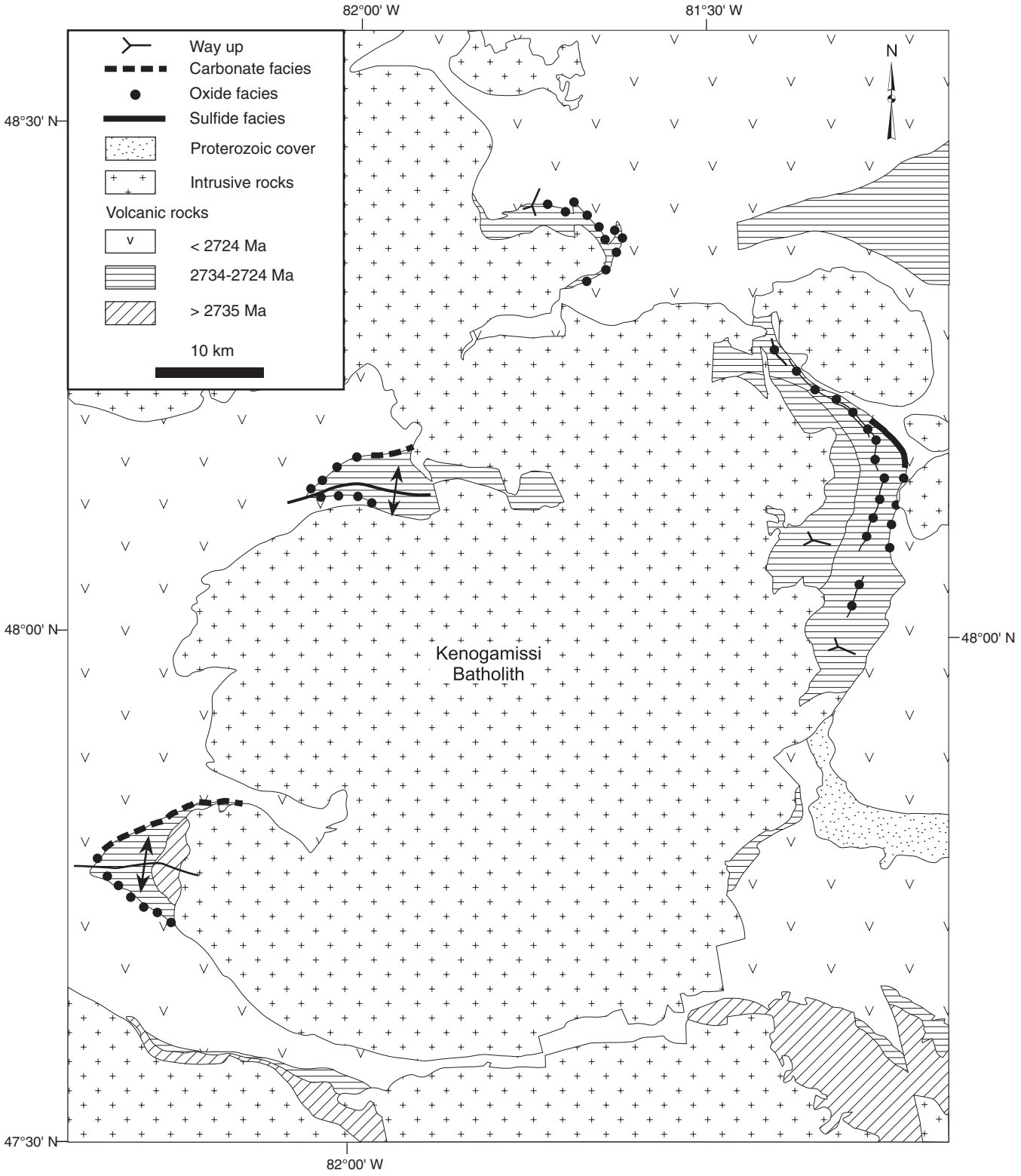

FIG. 8. Iron formation facies in the sedimentary interface zone capping the 2734 to 2724 Ma volcanic episode surrounding the Kenogamissi batholith. Note that the mixed carbonate-sulfide facies in the Woman River anticline is 3 to 30 m thick. Carbonate facies iron formation is spatially associated with altered underlying felsic metavolcanic rocks suggesting a proximal setting (Goodwin, 1965).

depositional gaps present but additional U-Pb zircon ages are required to better quantify their duration.

2719 to 2711 Ma volcanic episode (Kidd-Munro assemblage)

Units in this age range include the well-known Kidd-Munro assemblage of the southern Abitibi greenstone belt and units in the same age range in Québec. The Kidd-Munro assemblage, formerly a single stratigraphic unit with an age range of 2719 to 2711 Ma (Bleeker et al., 1999; Ayer et al., 2002a), is now subdivided (Ayer et al., 2005) into lower and upper parts.

In Ontario, the lower part of the Kidd-Munro assemblage (2719–2717 Ma) includes dominantly intermediate to felsic calc-alkaline volcanic rocks: (1) the former Duff-Coulson-Rand assemblage of Jackson and Fyon (1991) south of Lake Abitibi; (2) in Dundonald and Clergue townships in the central part of the western Abitibi greenstone belt where it is complexly infolded with upper Kidd-Munro assemblage rocks; and (3) west of Timmins in Thorburn and Loveland Townships, 2719.5 ± 1.7 Ma (Ayer et al., 2002a) calc-alkaline rocks are in tectonic contact with a northeast-facing unit of the upper part of the Kidd-Munro assemblage to the south (Hathway et al., 2008).

The upper part of the Kidd-Munro assemblage (2717–2711 Ma: Ayer et al., 2005) extends across the Abitibi greenstone belt, north of the Porcupine-Destor fault in Ontario (Fig. 2). It consists of tholeiitic and komatiitic units with minor centimetre- to meter-scale graphitic metasedimentary rocks and localized felsic volcanic centers. At the eastern end of the assemblage, its southern limit is the Porcupine-Destor fault. To the west, the southern contact is with Porcupine assemblage metasedimentary rocks across the Pipestone deformation zone, whereas west of the Buskegau River deformation zone, the southern contact is poorly known. West of the Matagami River fault, the assemblage is northeast facing, based on two new U-Pb zircon ages, and is in tectonic contact with the upper part of the Blake River assemblage in Jamieson Township (Hathway et al., 2008).

South of the Kamiskotia area, the base of the upper part of the Kidd-Munro assemblage is in contact with pillow basalts of the Deloro assemblage. The basal contact represents an ~13-m.y. gap between the 2727 ± 1 Ma Deloro assemblage and the 2712.2 ± 0.9 Ma Kidd-Munro felsic tuffs in Carscallen Township (Hall and Smith, 2002). Oxide facies iron formation containing chert breccia clasts, chert replacement of iron formation, and erosional features at this basal contact confirm that the basal contact is marked by a sedimentary interface zone (Fig. 4D; Table 4). Northwest of Timmins, in northernmost Robb and south-central Loveland Township, a drill hole through the contact between coherent rhyolites and overlying pillowed mafic flows revealed 2 m of "thin-bedded graphitic argillite and siltstone" at the top of the felsic unit (Hathway et al., 2005), suggesting locally developed volcanic hiatuses in the upper part of the Kidd-Munro assemblage. However, no major occurrences of iron formation conglomerate or chert breccia are known at this stratigraphic level.

In the upper Kidd-Munro assemblage between the Buskegau River fault (Fig. 2) and the interprovincial border, relationships are complex. The Kidd-Munro is tectonically juxtaposed with the younger Porcupine assemblage and a proportion of the Kidd-Munro stratigraphy has been removed by thrusting (Berger et al., 2007).

In the vicinity of the Kidd Creek mine, a significant age gap of at least 11 m.y. exists between the uppermost part of the Kidd-Munro assemblage and an overlying metasedimentary unit with a maximum depositional age of 2699 Ma in the Kidd 66 basin, located northeast of the deposit (Bleeker et al., 1999), and a heterolithic debris flow unit with a maximum depositional age of 2700 Ma overlies the rocks hosting the deposit in the Kidd West basin (W. Bleeker, pers. commun., 2005). These ages indicate a depositional gap between the upper part of the Kidd-Munro assemblage and rock units with ages correlative with the upper Blake River assemblage and suggests that a debris flow and/or clastic sediment sedimentary interface zone, without any obvious iron formation units, occurs between the Kidd-Munro and the Upper Blake River assemblage in the vicinity of the mine.

The Biscotasing Group (Heather, 2001) in the northern part of the Swayze greenstone belt is correlated by Ayer et al. (2002a) with the Kidd-Munro assemblage on the basis of rhyolite ages of 2715 ± 2 and 2718 ± 2 Ma (van Breemen et al., 2006). Here, the assemblage includes units of carbonate and oxide facies iron formation up to tens of meters thick with units of chert breccia up to 1 m thick, similar to that found above the Deloro assemblage south of Timmins.

The Lanaudière Formation of the Kinojévis Group, occurring north of the Porcupine-Destor fault, north of Rouyn-Noranda, may be equivalent to the lower part of the Kidd-Munro assemblage. This formation is in conformable contact with the underlying tholeiitic basalts of the Deguisier Formation considered to be part of the 2723 to 2720 Ma volcanic episode. The Lanaudière Formation is composed of intercalated basalt, andesite, tholeiitic rhyolite, and komatiitic basalt (Goutier and Lacroix, 1992; Goutier, 1997). A rhyolite within this unit with an age of 2718 ± 2 Ma, along with interdigitation of rhyolite and komatiitic basalt and the similarity of rhyolite geochemistry of this unit with Kidd-Munro assemblage rhyolites indicate that the unit is an equivalent of the Kidd-Munro assemblage.

Also in Québec, east of Rouyn-Noranda, are the La Motte-Vassan and Dubuisson Formations of the Malartic Group made up of komatiites and basalts for which a date of 2714 ± 3 Ma (Pilote et al., 2000) was obtained. The other temporal equivalents are the Lac Arthur Group near Amos (2714 ± 3 Ma: Labbé, 1999), lapilli tuffs of the Gonzague-Langlois mine (2718 ± 2 Ma: Davis et al., 2005), the Novellet Member situated 23 km southeast of the Gonzague-Langlois mine (2714 ± 1 Ma: Bandyayera et al., 2003), and the Macho Formation 74 km east-southeast of the Gonzague-Langlois mine (2717 ± 1 Ma: Bandyayera et al., 2002). The main possible depositional gap in the Val-d'Or area is about 8 m.y.

2710 to 2704 Ma volcanic episode (Tisdale assemblage)

Units in this age range include the 2710 to 2704 Ma Tisdale assemblage (Ayer et al., 2002a), the Jacola, Figuery, and Val-d'Or Formations in the southern Abitibi greenstone belt (east of Rouyn-Noranda) and the Urban Formation (lac Hébert area; 2707 ±3 Ma: Bandyayera et al., 2004) just north of the Fecteau Formation in the northern Abitibi greenstone belt.

Table 4. Stratigraphic Position and Character of Sedimentary Interface Zones

Age range (Ma)	Position	Condensed section	Chert replacement	Iron formation	Chert/iron formation breccia	Graphitic argillite
2704–2695	Top	Top of Bousquet Formation	Downward replacement			At geochemical discontinuities east of Timmins (Péloquin et al., 2005)
	5 internal within Noranda Fm.			Cherty iron formation and tuffite units		
2710–2704	Top of Lower unit			Cherty oxide and carbonate facies		East of Timmins in Lower Tisdale (Péloquin et al., 2005)
	Within Lower unit		Multiple chert units capping debris flows and reworked tuffs (Hutt Township)			
	Top of Upper unit		Replacing tuff unit (Gauthier Township)			
2719–2711	Top of upper unit	Thickness variation in carbonate iron formation			In Swayze belt above carbonate iron formation in Radio Hill iron formation (Ayer, 1995)	At geochemical discontinuities west of Timmins (Hathway et al., 2005)
	Top of lower unit			Iron formation unit, unknown characteer		
	Within Lower unit			Iron formation with chert breccia, graphitic pyritic argillite shallows up to tidal sands		
2723–2720	Top of unit		Chert unit, unknown character	Dussieux Formation Matagami area (Goutier, 2006)		
2734–2724	Top of unit	In iron formation, chert breccia unit with stratigraphic cutouts			South of Timmins and in Shaw Dome area along Deloro-Tisdale contact	
2750–2735	Top of unit	Proximal carbonate-oxide IF with chert breccia grades laterally to thin chert				
>2750		Lateral gradation from chert breccia to chert			At top of Pacaud assemblage in Shining Tree belt	

The Tisdale assemblage has been subdivided into a lower part and a upper part (Ayer et al., 2005). The lower part of the Tisdale assemblage consists of mafic tholeiitic flows with locally developed komatiite and intermediate to felsic calc-alkaline volcanic rocks and iron formation which forms the nose and limbs of a broad, west-verging, central syncline underlying the Blake River assemblage and truncated by the Porcupine-Destor fault to the north. It ranges in age from 2710 to 2706 Ma based on an age of 2710.1 ± 3.9 Ma for a heterolithic tuff breccia in Boston Township south of Kirkland Lake and a felsic flow with an age of 2710.5 ± 1.6 Ma in the core of the Halliday anticline in Midlothian Township (Ayer et al., 2002b). The basal contact with the Deloro assemblage south of Timmins and along the north and east flanks of the Shaw dome is characterized above in the description of the 2734 to 2724 Ma volcanic episode.

An internal sedimentary interface zone occurs in the lower part of the Tisdale assemblage in Hutt Township south of Timmins (Fig. 9A). Finely laminated felsic ash with pyritic argillite forms the bed tops. The contact between the heterolithic debris flows and the cherty unit capping each debris flow is gradational, whereas the upper contact of the chert unit is sharp. These contact relationships for the chert suggests that in these sequences it is diagenetic, by analogy

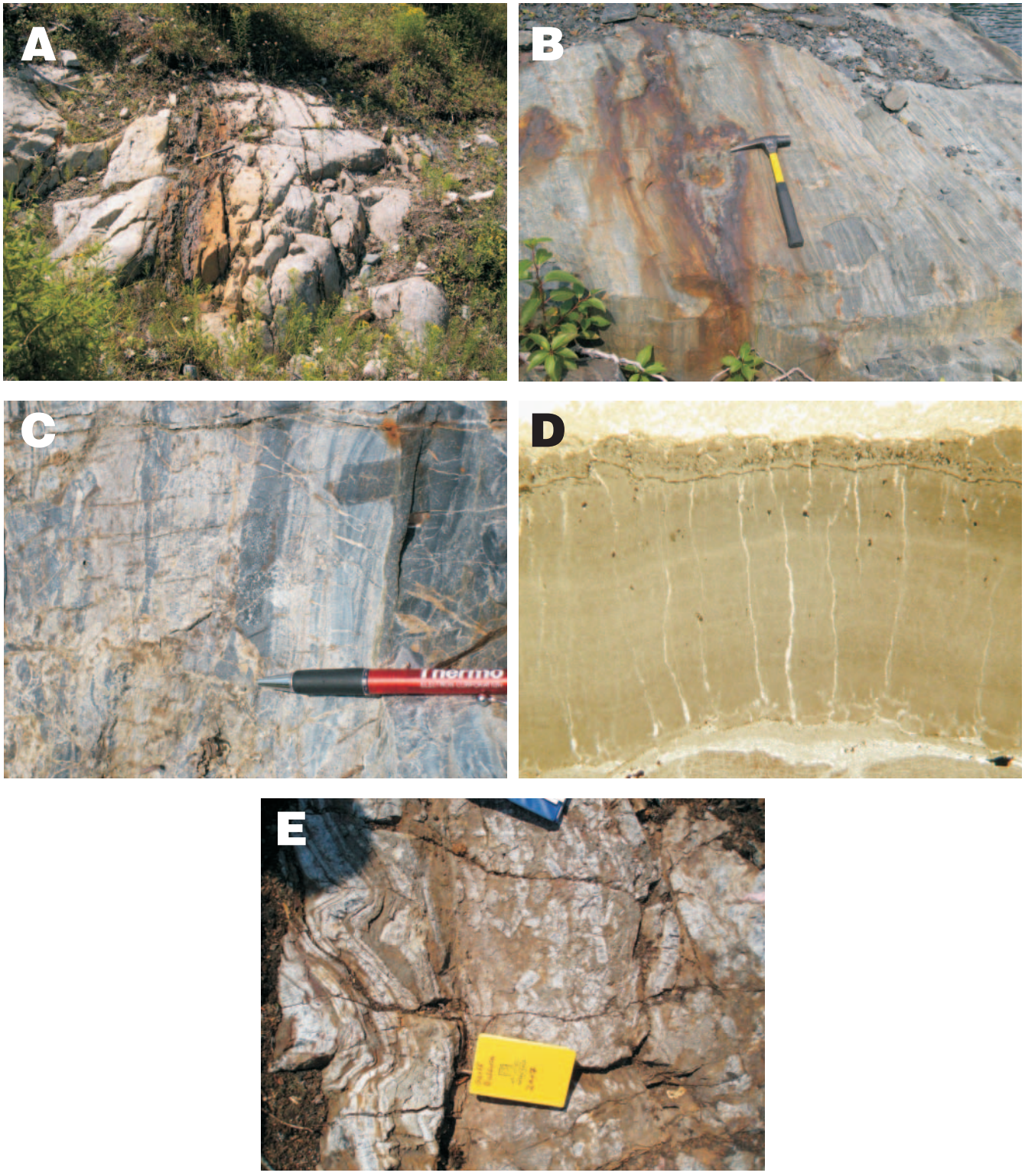

FIG. 9. A. Heterolithic felsic debris flow in the lower part of the Tisdale assemblage in Hutt Township. The debris flow (white) is overlain by pyritic chert (black and rust color) displaying a sharp upper contact (left on photo) and a diffuse lower contact. Hammer for scale is 35 cm long. B. Flaser bedded sandstones with a graphitic argillite clast in a unit capping oxide facies iron formation at the Adams mine in Boston Township south of Kirkland Lake. Hammer is 35 cm long. C. "Exhalite" metalliferous chert in the Noranda caldera of Gibson and Watkinson (1990). D. Turbiditic iron formation in the "sedimentary interface zone" capping the Stoughton-Roquemaure assemblage in the Burntbush segment of the Abitibi greenstone belt. The bed shown is 3 mm thick. E. Chert breccia bed overlain (to left of 21 cm field notebook) by chert and wacke beds, illustrating the synsedimentary nature of the chert breccia units. Photo taken in English Township on the powerline by Geoffrey Baldwin.

with similar relationships reported in the Brockman Iron Formation (Krapez et al., 2003). This association of chert and mass-flow units suggests that some internal contacts within this volcanic episode are likely submarine unconformities. The persistent presence of iron formation at the top of the lower part of the Tisdale assemblage in Cleaver, McNeil, Argyle, Hincks, and Robertson Townships south of Timmins (Ayer et al., 2004a) also suggests the presence of a volcanic hiatus and a possible depositional gap. In the area south of Kirkland Lake, a substantial thickness of iron formation occurs near the top of the lower part of the Tisdale assemblage in Boston Township at the Adams mine. The section there consists of basal graphitic argillite grading upward to oxide-facies iron formation with intercalations of chert breccia all capped by flaser bedded sandstones (Fig. 9B) and some intercalations of chert breccia and iron formation conglomerate.

The upper part of the Tisdale assemblage, the "Marker Horizon" of Corfu and Noble (1992) is characterized by 2706 to 2704 Ma calc-alkaline felsic to intermediate volcanic rocks. They include amygdaloidal flows, heterolithic debris flows and volcaniclastic units. The Marker Horizon forms the core of three east-trending synclines on the west flank of the Watabeag batholith southeast of Timmins. The presence of an iron formation toward the top of the unit in that area indicates a possible sedimentary interface zone marking a volcanic hiatus of approximately 2 m.y. between the upper part of the Tisdale assemblage and the overlying lower part of the Blake River assemblage.

In the Kirkland Lake area on the north flank of the Spectacle Lake anticline is another example of a volcanic hiatus represented by a sedimentary interface zone between the Upper Tisdale and Blake River assemblages. Here, the upper part of the Tisdale assemblage volcanic rocks are overlain by reworked pyroclastic units above which are, in ascending order, 10 to 20 m of tuff, a chert-basalt conglomerate, a laminated chert, and pillowed flows of the lower Blake River assemblage (Roberts and Morris, 1982).

The upper part of the Tisdale assemblage also forms an east-trending unit north of the Porcupine-Destor fault deformation zone in contact with the 2723 to 2720 Ma Stoughton-Roquemaure assemblage. The ~15 m.y.-age gap represents a basal depositional gap in this region. The presence of the 2704 ± 5 Ma mafic to ultramafic Mann intrusive complex (C. T. Barrie, 1999, unpub. report: The Kidd-Munro Extension Project: Year 3 Report, Ontario Geological Survey) at the assemblage contact clearly indicates the contact is not tectonic and also suggests an original depositional gap at the lower contact.

Broadly correlative units to the east of Rouyn-Noranda just north of the Larder Lake-Cadillac fault zone include the Val-d'Or and Jacola Formations (Scott et al., 2002). Recent geochronology indicating an age 2706 ± 3 Ma from the Figuery Formation (David et al., 2007) further indicates the presence of units within this episode north of the Porcupine Destor fault in Québec. There is a lack of dated units between 2706 and 2704 Ma in the Rouyn-Noranda area in Québec, indicating a possible depositional gap of as much as 2 m.y.

2704 to 2695 Ma volcanic episode (Blake River assemblage)

The volcanic rocks deposited over this time interval have been divided in Ontario into the lower Blake River assemblage ranging from 2704 to 2701 Ma and an upper Blake River assemblage ranging from 2701 to 2696 Ma (Ayer et al., 2005). The lower Blake River represents new nomenclature for the former Kinojevis assemblage of Ayer et al. (2002a) in order to remove confusion with the 2718 ± 2 Ma (Zhang et al., 1993) Kinojévis Group in Québec, which correlates with the Stoughton-Roquemaure and the Kidd-Munro assemblage in Ontario. In Québec, tholeiitic basalts beneath the Blake River Group are assigned to the Hébécourt Formation to distinguish them from geochemically similar, but older, Kinojévis Group basalts situated north of the Porcupine-Destor fault (Goutier, 1997).

In Ontario, the lower Blake River assemblage occupies the north and south margins of the Blake River synclinorium and the west flank of the Nat River batholith in the Kamiskotia area where it underlies the Kidd-Munro assemblage and extends east of the Matagami River fault. In the former area, the assemblage consists of high Fe and high Mg basalts with minor felsic volcanic units and turbiditic metasediments. In the latter area tholeiitic basalts and minor rhyolite flows and pyroclastic units occur. The lower contact of this unit with the underlying Tisdale assemblage is locally deformed and does not include iron formation breccia where exposed east of Timmins (Péloquin et al., 2005).

South of the Larder Lake-Cadillac fault in the Val-d'Or region, the temporal equivalents of this episode are the Héva Formation (2702 ± 2 Ma: Scott et al., 2002), which rests concordantly on the Val-d'Or Formation and the Villebon Group (2703 ± 1 Ma: Moorhead et al., 2000b). In the Rouyn-Noranda camp, the homogeneous and continuous basalt units of the Hébécourt Formation are physically connected with and temporally equivalent to the lower Blake River Group in Ontario (Goutier, 1997; Lafrance et al., 2003).

The upper part of this Blake River episode represents a time span from 2702 to 2695 Ma and occurs in a number of areas: (1) the major unit is the Blake River Group which occurs in the core of the Blake River synclinorium extending eastward from Ontario into Québec; (2) an east-facing homoclinal succession on the east flank of the Nat River batholith in the Kamiskotia area; (3) the Skead Formation in the Kirkland Lake area consisting of calc-alkaline intermediate to felsic volcanic rocks with an age of 2701 Ma (Ayer et al., 2005) overlying the Stoughton-Roquemaure assemblage on the eastern and southern flanks of the Round Lake batholith; and 4) the Swayze Group in the central part of the Swayze greenstone belt.

Cherty exhalites such as the key tuffite (Kalogeropoulos and Scott, 1983; Fig. 9C) represent small-scale depositional gaps in the volcanic evolution of the Noranda Formation. New dates and mapping indicate that the Bousquet Formation (2699–2698 Ma: Lafrance et al., 2005; Mercier-Langevin et al., 2007a) rests directly on the 2704 to 2701 Ma Hébécourt Formation (Lafrance et al., 2003) and thus there is probably a temporal hiatus between the two units (though the radiometric age errors are problematic). The upper contact of the felsic pyroclastic rocks of the Bousquet Formation is marked by silicification and pyritization proceeding from the sharp upper contact with graded beds of wacke of the Cadillac Group downward on a scale of centimeters to a diffuse lower contact with less-altered pyroclastic rocks. This contact thus

represents a depositional gap (Mercier-Langevin et al., 2007a during which a condensed section was produced involving water-rock interaction and silica and pyrite replacement of the Bousquet Formation during a depositional hiatus of about 5 to 10 m.y.

At Kamiskotia, the basal contact of the upper part of the Blake River assemblage is cut out by the Kamiskotia Gabbroic Complex (Barrie, 1992). Hart (1984) divided the Kamiskotia rhyolites into a lower, primitive (FII of Lesher et al., 1986) and an overlying more evolved FIIIb type. Finamore (Hocker) et al. (2008) have identified an unconformity at the top of the FII rhyolite unit by virtue of the fact that a synvolcanic mafic intrusion cutting the upper part of the assemblage also cuts the lower part of the FIII unit.

The former Skead assemblage (Jackson and Fyon, 1991) rests upon rocks of the 2723 to 2720 Ma Stoughton-Roquemaure assemblage (Ayer et al., 2002a), representing a substantial depositional gap (see discussion of the 2723–2720 Ma volcanic episode).

The Swayze Group in the Swayze greenstone belt dated at 2695 ± 2 Ma (van Breemen et al., 2006) is correlated with the upper part of the Blake River Group and lies directly upon rocks of the 2705 ± 2 Ma Trailbreaker Group, again representing a depositional gap.

Sedimentary interface zones

The sedimentary interface zones of the Abitibi greenstone belt are 1- to 350-m-thick zones of chemical and minor clastic sedimentary rocks at the top, as well as within, the major volcanic sequences. They are dominated by oxide facies iron formation, with lesser sulfide facies iron formation, chert breccia units, chert, terrigenous heterolithic debris flows, and conglomerates, as detailed in Table 4. Sedimentary interface zones occur at the top of mafic to felsic volcanic cycles and at geochemical transitions in volcanic units of greenstone belts worldwide, for example, the Pilbara Supergroup of the Pilbara craton (Vearncombe et al., 1998; Hickman and Van Kranendonk, 2004; Van Kranendonk, 2006), the Belingwe greenstone belt, Zimbabwe craton (Bickle et al., 1994), the Barberton greenstone belt, Kaapvaal craton (Lowe et al., 1999), and the Red Lake greenstone belt of the western part of the Superior province (Sanborn-Barrie et al., 2001).

Sedimentary interface zone units commonly include mass-flow deposits at the stratigraphic base or intercalated within the sedimentary interface zone succession. At the interface between the Deloro and Tisdale assemblages, heterolithic, largely volcanic, ungraded, unbedded mass flows occur with the sedimentary interface zone iron formations (Table 3, locs. 2, 3, 5, 10, 11, and 12). A typical section of a sedimentary interface zone in the Abitibi greenstone belt is that developed along the Deloro-Tisdale assemblage contact south of Timmins (Table 3, loc. 5), which consists of a 23- to 34-m-thick unit with a basal 2- to 3-m-thin bedded chert, succeeded by 5 to 8 m of heterolithic breccia, 2 to 3 m of iron formation breccia, 4 to 5 m of wacke and conglomerate, with scour structures, and capped by 10 to 15 m of heterolithic breccia. Just to the north this sedimentary interface zone consists of three iron formation units, two oxide facies, and one sulfide facies (Houlé, 2006; Table 3, loc. 6). Around the Shaw dome south of Timmins, the Deloro-Tisdale sedimentary interface zone is represented by 10 to 60 m of iron formation and iron formation breccia and related chert units (Table 3, locs. 1–3).

Some sections, such as the Woman River antiform in the Swayze greenstone belt, consist of up to 350 m of iron formation, iron formation breccia, and minor clastic units, although some fold-related repetition is suggested (Heather, 2001). The unit consists of carbonatized felsic volcanic rocks overlain by one unit of carbonate facies iron formation with minor sulfide facies overlain by cherty material succeeded by two chert-oxide facies units (Table 3, loc. 8).

The bulk of the iron formation within sedimentary interface zone units is thin bedded (<5 cm), silt-grade wacke, felsic ash, or cherty turbidites grading up to oxide-rich upper units (Fig. 9D). Toward the top of some meter-scale sequences of iron formation (e.g., the top of the Deloro assemblage; Table 3, loc. 10), a 4.5-m thickness of silty iron formation turbidites (1–3 cm thick) has been replaced by fine chert. The replacement relationship is seen in the progressive obscuring of bed contacts and diminishing thickness of the iron-oxide–rich part of individual turbidite beds along strike. The chert replacement zone has a sharp upper contact and a diffuse lower contact. At this location, the iron formation includes clasts of iron formation breccia toward the base of one of the two depositional units. The minor clastic units of the sedimentary interface zones are thin-bedded argillites and rare wackes, conglomerates, and reworked volcanic rocks representing relatively distal facies. Possible similar units exist within the Tisdale and Blake River assemblages.

Chert breccia and iron formation conglomerate form significant parts of sedimentary interface zones. The chert breccia units form two types: crosscutting chert breccia cemented by iron carbonate which cut thinly laminated oxide-facies iron formation (Figs. 4A, 5), and strata-bound, stratiform units of chert fragments cemented by iron-oxide, biotite, and quartzofeldspathic material. The chert breccia units commonly overlie 3- to 5-m-thick unbedded, ungraded, coarse to fine heterolithic debris flows. The intercalation of the chert breccia units with undisturbed, finely laminated chert at the top of the Deloro assemblage (Table 3, loc. 5, Fig. 4D) suggests that the breccia units are synsedimentary and represent either episodic downslope movement of iron formation from its formative environment (Heather, 2001), products of hydrothermal brecciation (Van Kranendonk, 2006), and/or dewatering structures (Krapez et al., 2003). South of Timmins, chert breccia units at the top of the Deloro assemblage grade upward from undisturbed chert to banded iron formation through rhyolitic debris flows to chert breccia or conglomerate to laminated, graded wackes and pebble conglomerate with chert clasts cut by an erosional channel filled with a rhyolitic debris flow (Fig. 6). A similar vertical succession occurs in the Deloro assemblage west of Timmins, where a basal 5.5-m-thick tholeiitic pillow breccia is overlain by 4.5 m of banded iron formation (Fig. 4D), 4 m of chert breccia and/or conglomerate, capped by 7 m of carbonatized tholeiitic flows of the Kidd-Munro assemblage. The lateral transition from centimeter-scale bedded graphitic argillite overlying debris flows to meter-scale thickness of iron formation breccia suggests that the thicker zones of chert breccia are downslope from the zone of iron formation accumulation on the shelf and that the debris flows overlain by thin graphitic argillite

are the distal equivalent of the breccia zones. Chert breccia in the Shining Tree greenstone belt consists of several tens of meters of crosscutting chert breccia cemented by iron carbonate (Figs. 4A, 5).

Iron formation conglomerate consists of meter-scale thicknesses of unbedded, ungraded conglomerate containing clasts of oxide-facies iron formation, arkose, and shale. The conglomerates occur in the sedimentary interface zone above the 2734 to 2724, 2719 to 2711, and 2710 to 2704 Ma units. The conglomerates represent multiple generations of downslope movement of iron formation. Early, angular breccias of dismembered chert beds are incorporated into iron formation clasts (Fig. 4B), suggesting that the iron formation conglomerate units represent multiple episodes of resedimentation of partially to wholly consolidated banded iron formation (e.g., Heather, 2001; Pickard et al., 2003).

Whereas mass flows can be typical of the waning phases of felsic volcanism (McPhie et al., 1993), the above described vertical changes from volcaniclastic debris flows to iron formation breccia and/or conglomerate and the laterally extensive occurrence of these units in the sedimentary interface zone at the tops of stratigraphic units indicate that they are related to postvolcanism sedimentary processes.

Iron formation units within the sedimentary interface zones of the Abitibi greenstone belt generally represent a variety of precursor lithologic units, including felsic tuff, silt, wacke, and chert with replacement by iron carbonates, oxides, sulfides, and silicates. There is a tendency for stratigraphy at the Deloro sedimentary interface zone to contain thin basal sulfidic argillite succeeded by a mixture of oxide and silicate facies. The basal unit on the west flank of the Kenogamissi batholith (Table 3, loc. 10) has an extensive 3- to 13-m-thick bedded carbonate facies iron formation. However the most common mode of occurrence of carbonate facies iron formation is as hydrothermal breccias (Figs. 4A, 5). The stratigraphic position of banded iron formation and chert breccia units at or near the tops of assemblages, the chert-rich tops of iron formation units, and precompaction origin of the chert clearly indicate they represent chert development largely but not exclusively during diagenesis. The associated debris flows represent downslope movement of coarse clastic units from the site of original deposition to a more distal environment in which they are intercalated with thin-bedded iron formation turbidites in a distal setting representing bypass sedimentation (cf. Krapez et al., 2003). The synsedimentary timing of sedimentary interface zone units (based on fluidization textures) and syndiagenesis timing of chert replacement based on contrasts in thickness of laminations within and beyond chert nodules (based on the criteria of Krapez et al., 2003) and debris-flow depositional mechanism suggest that the debris flows and associated chert breccia and iron formation conglomerate units are time equivalents of upslope iron formation units. A full range of depositional settings may be present from relatively distal settings with thinly laminated ash beds and thinly laminated relict turbidite beds to the flaser-bedded sandstones laterally equivalent to the iron formation at the Adams mine, indicative of a tidal or shelf environment (Fig. 9B).

Graphitic argillite units are centimeter- to meter-scale thicknesses of graphitic argillite, commonly with framboidal pyrite, which display thin, A-E laminations typical of distal turbidites and contain very little terrigenous, quartzo-feldspathic material. They occur at geochemical discontinuities in volcanic stratigraphy (Table 4) and are interpreted to represent very low rates of sedimentation in a basinal setting.

In summary, there are four types of sedimentary interface zone (Table 4): (1) units with pronounced lateral thickness variation from several tens of meters of carbonate-facies iron formation and/or iron formation breccia and/or conglomerate to a few meters of oxide-facies iron formation that are interpreted herein to represent condensed sections; (2) oxide-facies iron formation and felsic tuff with chert replacement of upper parts of depositional units, which is interpreted as possibly representing diagenetic replacement; (3) graphitic argillite units intercalated with volcanic rocks at geochemical transitions; and (4) chert breccia and/or iron formation conglomerate units. Chert breccia and/or conglomerate units are developed in association with chert and iron formation at the top of three episodes (Table 4). In these instances, evidence has been presented that these sections represent condensed sections. For example, a unit of iron formation clast-bearing conglomerate, about 6 m thick with a <1-m thickness of chert breccia and/or conglomerate, occurs at the top of the 2720 Ma Dussieux Formation in the Matagami area (Goutier, 2006), suggesting that the top of the 2723 to 2720 Ma episode may represent a condensed section.

Thus, sedimentary interface zone capping major volcanic successions of the Abitibi greenstone belt provide some evidence for the existence of depositional gaps, condensed sections typified by iron formation and chert breccia and/or conglomerate, sections with low sedimentation rates accompanied by hydrothermal circulation, and deposition of chert breccias and sections with no sedimentation and early diagenetic replacement by chert. Recent sequence stratigraphic models (Miall, 1994; Catuneanu, 2003) equate condensed sections, low sedimentation rates, and periods of no sedimentation with so-called correlative conformities. Mitchum (1977) defined a correlative conformity as the seaward continuation of an unconformity surface nearer shore. The surface is marked by parallel strata in the basin. We therefore conclude that the top of the major volcanic episodes may represent correlative conformities. However, as we lack the nearshore equivalents with mapped unconformities, we suggest use of the term submarine disconformity. The presence of similar features within the lower Tisdale assemblage (see discussion of the 2710–2704 Ma volcanic episode above) and within the upper Blake River Group in the Rouyn-Noranda area (see 2704–2695 Ma episode above) suggests that submarine unconformities in some instances exist at the formation and member levels as well.

Successor Basins

Two types of successor basins are present in the Abitibi greenstone belt: early turbidite-dominated (Porcupine assemblage; Ayer et al., 2002a) laterally extensive basins succeeded by areally more restricted alluvial-fluvial or Timiskaming-style (Thurston and Chivers, 1990) basins. The Porcupine-type sedimentary basins form wacke-dominated, kilometer-scale sequences unconformably overlying the metavolcanic and sedimentary rocks of the Abitibi greenstone belt and are transitional into much more extensive basins such as the

wacke-dominated Quetico subprovince to the north and the Pontiac subprovince to the south. In the southern Abitibi greenstone belt, the Porcupine-type successor basin is 2690 to 2685 Ma in age based on the crystallization age of the basal Krist volcanic unit and detrital zircons in the overlying wackes in the Timmins area (Ayer et al., 2005). The basal contact of this assemblage in the Timmins area is a low-angle unconformity (Bateman et al., 2008). However, in the Shining Tree area to the south, the contact between the volcanic rocks and the Natal Group wackes of the Porcupine assemblage varies from unconformable to paraconformable (Ayer et al., 1999). In the Timmins area, the contact typically lacks regoliths or paleosol (Ayer et al., 2002a) and is therefore interpreted as submarine. Direct equivalents of the Porcupine assemblage in Québec, south of the Porcupine-Destor fault in the Rouyn-Noranda area, include the Kewagama Group (including the Caste Formation) and the Cadillac Group, both of which lie paraconformably on the volcanic rocks of the Blake River Group (Goutier, 1997; Lafrance et al., 2003; Mercier-Langevin et al., 2007b).

The remnants of the early successor basin within the Abitibi greenstone belt were previously separated into two distinct cycles of basin development in part as a function of the division of the Abitibi greenstone belt into northern and southern parts (Chown et al., 1992; Mueller and Donaldson, 1992b). New U-Pb zircon ages show that the various early turbiditic basins in the northern and southern Abitibi greenstone belt (e.g., Porcupine assemblage and Taibi Group) contain both young and old detrital zircons (2685, 2700, >2750, and in some cases >2800 Ma: Pilote et al., 1999; Ayer et al., 2002a, 2007; Davis, 2002; Lafrance et al., 2005).

The Timiskaming assemblage of dominantly sedimentary rocks represents the youngest supracrustal unit in the Abitibi greenstone belt. The rocks include alluvial-fluvial conglomerates, sandstones, turbidites, and alkalic to calc-alkaline volcanic rocks that unconformably overlie metavolcanic rocks and/or Porcupine assemblage units with numerous examples of erosional discordance and development of paleosols (Jackson and Fyon, 1991; Mueller, 1991; Chown et al., 1992). At South Porcupine, east of Timmins, the lower contact of the Timiskaming assemblage is a sharp erosional angular unconformity with the underlying Porcupine assemblage, with no evidence of subaerial weathering (Born, 1995). In the Timmins, Kirkland Lake, and Larder Lake area, the Timiskaming assemblage ranges in age from 2677 to 2670 Ma, based on U-Pb detrital and magmatic zircon age determinations (Corfu et al., 1991; Ayer et al., 2005). Conglomerates and alkaline volcanic rocks in the northern Abitibi greenstone belt, such as the Matagami Group and the Haüy Formation, were previously assigned to older episodes between 2715 to 2705 Ma (Mueller and Donaldson, 1992b). However, new geochronological data clearly indicate that they are younger than these ages. This includes detrital zircons with an age of 2701 ± 1 Ma in a conglomerate of the Matagami Group (Goutier et al., 2004) and 2692 ± 3 Ma in a conglomerate of the Haüy Formation (David et al., 2007). Moreover, an age of 2688 ± 1 Ma for the Berthiaume Syenite (Davis et al., 2005) and of 2691 Ma for carbonatite from the Lac Shortt mine (Joanisse, 1994) indicate alkaline magmatism was at least 10 m.y. older than in the southern Abitibi greenstone belt. This suggests alkaline magmatism, accompanied by shallow water sedimentation and emergent continental masses started earlier in the northern Abitibi greenstone belt, representing temporal variation differing from the models of Chown et al. (1992), Mueller and Donaldson (1992b), and Daigneault et al. (2004).

New Geochronological Data Supporting Autochthonous Evolution

Geochronologic evidence provides critical support for autochthonous construction of the Abitibi greenstone belt (details of geochronologic methods are provided in Ayer et al. (2005) and description of samples and analytical data are provided in App. 2). The evidence includes ages for feeder dikes and large mafic to ultramafic intrusions. Mafic feeder dikes cutting older stratigraphic units in the southern Abitibi greenstone belt match the age of overlying stratigraphic units (see also van Breemen et al., 2006). Specifically, the Muskasenda gabbro has numerous east-trending, quartz-bearing tholeiitic leucogabbro dikes, dated at 2705.7 ± 4 Ma (Fig. 10A), which cut the 2730 to 2724 Ma Deloro assemblage, demonstrating that the Deloro assemblage was in place during ~2710 Ma Tisdale volcanism, a relationship reminiscent of the synvolcanic gabbro at Woman Lake in the Confederation Lake greenstone belt (Rogers, 2000). The 2719 to 2711 Ma Kidd-Munro assemblage is cut by numerous Tisdale-aged mafic-ultramafic intrusions, including the 2712.4 ± 1.1 Ma Ghost Range sill (Fig. 10B) and the 2706.8 ± 1.2 Ma Centre Hill intrusion (Fig. 10C), indicating that the Kidd-Munro assemblage was in place at the time of Tisdale volcanism.

Rates of volcanic accumulation

The tectonic evolution of the Abitibi greenstone belt represents a mix of arc and plume magmatism (e.g., Ayer et al., 2002a; Sproule et al., 2002; Wyman et al., 2002). Based on the estimates of magma production in arc and plume systems (Table 5), we assume that, for example, the 2734 to 2724 Ma episode has a maximum volume of about 750,000 km^3 constrained by a 5-km thickness (Ayer et al., 2002a), a strike length of ~600 km, and a width of ~250 km (Fig. 2). The assumed lateral extent of volcanic units of this age is further supported by the presence of numerous zircon xenocrysts of this age within younger episodes. Using the various rates of influx of mafic magma of Shaw (1985; Table 5) yields an accumulation time for the 2734 to 2724 Ma episode of 7500 to 75,000 yr, and using the rate of magma influx in plume systems (0.15–8.2 km/yr: Condie, 2001) yields accumulation times ranging from ~100,000 yr to 5 m.y. Using the estimate of 2 to 3 km^3/yr (total magma production) per km of arc length (Scholl and von Hueme, 2004) for a 600-km-long arc yields 1,800 km^3/yr and an accumulation time of about 4.1 × 10^3 yr. However, stratigraphy within Abitibi greenstone belt episodes accumulated over a mean duration of 6.8 m.y. based on over 450 U-Pb zircon ages. Given the assumption that rates of igneous processes used here are based on the cooler Phanerozoic Earth and hence the rates of magma influx in the Phanerozoic are minima, the volcanic units of the Abitibi greenstone belt probably accumulated over even shorter intervals of time. The disparity described above between the duration of volcanic episodes based on U-Pb ages and volcanic accumulation rates based on the above simplistic modeling

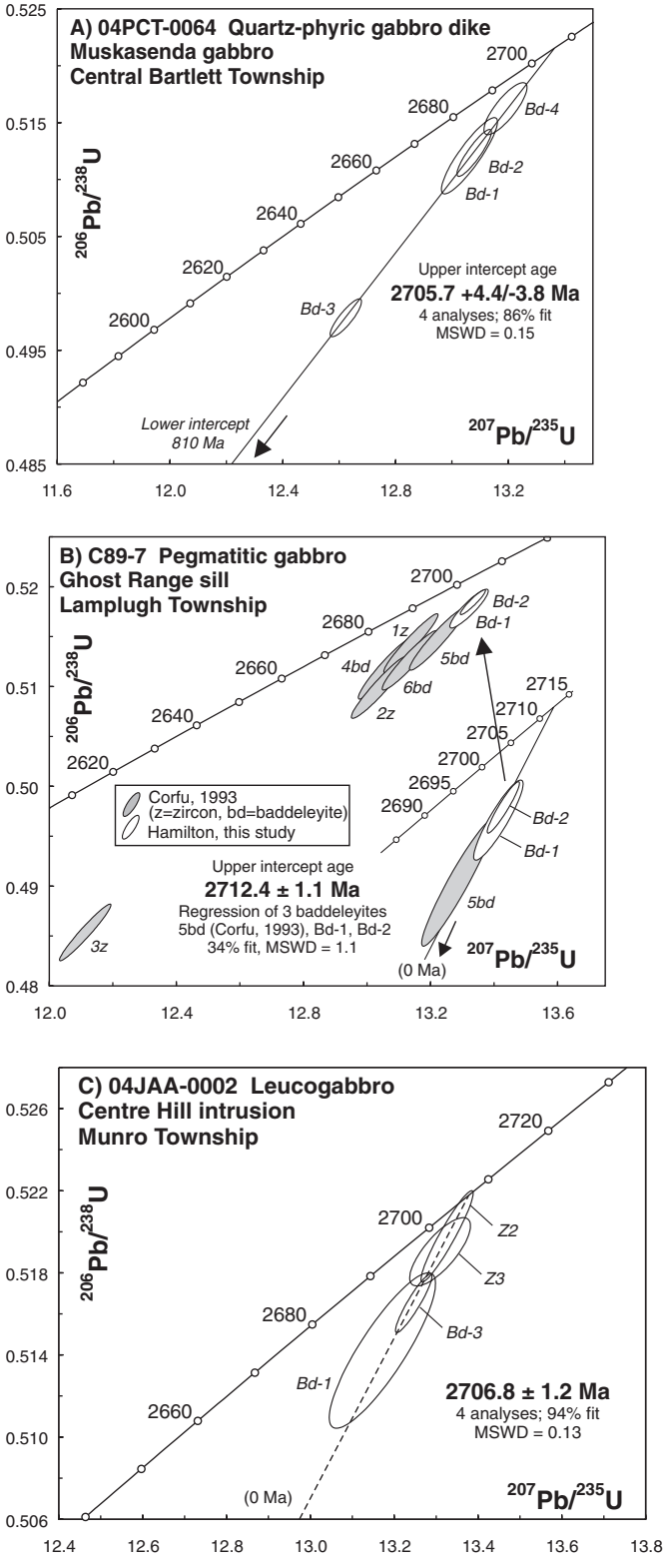

FIG. 10. Concordia diagrams for U-Pb zircon ages, demonstrating autochthonous nature of the Abitibi greenstone belt. A. Concordia diagram for U-Pb zircon age on Muskasenda gabbro dikes cutting the Deloro assemblage south of Timmins. B. Concordia diagram for U-Pb zircon age of the Ghost Range sill in Lamplugh Township. C. Concordia diagram for U-Pb zircon age of the Centre Hill intrusion in Munro Township.

TABLE 5. Estimated Rates of Magma Production in the Modern Earth

Rate of magma production	Type of system	Reference
0.01–1 km^3/yr	Estimated influx rate for mafic magma into the base of silicic ash-flow–producing systems	Shaw (1985)
5 km^3/year/km of arc length	Overall estimate of the total production rate for several arc systems	Scholl and von Hueme (2004)
0.15–8.2 km^3/year	Overall rate of volcanic production for plume systems	Condie (2001)

may indicate that the sedimentary interface zone between major volcanic units represents the apparent time gaps.

The sole geochronological test of this hypothesis is in the Swayze greenstone belt (Fig. 2) where rhyolites immediately underlying and overlying the lower of two iron formation in the Marion Group have ages indicating that the lower sedimentary interface zone required 4 to 10 m.y. for deposition (van Breemen et al., 2006). Therefore, it is quite probable that chemical and clastic sedimentary units between volcanic units represent substantial time intervals.

Discussion and Interpretations

Significance of the sedimentary interface zone and depositional gaps

Three alternative explanations for the sedimentary interface zones have been suggested above.

Condensed section model: In modern environments "condensed sections," representing very low rates of sedimentation, develop downdip from thicker, near-shore sections in a shelf environment. The condensed sections develop during sea-level rise when newly developed estuaries trap clastic sediment, yielding very low volumes in the basin (Catuneanu, 2003). The central Pacific Ocean represents such a deep marine environment with a very low sedimentation rate through lack of terrigenous input and very low rates of infall of dust with a sedimentation rate of 0.3 to 2 mm/ky (Gleason et al., 2004). Condensed sections should be traceable to thicker sections closer to source.

Hydrothermal circulation model: During a hiatus in volcanism, hydrothermal circulation produces chert breccia units crosscutting volcanic stratigraphy (Van Kranendonk, 2006), and meter-scale metalliferous stratiform cherts and/or iron formation proximal to VMS deposits (Kalogeropoulos and Scott, 1983; Van Kranendonk, 2006).

Rock-water exchange model: Very low to negligible rates of sedimentation on a shelf or in the abyssal environment result in production of hard ground, manganese nodules, glauconite sand, sulfide zones, and/or chert replacement of existing sediment by water-rock interaction (Krapez et al., 2003).

The important features of the sedimentary interface zones in the Abitibi greenstone belt are summarized in Table 4. We suggest that there are examples of all three models listed above for deposition of sedimentary rocks in sedimentary interface zones in the Abitibi greenstone belt.

Where the sedimentary interface zones represent condensed sections (model 1), we observe lateral transitions from relatively proximal, near-shore, thicker sections, to relatively distal environments with attendant thinning of the section. Table 3 demonstrates that the thickness of the sedimentary interface zone varies by one to two orders of magnitude at the top of the 2734 to 2724, 2723 to 2720, 2719 to 2711, 2710 to 2704, and 2704 to 2695 Ma volcanic episodes. At the top of the 2734 to 2724 and 2719 to 2711 Ma volcanic episodes there is commonly a lateral transition from relatively proximal zones with bedded, thinly laminated iron formation and crosscutting chert-iron carbonate breccia zones (carbonate facies iron formation) to well stratified, oxide-facies iron formation and stratiform chert breccia units at the top (based on a comparison of stratigraphy in the northern Swayze area (Ayer, 1995) and Carscallen Township area (Hall and Smith, 2002)). At the top of the 2734 to 2724 Ma succession in the Shaw dome south of Timmins, there is a lateral transition from multiple chert-iron formation units over 200 to 300 m thick on the northeast part of the structure to thinner sections (<100 m) with fewer iron formation units on the northwest side of the structure (Hall and Houlé, 2003; Houlé and Guilmette, 2004). Thus, the variation in thickness of the sedimentary interface zone indicates that many of the zones represent condensed sections.

In the Abitibi greenstone belt, the hydrothermal circulation model (model 2) is represented by crosscutting carbonate-matrix chert breccia dikes in the sedimentary interface zone in the Swayze greenstone belt, which transition to stratiform, laterally extensive chert breccia units. South of Timmins, we observed a transition from slump-folded, bedded chert to overlying stratiform chert breccia, suggesting development of the breccia units by fluid overpressure (see also Krapez et al., 2003). This implies regular arrival of new sediment to prompt dewatering events. The crosscutting chert breccia dikes, such as the one capping the 2734 to 2724 Ma volcanic episode in the Shining Tree greenstone belt (Figs. 4A, 5), is interpreted to represent a deposit resulting from the hydrothermal circulation (model 2), as do the various "exhalite" units of metalliferous chert in the Rouyn-Noranda camp (Kalegeropoulous and Scott, 1983; Gibson and Gamble, 2000).

The chert breccia units within the sedimentary interface zone could be produced by dewatering, possibly related to downslope movement of proximal chert-rich sedimentary units or faulting (e.g., the gravity sliding of overlying volcanic units). Figure 9E shows chert breccia overlain by a wacke and/or chert unit, demonstrating the synsedimentary nature of the chert breccia units capping the 2734 to 2724 Ma volcanic episode south of Timmins. We discount the possibility of production of these breccias during tectonism and/or thrusting because (1) at the scale of the Abitibi greenstone belt, stratigraphy is uniformly upward facing and upward younging (Heather, 2001; Ayer et al., 2005; Goutier and Melançon, 2007), there is very little out-of-sequence stratigraphy and none in the region of the chert breccias (Ayer et al., 2005; Goutier and Melançon, 2007); (2) the chert breccias do not exhibit mylonitic textures, there are no pronounced gradients in fragment size or morphology typical of cataclastic breccias (cf. Higgins, 1971); (3) chert breccia units, while continuous over a few kilometers, do not persist over the tens to hundreds of kilometers length separating volcanic units of differing ages; and (4) we observe a few transitions from bedded chert to chert breccia at culminations of synsedimentary folds suggestive of dewatering.

Model 3 is based on modern ocean sediments in areas removed from terrigenous input, which are characterized by very slow sedimentation of mixtures of eolian dust and hydrothermal components (Gleason et al., 2004, and references therein). Graphitic argillite units ranging from a few centimeters at the top of the 2734 to 2724 Ma volcanic episode in Bartlett Township south of Timmins (Pyke, 1978) to centimetre- to meter-scale units in the upper Kidd-Munro assemblage in Jamieson Township (Hathway et al., 2005) are possible analogues based on the presence of pyrite horizons and graphite-rich beds, both indicative of extended water-rock interaction (Van Wagoner et al., 1990).

Extremely low rates of sedimentation result in exposure of sediment to processes of rock-water interaction. This is exemplified by chert horizons above heterolithic felsic debris flows (Tisdale assemblage, south of Timmins; Bright, 1984), thin-bedded iron formation turbidites at the top of the Kidd-Munro assemblage (Carscallen Township, west of Timmins; Hall and Smith, 2002), and felsic tuff at the top of the Tisdale assemblage in Gauthier Township. (C. Page, Queenston Mining Inc., pers. commun.). In each case, the chert unit has a sharp upper contact and a diffuse lower contact (e.g., Figs. 4D, 9A). Alternative hypotheses for development of this style of chert replacement include water-rock interaction at low temperature in which silica-saturated sea water replaces the rock unit from the top down (e.g., Siever, 1992; Krapez et al., 2003); and water-rock interaction in which sea water rich in silica and metals derived from hydrothermal circulation through subjacent volcanic rocks replaces existing rock units (Franklin et al., 2005).

Depositional environment and origin of the sedimentary interface zones

To fully understand the sedimentary interface zones, the depositional gaps and their connection to mineralization, it is important to understand the paleoenvironmental setting for the sedimentary interface zone. Recent syntheses (Simonson and Hassler, 1996; Krapez et al., 2003; Pickard et al., 2003; Clout and Simonson, 2005; van den Boorn et al., 2007) make the following points about the genesis of Archean iron formation: (1) iron formation is made up of thinly laminated siliciclastic or siliciclastic-volcaniclastic rocks, mudstones and/or wackes, and variably reworked bedded ash; (2) the iron is derived from hydrothermal alteration of volcanic rocks; and (3) intercalated cherts represent either silica replacement of precursor sedimentary and/or volcanic components commonly during diagenesis in a proximal setting or direct chemical precipitation of chert on the sea floor or in a hydrothermal conduit in a more distal setting. These authors appeal to precipitation of the iron-rich sediment during a sea-level highstand, which allowed Fe-rich, anoxic bottom water to have access to the shelf where the iron-rich gels and muds were initially deposited, followed by resedimentation. The replacement and/or diagenetic origin of the iron-bearing minerals after original iron oxyhydroxides (Krapez et al., 2003; Clout and Simonson, 2005) and of chert-rich bands renders identification of primary sedimentary structures, and hence the nature of the depositional environment, difficult.

Sparse sedimentologic data indicate that Algoma-type iron formation within greenstone belts of the Superior province is deposited in a variety of settings ranging from shallow-water platforms (Wilks and Nisbet, 1988; Hofmann et al., 1991; Hofmann and Masson, 1994) to mafic plain or starved basins (Trowell, 1986). The "deep water" iron formation of Kimberly (1978), which is broadly comparable to the Hamersley iron formation and consists of fans of thin-bedded carbonate and siliciclastic muddy turbidites overlain by iron formation deposited on a basin floor or in the deep sea, also can represent condensed sections but these are not found in the Abitibi (Krapez et al., 2003; Pickard et al., 2003). Primary structures constraining the depositional environment of Abitibi greenstone belt sedimentary interface zone iron formations are listed in Table 6.

Iron formations within the sedimentary interface zone of the Abitibi greenstone belt have some elements in common with the Hamersley iron formation: (topdown silicification of depositional units, the presence of diagenetic chert, replacement of bed contacts by chert and the presence of conglomerates and reworked ash beds interpreted in terms of the ubiquitous nature and timing of the silicification, extensive rock-water interaction, and the existence of condensed sections). However, the lack of shaley units intercalated with Abitibi greenstone belt sedimentary interface zone and the presence of conglomeratic interbeds both suggest that Abitibi greenstone belt sedimentary interface zone units do not represent a deep basin floor like the Hamersley iron formations. Rather, the sparse primary structure data (Table 6) suggest that some Abitibi greenstone belt sedimentary interface zone iron formations may represent a somewhat shallower depositional setting.

The following is evidence for a basinal setting for the sedimentary interface zones of the Abitibi greenstone belt: (1) the iron formation units are marine sediments with rare associated terrigenous sedimentary rocks; (2) the iron formation is characterized by thin-bedded turbidites, suggestive of a relatively distal setting; and (3) the presence of iron formation conglomerates in most of the sedimentary interface zones suggest multiple cycles of downslope movement of previously deposited iron formation. The sedimentary interface zone units are not interpreted as deformed sedimentary rocks produced by tectonic sliding based on the consistent upward facing and younging, the lack of cataclastic textures, and the lack of gradations in fragment sizes typical of such an origin.

Stratigraphic implications

To develop nomenclature for the sedimentary interface zones in the Abitibi greenstone belt, we review some aspects of stratigraphic terminology. Workers in sequence stratigraphy define an unconformity as "a surface separating younger from older strata, along which there is evidence of subaerial erosional truncation (and, in some cases, correlative submarine erosion) or subaerial exposure, with a significant hiatus indicated" or downdip correlative conformities marking a hiatus in sedimentation (Vail et al., 1977). Related terms include disconformity, paraconformity, and the notion of the "condensed section" defined as "a thin marine stratigraphic interval characterized by very slow depositional rates (<1–10 mm/yr; Vail et al., 1984). Condensed sections commonly consist of hemipelagic and pelagic sediments, starved of terrigenous materials, deposited on the middle to outer shelf, slope, and basin floor during a period of maximum relative sea level rise and maximum transgression of the shoreline (Loutit et al., 1988).

Shanmugam (1988) summarized submarine unconformities as being typified by the presence of debris flows, slump deposits, and hemipelagic mudstones, as well as horizons produced by extended exposure of a given horizon to seawater, producing manganese nodules, glauconitic minerals, sulfide, and dolomitization fronts. Siever (1992) drew attention to development of chert during extended periods of rock-water interaction given the greater Si content of Precambrian oceans.

In general, the major parts of some sedimentary sections represent long intervals of nondeposition (Miall, 1990, 1994), with short intervals of sediment deposition. However, the calculation of the rates of accumulation of volcanic rocks described above, combined with the geochronological evidence for gaps between major volcanic episodes, leaves little doubt that the sedimentary interface zone of the Abitibi greenstone belt represents depositional gaps. The issue is whether the depositional gaps are submarine unconformities (i.e., periods of nondeposition) or that they represent low rates of sedimentation and potential condensed sections. Below, we describe the features of the sedimentary interface zone that bear upon their origin and metallogenic importance.

Mechanism for development of sedimentary interface zones in the Abitibi greenstone belt

The evidence presented in this paper for orderly development of vertically stacked or laterally accumulated stratigraphy

Table 6. Constraints on Depositional Environment of Iron Formation in the Abitibi Greenstone Belt

Volcanic episode	Primary structures	Interpreted depositional environment	Reference
2704–2695 Ma	Thin-bedded BIF	?	
2710–2704 Ma	Flaser bedded wackes	Tidal	This study
2719–2711 Ma	Thin-bedded argillite and thinly laminated iron formation	Deep water?	Barrie (2005); Hathway et al. (2005)
2723–2720 Ma	Nil reported	?	
2734–2725 Ma	Stromatolites	Shallow water	Hofmann et al. (1991); Hofmann and Masson (1994)
2750–2735 Ma	Crosscutting carbonate matrix chert breccia	Hydrothermal breccia cutting thinly laminated BIF	This study

over close to 100 m.y. of Abitibi greenstone belt history is clear. However, stratigraphic sections and geochronological data on the margins of the Kenogamissi, Round Lake, and Nat River batholiths at the west end of the southern Abitibi greenstone belt reveal substantial depositional gaps between major volcanic episodes (Fig. 3) marked by chemical and minor clastic sedimentary rocks. The most prominent depositional gap is above the 2734 to 2724 Ma Deloro assemblage and likely key to understanding the development of a laterally extensive hiatus in volcanism and related submarine correlative conformities and unconformities. The 2734 to 2724 Ma episode is characterized by dominantly calc-alkaline magmatism (Chown et al., 2002; Becker and Benn, 2003; Peschler et al., 2004; Ketchum et al., 2008) extending the full length of the Abitibi greenstone belt, which is in contrast to preceding and later volcanic episodes representing magmas derived from arc-plume interaction (Ayer et al., 2002a; Wyman et al., 2002). This 2734 to 2724 Ma calc-alkaline magmatism is associated with extensive tonalite-trondhjemite-granodiorite (TTG) plutonism that is more voluminous than in other intervals of magmatism in the Abitibi greenstone belt. The TTG plutons were emplaced diapirically and produced related tilting of strata (Becker and Benn, 2003). Evidence for tilting of >2724 Ma strata is seen in the presence of stratigraphic cutouts of the Deloro assemblage along the flanks of the Shaw dome and in the region south of Timmins, where successive iron formation markers in the Deloro assemblage are cut out in Bartlett and McArthur Townships (Fig. 7; Pyke, 1978; Ayer et al., 2004a) by synvolcanic faulting of unknown character. The interpretation of tilting is also supported by erosional features in the stratigraphy of this sedimentary interface zone in the area shown in Figure 6. Contributing to development of the depositional gap, along with diapirism-related tilting of strata, is the off-lapping distribution of younger units (e.g., the 2723–2720, 2719–2711, and the 2710–2704 Ma volcanic episodes, Fig. 2). Similar (quite major in places) tilting of greenstone belt strata is seen in the Pilbara craton (Van Kranendonk et al., 2002, 2004; Van Kranendonk, 2006). Therefore, we conclude that the top of the 2734 to 2724 Ma volcanic episode represents an angular unconformity south of Timmins in English and Bartlett Townships.

The 2734 to 2724 Ma volcanic episode was followed by development of the Stoughton-Roquemaure assemblage and the equivalent groups of the 2723 to 2720 Ma episode in the eastern and northern parts of the Abitibi greenstone belt, and by the Kidd-Munro assemblage and the equivalent groups of the 2719 to 2711 Ma episode in the southern and western Abitibi greenstone belt. The lack of abundant 2723 to 2720 Ma activity in the western and southern parts of the belt produced a hiatus in volcanism during which a laterally extensive series of correlative conformities or submarine unconformities developed.

Sedimentary interface zones form the upper part of all remaining volcanic units of the Abitibi greenstone belt, containing condensed sections, evidence for water-rock interaction in the form of chert replacement of the upper part of iron formation units, and unusual iron formation breccias which are an essential part of the sedimentary interface zone capping the 2734 to 2724 Ma volcanic episode. However, the other volcanic units do not display the off-lapping relationship associated with the 2734 to 2724 Ma volcanic episode, nor do the other episodes have the same abundance of coeval TTG magmatism, save for the ca. 2715 Ma TTG magmas of the Round Lake batholith (Ketchum et al., 2008). On the basis of the similar rock-type associations, the evidence of chert replacement of iron formation and other units and the presence of condensed sections, we believe that the sedimentary interface zones above the other major volcanic episodes in the Abitibi greenstone belt represent correlative conformities and related submarine unconformities.

Our model for the development of correlative conformities or submarine unconformities and related condensed sections in the Abitibi greenstone belt is illustrated in Figure 11. The build-up of stratigraphic thickness during an episode of volcanism, assuming no synvolcanic subsidence and given the lack of sector collapse features, would result in relatively shallow water deposition in the upper felsic parts of the volcanic sequences (Fig. 11A). There are no unequivocal indicators of a shallow depositional environment for the felsic volcanic units capping the 2734 to 2724 Ma volcanic episode. However, the scattered presence of stromatolite-bearing carbonate metasediments capping the felsic volcanic rocks (Hofmann et al., 1991; Hofmann and Masson 1994) is likely of significance, as most but not all stromatolites are interpreted to have developed in relatively shallow water (e.g., Allwood et al., 2007).

The succeeding chemical sediments represent a sea-level highstand (Fig. 11B) based on the depositional model for iron formation of Simonson and Hassler (1996). We have described above the evidence for at least some of the chert deposited at this time being diagenetic in origin, thereby explaining the development of condensed sections in iron formation during volcanic hiatuses. Further evidence of a possible sea-level highstand is the off-lapping nature of younger volcanic episodes in the Abitibi greenstone belt (Fig. 2), which suggests that in the western part of the Deloro assemblage this unit was exposed for several million years. During this period of exposure, extensive water-rock interaction associated with the development of a condensed section model (Loutit et al., 1988; Van Wagoner et al., 1988) resulted in silicification of preexisting units and production of iron formation. The evidence for such an origin in the 2734 to 2724 Ma stratigraphic interval of the Abitibi greenstone belt is the top-down silicification of units resulting in the development of substantial thicknesses of iron formation, a feature which is common with numerous iron formation units worldwide (van den Boorn et al., 2007).

Speculation on paleotopography and tectonics

The Superior province has been viewed in terms of allochthonous processes involved in final assembly at the scale of the orogen for some time (Langford and Jensen, 1976; Card, 1990; Percival, 2007). However, within subprovinces and domains, individual greenstone belts, including the Abitibi greenstone belt, developed autochthonously (e.g., Ayer et al., 2002a; Thurston, 2002). In the preceding sections, we demonstrated that the stratigraphic and lithotectonic units of the Abitibi greenstone belt have a somewhat irregular distribution brought about by poor preservation of early units assimilated during intrusion of synvolcanic batholiths and that

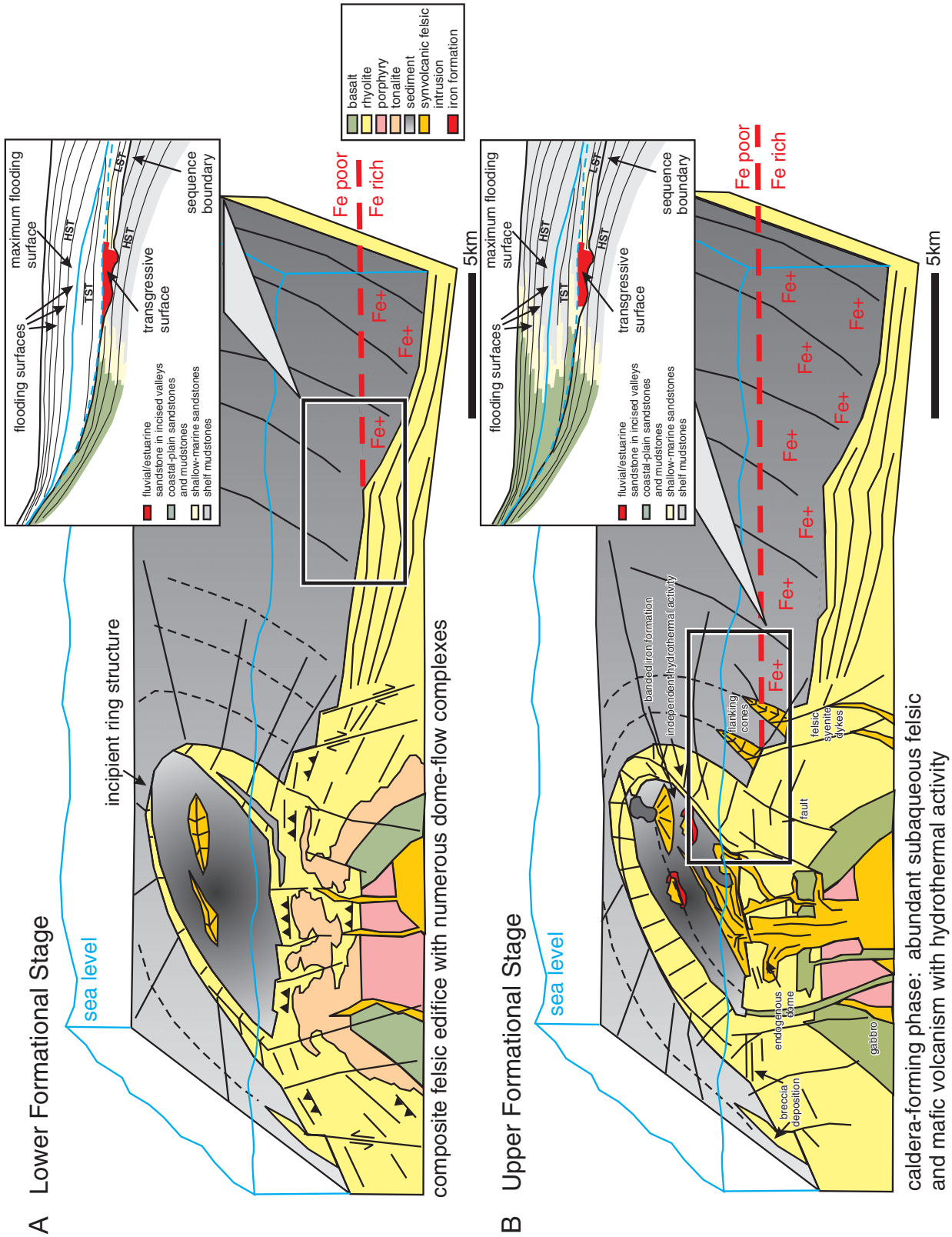

FIG. 11. Schematic diagram illustrating development of submarine unconformities and correlative conformities. Modified after Mueller and Mortensen (2002). A. Conditions during a low stand of sea level where there is free access of clastic material to the basin and no deposition of iron formation in that Fe-rich bottom water does not have access to the depositional area. B. Conditions during a high stand of sea level where Fe-rich bottom water has access to a shelf where iron formation is deposited.

later units define batholith-centered crustal sections and complex off-lapping patterns. Important aspects of these patterns for understanding the paleogeography of the belt are (1) a >2750 Ma volcanic episode preserved as fragments on the northeastern and southwestern extremities of the belt (Fig. 2); (2) a 2750 to 2735 Ma episode found as remnants on the margins of the Mistaouac, Round Lake, Kenogamissi, and Ramsey Algoma batholiths; and (3) a 2734 to 2724 Ma volcanic episode, which is more widespread, occurring on the margins of batholiths in the western Abitibi greenstone belt and forming extensive units in the northern Abitibi greenstone belt. The 2723 to 2720 Ma volcanic episode represents the most areally extensive volcanic unit and was erupted over a short time period, concentrated in the northern parts of the Abitibi greenstone belt. The 2719 to 2711 Ma volcanic episode is concentrated in the central part of the Abitibi greenstone belt, extending from the eastern to the western margin. The 2710 to 2704 Ma volcanic episode is concentrated on the southern flank of the Abitibi greenstone belt. The 2704 to 2695 Ma volcanic episode is concentrated in the Rouyn-Noranda camp and in the Kamiskotia area to the west of Timmins. We note that there is no simple north-to-south younging (such as observed on the south margin of the North Caribou terrane: Williams et al., 1992) of the ages of volcanism that might be expected in an allochthonous origin, but the beginning of sedimentation of successor basins may have started up to 10 m.y. earlier for the Timiskaming episode in the north part of the Abitibi greenstone belt.

The presence of the central syncline in the southern Abitibi greenstone belt, the younging of strata with increasing distance from batholiths throughout the Abitibi greenstone belt (Fig. 2), as well as the lack of large-scale thrusting in surface mapping results and seismic images (Snyder et al., 2008) leads to the conclusion that the relationships documented above are predominantly depositional features representing primary architecture.

Exploration Implications

The distribution of VMS mineralization in all major units of the Abitibi greenstone belt indirectly identifies volcanic centers (Table 7). The scatter of the centers does not display any discernible trend within or between the major units of the Abitibi greenstone belt. While large proportions of the metals in VMS deposits are concentrated in the southern part of the Abitibi greenstone belt, the authors suspect that this is a function of older mapping, extensive Quaternary cover and less exploration effort in the relatively poorly accessible northern parts of the belt. Syngenetic mineralization such as volcanogenic Zn-Cu, volcanogenic Cu-Zn-Au, and komatiite-related Cu-Ni-PGE are critically dependent upon stratigraphic and lithologic controls (Dubé et al., 2007; Eckstrand and Hulbert, 2007; Galley et al., 2007, Houlé et al.,

TABLE 7. Syngenetic Mineralization in Major Volcanic Units of the Abitibi Greenstone Belt

Time interval	VMS mineralization	Komatiite-associated Cu-Ni-PGE mineralization	Reference
2704-2695 Ma	Jameland, Kam-kotia, Can. Jamieson,		Ayer et al. (2003); Hathway et al. (2005)
	Rouyn-Noranda Camp (ex. Horne), Bousquet-Laronde Penna		Chartrand and Cattalani (1990); Gibson and Watkinson (1990); Kerr and Gibson (1993) Tourigny et al. (1993); Dubé et al. (2007), Mercier-Langevin et al. (2007a, 2007b)
2710-2704 Ma	Val-d'Or Camp (e.g., Louvicourt)		Chartrand and Cattalani (1990); Pilote et al. (2000); Moorhead et al. (2000a).
		Langmuir	Stone and Stone (2000); Ayer et al. (2004)
		Redstone	
		Texmont	Houlé et al. (2008b)
2719-2711 Ma	Kidd Creek mine		Ayer et al. (2004); Ayer et al. (2005)
	Potter mine		Gibson and Gamble (2000)
	Potterdoal mine		Epp (1997)
	Langlois mine		Théberge et al. (1999)
		Alexo, Dundonald,	Houlé et al. (2001)
		Dumont, Marbridge	Giovenazzo (2000)
2723-2720 Ma	Estrades		Chartrand and Cattalani (1990); O'Dowd (1989)
2734-2724 Ma	Shunsby		
	Hunter mine,		Dufresne (1959)
	Normétal mine,		Brown (1948)
	Selbaie mines,		Faure et al. (1990)
	Matagami Camp (e.g.,		Piché et al. (1990); Piché et al. (1993)
	Mattagami Lake),		Chartrand and Cattalani (1990)
	Lemoine,		Daigneault and Allard (1990)
	Joutel Camp (e.g.,		Legault et al. (2002)
	Poirier)		
2750-2735 Ma	Tretheway-Ossian		Ayer et al. (2004)
	Amity		Ayer et al. (2004)
	Gemini-Turgeon		Girard et al. (2000)
Pre-2750 Ma	Drill hole FEC-98-01		Bandyayera et al. (2004)

2008); hydrothermal systems which transport the metals and give rise to the Zn-Cu and Cu-Au deposits develop during hiatuses in volcanism.

Volcanogenic Zn-Cu

These deposits develop by subvolcanic pluton-centered hydrothermal circulation through the volcanic succession (Franklin et al., 2005). Mineralization is produced during a hiatus in volcanism when a hydrothermal system leaches metals from underlying source rocks and deposits them on or immediately beneath the sea floor (Franklin et al., 2005).

VMS mineralization developed at various stratigraphic levels within individual volcanic units throughout the Abitibi greenstone belt. Table 7 lists representative VMS deposits associated with the stratigraphic packages within each of the volcanic episodes identified in this paper. In more detail, volcanogenic mineralization occurs at hiatuses at the group, formation, and member level. For example, in the Rouyn-Noranda VMS camp, mineralization occurs associated with cherty units capping members within the Blake River Group. In contrast, in the Matagami camp, mineralization is largely at the top of the Lac Watson Group (Sharpe, 1968; Piché et al., 1990, 1993), and in the Chibougamau camp it occurs at the top of various formation-level felsic centers in the Chibougamau camp (Pilote, 2006). The Normétal (Brown, 1948; Lafrance et al., 2000) and Selbaie (Faure et al., 1990) deposits also occur in, and above, felsic metavolcanic rocks during volcanic hiatuses in this episode. In the Swayze greenstone belt, the Shunsby VMS mineralization is at the top of the 2734 to 2724 Ma volcanic episode (Heather, 2001).

The Estrades mineralization represents relatively rare evidence for VMS mineralization during the 2723 to 2720 Ma episode. Detailed chemostratigraphy of the 2719 to 2711 Ma volcanic episode shows that the mineralized zones within the Kidd-Munro assemblage occur at various stratigraphic levels, rather than simply at the top (Bleeker, 1999; Gibson and Gamble, 2000; Hathway et al., 2005). In detail, the world-class Kidd Creek deposit occurs at the top of a rhyolitic succession (formation?) overlying basal komatiites. Argillaceous units were deposited at the Kidd Creek deposit and through the upper part of the 2717 to 2711 Ma volcanic episode, reflecting additional hiatuses in volcanism and possible submarine correlative conformities. However distribution of the argillites is discontinuous and not traceable at a regional scale. The Potter mine, within the 2719 to 2711 Ma Kidd-Munro assemblage, lies at the top of a tholeiitic succession and beneath a komatiitic flow succession (Gibson and Gamble, 2000). Mineralization during the 2710 to 2704 Ma volcanic episode occurs principally east of Rouyn-Noranda, where the Manitou and Louvicourt deposits lie at the top of small felsic centers in the Val-d'Or Formation (Scott et al., 2002). In the Rouyn-Noranda camp, VMS-mineralized volcanic hiatuses occur at several stratigraphic levels within the 2704 to 2695 Ma Blake River Group (Gibson and Watkinson, 1990). The mineralization within the upper Blake River assemblage in the Kamiskotia area west of Timmins is also essentially at the top of the assemblage immediately underlying an epiclastic unit of unknown age (Hathway et al., 2005). The gold-bearing VMS mineralization of the LaRonde Penna deposit (Dubé et al., 2007; Mercier-Langevin et al., 2007a, b) represents VMS mineralization related to a shallow-level hydrothermal system emplaced near the top of the Blake River Group, where it is unconformably overlain by turbidites of the Cadillac Group.

Komatiite-hosted Ni

In the case of the komatiite-related mineralization, relatively unevolved, sulfur-undersaturated melts yield metal-rich sulfides upon attaining sulfur saturation at or near surface. Mineralization is either basal massive-dissseminated (type I of Lesher and Keays, 2002) or strata bound internally disseminated (type II). Komatiite-hosted mineralization occurs in the 2750 to 2735 Ma Pacaud assemblage, the 2723 to 2720 Ma Stoughton-Roquemaure assemblage, the 2719 to 2711 Ma Kidd-Munro assemblage, and the 2710 to 2704 Ma Tisdale assemblage. Critical parameters controlling the presence or absence of mineralization include the primary magmatic composition, the availability of a suitable substrate, and most critically the physical volcanology (Lesher, 1989; Sproule et al., 2002, 2005; Houlé et al., 2008). The synthesis of Sproule et al. (2005) indicates that type I mineralization occurs mainly within the Tisdale assemblage (e.g., Hart, Langmuir, McWatters, and Redstone deposits in the Shaw dome; Texmont, Sothman, and Bannockburn C deposits in other domes south of Timmins). These deposits occur immediately above iron formation units capping felsic volcanic units of the 2734 to 2724 Ma volcanic episode. Type I deposits also occur in the Kidd-Munro assemblage, including the Alexo mine, the Dundeal, Dundonald, and Marbridge deposits east of Timmins (Houlé et al., 2008). Type II deposits have been identified in the 2710 to 2704 Ma Tisdale assemblage (Bannockburn A, B, and BT zones) and in the Kidd-Munro assemblage (Dumont) (Sproule et al., 2005). The stratigraphic controls on the Kidd-Munro assemblage komatiite-associated Ni deposits are less clear.

Recognition of the volcanic hiatuses and associated submarine unconformities below the komatiite successions is important. At the Dundonald deposit, the komatiite-associated Ni-Cu mineralization occurs at the transition from the calc-alkaline–dominated lower Kidd-Munro assemblage of Ayer et al. (2002a), a group level unit, into komatiites and tholeiites of the upper Kidd-Munro assemblage (Houlé et al., 2008). The profound shifts from calc-alkaline to komatiitic and tholeiitic basaltic flows and the presence of argillaceous metasedimentary units toward the top of the geochemically defined units represent volcanic hiatuses and possible group level unconformities of limited duration. In the Shaw dome area, the Ni-Cu-PGE deposits in the Tisdale assemblage (Stone and Stone, 2000) are associated with a basal komatiite unit within a komatiite-tholeiite flow package overlying the rhyolitic rocks of the Deloro assemblage. This transition represents a major depositional gap of about 18 m.y.

Lode and syngenetic gold

Given the well-known affinity of lode gold deposits for Fe-rich lithologic units, the iron formation units associated with the submarine unconformities make reasonable targets for lode gold-style mineralization. Several examples of iron formation-hosted gold occur at the top of the 2734 to 2723 Ma volcanic episode in the Shining Tree greenstone belt (Golden Sylvia; KRL Resources prospect). The gold mineralization at

the Upper Beaver mine in Gauthier Township east of Kirkland Lake in the 2710 to 2704 Ma Tisdale assemblage has been considered stratigraphically controlled (Roberts and Morris, 1982), hosted in fragmental rocks at the top of the assemblage. The present interpretation is that the conglomerates here are related to the development of a sedimentary interface zone at the top of the Tisdale assemblage; however, the mineralization is presently viewed to be of uncertain origin (C. Page, Queenston Mining Inc., pers. commun.).

Volcanic hiatuses and mineralization

The lithotectonic assemblage subdivisions correspond in a general way with group-level stratigraphic subdivisions in that several mappable units representing a definite time interval and depositional setting comprise an assemblage (Thurston, 1991), but there are also unifying features such as magma clan affiliation and geographic extent. Assemblages as proposed by Ayer et al. (2002a) have subsequently been subdivided (Ayer et al., 2005), but based on the principles listed above are still roughly equivalent to stratigraphic groups. Our work, mainly in the southern Abitibi greenstone belt, has identified volcanic hiatuses which represent submarine unconformities or disconformities at what would be considered (using stratigraphic nomenclature) the group, formation, and possibly the member level. At the group level, the most extensive submarine unconformity or disconformity is at the top of the 2734 to 2724 Ma Deloro assemblage, with less extensive submarine unconformities or disconformities at the tops of the 2750 to 2735 Ma Pacaud assemblage and the 2723 to 2720 Ma Stoughton-Roquemaure assemblage. VMS deposits associated with these major depositional hiatuses could be explored for in suitable volcanic units beneath the disconformity. This stratigraphic relationship, with iron formation overlying largely mafic metavolcanic units, is critical in that it is reasonably common in the Abitibi greenstone belt (Gibson and Watkinson, 1990; Ayer et al., 2005) and elsewhere in the Superior province (Rogers, 2002) to have iron formation units capping VMS-mineralized dominantly basaltic stratigraphy. The conventional VMS model then calls for identification of felsic centers in close spatial association with VMS mineralization. We assert that the critical volcanic hiatus can be identified by a variety of means, including the presence of disconformities marked by iron formation or chert. Once the hiatus is identified, mineralization may be found in mafic units on strike with or above the hiatus especially associated with local felsic units, as in the Rouyn-Noranda camp (Gibson and Watkinson, 1990; Ayer et al., 2005; Goutier and Melançon, 2007). At the group level, VMS mineralization at the top of the 2734 to 2724 Ma assemblage includes the Shunsby mineralization in the Swayze greenstone belt (Heather, 2001) and the Normétal and associated deposits in the northern Abitibi greenstone belt (Chartrand and Cattalani, 1990). At the formation level, submarine unconformities have been identified within the Tisdale and Blake River assemblages. We have found evidence of graphitic horizons within the Kidd-Munro assemblage (Ayer et al., 2005), which are indicative of a volcanic hiatus between two geochemical types of volcanism. Graphitic horizons of this type are probably more directly related to volcanism and form very direct targets similar to the exhalite units of the Rouyn-Noranda camp. The presence of a submarine unconformity within the Blake River assemblage in the Genex area (Finamore (Hocker) et al., 2008) suggests that similar unconformities may be found elsewhere in the Blake River assemblage given the complexity of its evolution (Gibson and Watkinson, 1990; Pearson, 2005).

Conclusions

In this contribution we have used an extensive stratigraphic and geochronologic database to document the character of geochronologically defined volcanic episodes within the Abitibi greenstone belt. Each of the seven episodes is summarized in terms of the character of the constituent units and stratigraphic relationships to neighboring units. The distribution patterns of the units making up the seven volcanic episodes across the entire Abitibi greenstone belt are shown in a generalized stratigraphic map. The presence of numerous batholith-centered outward-younging sequences indicates that the belt consists of batholith-cored crustal section. Stratigraphy throughout the belt is upward-facing, upward-younging intact stratigraphy folded about regional-scale fold axes and not significantly displaced by thrusting. Stratigraphic sections in many parts of the Abitibi greenstone belt demonstrate the presence of depositional gaps between some of the major volcanic episodes. At the top of each of the volcanic episodes is a sedimentary interface zone consisting largely of chemical sedimentary rocks characterized by unusual chert breccia units, iron formation, and chert. Sedimentary interface zone units also occur at the formation level in some units such as the 2710 to 2704 Ma episode.

Calculation of volcanic accumulation rates and a U-Pb zircon constraint on the rate of chemical sedimentation suggest that the sedimentary interface zone represents very low to negligible rates of sedimentary accumulation. Therefore the sedimentary interface zone units are interpreted to represent condensed sections and hydrothermal circulation in the volcanic rocks culminating in production of chert and/or iron formation units during volcanic hiatuses. Therefore, the sedimentary interface zone represents submarine correlative conformities, disconformities, or submarine unconformities, leading to the conclusion that Keewatin units of the Abitibi greenstone belt represent unconformity-bounded units. This, in conjunction with the stratigraphic map, leads to the ability to provide group-level correlation across the Abitibi greenstone belt. The extensively developed sedimentary interface zone at the top of the 2734 to 2724 Ma episode complete with stratigraphic cutouts in one region suggest some of the sedimentary interface zone is due to tilting of stratigraphy by synvolcanic batholiths or perhaps subtle indications of the beginnings of orogenic activity.

Exploration implications of the volcanic hiatuses and correlative conformities for VMS and komatiite-associated Cu-Ni-PGE mineralization include: (1) the ability to correlate mineralized packages at the group and formation level, using the sedimentary interface zone; (2) an additional indicator of a volcanic hiatus consisting of graphitic argillite units at geochemical discontinuities in stratigraphy, representing member-level discontinuities; (3) the correlations at the formation and member level serve to define time intervals during which mineralization can occur; for example, at Kidd Creek footwall rhyolites are dated at 2711 to 2715 Ma with a 4-m.y. gap to a

quartz-feldspar porphyry in the hanging wall, (4) the depositional gaps and associated sedimentary interface zone represent episodes of hydrothermal activity which, in a proximal setting, give rise to VMS mineralization.

Acknowledgments

The field work and geochronology upon which this work is based was funded by Discover Abitibi, a community-based geoscience program, and by a National Research Council of Canada (NSERC) Discovery grant to Thurston. This paper was significantly improved by review of a previous version by John Percival of the Geological Survey of Canada and reviews by Phil Fralick and Martin Van Kranendonk. The various researchers working on the Discover Abitibi project contributed through provision of stimulating discussion during the course of the project. R. Marquis of Géologie Québec provided encouragement to prepare an external publication. The base geology for Figure 7 was supplied by Michel Houlé. Figure 9E was supplied by Geoff Baldwin. This is contribution number MRNF 2007-8430-08 of the Ministère des Resources naturelles et de la Faune du Québec.

REFERENCES

Allwood, A.C., Walter, M.R., Burch, I.W., and Kamber, B.S., 2007, 3.43 billion-year-old stromatolite reef from the Pilbara craton of Western Australia: Ecosystem-scale insights to early life on Earth: Precambrian Research, v. 158, p. 198–227.

Ayer, J., 1995, Precambrian geology, northern Swayze greenstone belt: Ontario Geological Survey Geological Map 2627.

Ayres, L.D., and Thurston, P.C., 1985, Archean supracrustal sequences in the Canadian Shield: An overview: Geological Association of Canada Special Paper 28, p. 343–380.

Ayer, J.A., Trowell, N.F., Amelin, Y., and Corfu, F., 1998, Geological compilation of the Abitibi greenstone belt: Toward a revised stratigraphy based on compilation and new geochronology results: Ontario Geological Survey Miscellaneous Paper 169, p. 4-1–4-14.

Ayer, J., Amelin, Y., Corfu, F., Kamo, S., Ketchum, J.F., Kwok, K., and Trowell, N.F., 2002a, Evolution of the Abitibi greenstone belt based on U-Pb geochronology: Autochthonous volcanic construction followed by plutonism, regional deformation and sedimentation: Precambrian Research, v. 115, p. 63–95.

Ayer, J.A., Ketchum, J., and Trowell, N.F., 2002b, New geochronological and neodymium isotopic results from the Abitibi greenstone belt, with emphasis on the timing and the tectonic implications of Neoarchean sedimentation and volcanism: Ontario Geological Survey Open File Report 6100, p. 5-1–5-16.

Ayer, J.A., Barr, E., Bleeker, W., Creaser, R.A., Hall, G., Ketchum, J.W.F., Powers, D., Salier, B., Still, A., and Trowell, N.F., 2003, Discover Abitibi: New geochronological results from the Timmins area: Implications for the timing of late-tectonic stratigraphy, magmatism and gold mineralization: Ontario Geological Survey Open File Report 6120, p. 33-1–33-11.

Ayer, J.A., Trowell, N.F., and Josey, S., 2004a, Geological compilation of the Abitibi greenstone belt: Ontario Geological Survey Map P3565.

Ayer, J.A., Thurston, P.C., Dubé, B., Gibson, H.L., Hudak, G.J., Lafrance, B., Lesher, C.M., Piercey, S.J., Reed, L.E., and Thompson, P.H., 2004b, Discover Abitibi Initiative Greenstone Architecture Project: Overview of results and belt-scale implications: Ontario Geological Survey Open File Report 6145, p. 37-1–37-15.

Ayer, J.A., Thurston, P. C., Bateman, R., Dubé, B., Gibson, H. L., Hamilton, M. A., Hathway, B., Hocker, S.M., Houlé, M., Hudak, G.J., Ispolatov, V., Lafrance, B., Lesher, C.M., MacDonald, P.J., Péloquin, A.S., Piercey, S.J., Reed, L.E., and Thompson, P.H., 2005, Overview of results from the Greenstone Architecture Project: Discover Abitibi Initiative: Ontario Geological Survey Open File Report 6154, 125 p.

Ayer, J.A., Chartrand, J.E., Grabowski, G.P.D., Josey, S., Rainsford, D., and Trowell, N.F., 2006, Geological compilation of the Cobalt-Temagami area, Abitibi greenstone belt: Ontario Geological Survey Preliminary Map P3581.

Ayer, J.A., Dubé, B., Ross, P.-S., Beakhouse, G.P., Berger, B.R., Bleeker, W., Brouillette, P., Chapman, J., Dinel, E., Dion, C., Dumont, R., Fowler, A.D., Friedman, R., Gibson, H.L., Goutier, J., Grunsky, E.C., Hamilton, M.A., Hannington, M.D., Houlé, M.G., Keating, P., Kontak, D., Laurin, J., Layton-Matthews, D., Lesher, C.M., McNicoll, V.J., Mercier-Langevin, P., Monecke, T., Moulton, B.J.A., Paradis, S.J., Percival, J.A., Peter, J.M., Potvin, J., Roy, M., Sharman-Harris, E., Taranovic, V., Taylor, B.E., Thurston, P.C., Trowel, N.F., van Breemen, O., Veillette, J.J., Wilson, R., and Wing, B.A., 2007, The Abitibi greenstone belt: Update of the Precambrian Geoscience Section Program, the Targeted Geoscience Initiative III Abitibi and Deep Search Projects: Ontario Geological Survey Open File Report 6213, p. 3-1–3-44.

Bandyayera, D., Théberge, L., and Fallara, F., 2002, Géologie de la région des lacs Piquet et Mesplet (32G/04 et 32B/13): Ministère des Ressources naturelles du Québec rapport RG 2001-14, 48 p.

Bandyayera, D., Daigneault, R., and Sharma, K.N.M., 2003, Géologie de la région du lac de la ligne (32F/01): Ministère des Ressources naturelles du Québec rapport RG 2002-12, 31 p.

Bandyayera, D., Rhéaume, P., Doyon, J., and Sharma, K. N. M., 2004, Géologie de la région du lac Hébert: Ministère des Ressources naturelles et de la Faune du Québec rapport RG 2003-07, 57 p.

Barrett, T.J., and MacLean, W.H., 1994, Chemostratigraphy and hydrothermal alteration in exploration for VHMS deposits in greenstones and younger volcanic rocks: Geological Association of Canada Short Course Notes, v. 11, p. 433–467.

Barrie, C.T., 1992, Geology of the Kamiskotia area: Ontario Geological Survey Open File Report 5829, 180 p.

——2005, Geochemistry of exhalites and graphitic argillites near VMS and gold deposits: Ontario Geological Survey Miscellaneous Release Data 173, 126 p.

Barrie, C.T., and Corfu, F. 1999, The Kidd–Munro extension project: Results of U-Pb geochronology for Year 1: Ontario Geological Survey Miscellaneous Paper 169, p. 74–81.

Barrie, C. T., and Davis, D., 1990, Timing of magmatism and deformation in the Kamiskotia-Kidd Creek area, western Abitibi subprovince, Canada: Precambrian Research, v. 46, p. 217–240.

Barrie, C.T., and Krogh, T.E., 1996, U-Pb zircon geochronology of the Selbaie Cu-Zn-Ag-Au mine, Abitibi subprovince, Canada: Economic Geology, v. 91, p. 563–575.

Bateman, R., Ayer, J.A., and Dubé, B., 2008, The Timmins-Porcupine gold camp, Ontario: Anatomy of an Archean greenstone belt and ontogeny of gold mineralizations: Economic Geology, v. 103, p. 1285–1308.

Becker, J.K., and Benn, K., 2003, The Neoarchean Rice Lake batholith and its place in the tectonomagmatic evolution of the Swayze and Abitibi granite-greenstone belts, north-eastern Ontario: Ontario Geological Survey Open File Report 6105, 41 p.

Benn, K., and Peschler, A.P., 2005, A detachment fold model for fault zones in the Late Archean Abitibi greenstone belt: Tectonophysics, v. 400, p. 85–104.

Berger, B., Ayer, J., McNicoll, V.J., and Bleeker, W., 2007, The Kidd-Munro project: Stratigraphy of the Kidd-Munro assemblage in Prosser Tp. and area based on geology, geochemistry and new geochronology: Ontario Geological Survey Open File Report 6213, p. 5-1–5-8.

Bickle, M.J., Nisbet, E.G., and Martin A., 1994, Archean greenstone belts are not oceanic crust: Journal of Geology, v. 102, p. 121–138.

Bleeker, W., 1999, Structure, stratigraphy, and primary setting of the Kidd Creek volcanogenic massive sulfide deposit: A semi-quantitative reconstruction: Economic Geology Monograph 10, p. 71–123.

——2002, Archaean tectonics: A review, with illustrations from the Slave craton: Geological Society Special Publication 199, p. 151–181.

Bleeker, W., Parrish, R.R., and Sager-Kinsman, S., 1999, High precision U-Pb geochronology of the Late Archean Kidd Creek deposit and surrounding Kidd volcanic complex: Economic Geology Monograph 10, p. 43–69.

Born, P., 1995, A sedimentary basin analysis of the Abitibi greenstone belt in the Timmins area, northern Ontario, Canada: Unpublished Ph.D. thesis, Ottawa, ON, Carleton University, 489 p.

Bright, E.G., 1984, Geology of the Ferrier Lake-Canoeshed Lake area, District of Sudbury: Ontario Geological Survey Geological Report 231, 60 p.

Brown, W.L., 1948, Normetal mine: Canadian Institute of Mining and Metallurgy, Structural Geology of Canadian Ore Deposits Volume, p. 683–692.

Card, K.D., 1990, A review of the Superior province of the Canadian Shield, a product of Archean accretion: Precambrian Research, v. 48, p. 99–156.

Catuneanu, O., 2003, Sequence stratigraphy of clastic systems: Geological Association of Canada Short Course Notes, v. 16, 248 p.
Chartrand, F., and Cattalani, S., 1990, Massive sulfide deposits in northwestern Quebec: Canadian Institute of Mining and Metallurgy Special Volume 43, p. 77–92.
Chown, E.H., Daigneault, R., Mueller, W., and Mortensen, J.K., 1992, Tectonic evolution of the Northern volcanic zone, Abitibi belt, Quebec: Canadian Journal of Earth Sciences, v. 29, p. 2211–2225.
Chown, E.H., N'Dah, E., and Mueller, W.U., 2000, The relation between iron-formation and low temperature hydrothermal alteration in an Archean volcanic environment: Precambrian Research, v. 101, p. 263–275.
Chown, E.H., Harrap, R.M., and Moukhsil, A., 2002, The role of granitic intrusion in the evolution of the Abitibi belt, Canada: Precambrian Research, v. 115, p. 291–309.
Clout, J.M.F., and Simonson, B.M., 2005, Precambrian iron formations and iron formation-hosted iron ore deposits: Economic Geology 100th Anniversary Volume, p. 643–680.
Condie, K.C., 2001, Mantle plumes and their record in earth history: Cambridge, Cambridge University Press, 306 p.
Corfu, F., 1993, The evolution of the southern Abitibi greenstone belt in light of precise U-Pb geochronology: Economic Geology, v. 88, p. 1323–1340.
Corfu, F., and Noble, S.R., 1992, Genesis of the southern Abitibi greenstone belt, Superior province, Canada: Evidence from zircon Hf isotope analyses using a single filament technique: Geochimica et Cosmochimica Acta, v. 56, p. 2081–2097.
Corfu, F., Krogh, T.E., Kwok, Y.Y., and Jensen, L.S., 1989, U-Pb geochronology in the south-western Abitibi greenstone belt, Superior province: Canadian Journal of Earth Sciences, v. 26, p. 1747–1763.
Corfu, F., Jackson, S.L., and Sutcliff, R.H., 1991, U-Pb ages and tectonic significance of late Archean alkalic magmatism and nonmarine sedimentation: Timiskaming Group, southern Abitibi belt, Ontario: Canadian Journal of Earth Sciences, v. 28, p. 489–503.
Daigneault, R., and Allard, G.O., 1990, Le Complexe du Lac Doré et son environnement géologique (région de Chibougamau-sous-province de l'Abitibi): Ministère de l'Énergie et des Ressources du Québec rapport MM 89-03, p. 113–129.
Daigneault, R., Mueller, W.U., and Chown, E.H., 2004, Abitibi greenstone belt plate tectonics: A history of diachronic arc development, accretion and collision, *in* Eriksson, K.A., Altermann, W., Nelson, D.R., Mueller, W., Catuneanu, O., and Strand, K., eds., The Precambrian earth: Tempos and events: Amsterdam, Elsevier, Developments in Precambrian Geology 12, p. 88–103.
David, J., Dion, C., Goutier, J., Roy, P., Bandyayera, D, Legault, M., and Rhéaume, P., 2006, Datations U-Pb effectuées dans la Sous-province de l'Abitibi à la suite des travaux de 2004–2005: Ministère des Ressources naturelles et de la Faune du Québec rapport RP-2006-04, 22 p.
David, J., Davis, D.W., Dion, C., Goutier, J., Legault, M., and Roy, P., 2007, Datations U-Pb effectuées dans la Sous-province de l'Abitibi à la suite des travaux de 2005–2006: Ministère des Ressources naturelles et de la Faune du Québec rapport RP-2007-01, 17 p.
Davis, D.W., 2002, U-Pb geochronology of Archean metasediments in the Pontiac and Abitibi subprovinces, Québec: Constraints on timing, provenance and regional tectonics: Precambrian Research, v. 115, p. 97–117.
Davis, D., David, J., Dion, C., Goutier, J., Bandyayera, D., Rhéaume, P., and Roy, P., 2005, Datations U-Pb effectuées en support aux travaux de cartographie géologique et de compilation géoscientifique du SGNO (2003–2004): Ministère des Ressources naturelles et de la Faune du Québec rapport RP-2005-02, 20 p.
Davis, W.J., Lacroix, S., Gariepy, C., and Machado, N., 2000, Geochronology and radiogenic isotope geochemistry of plutonic rocks from the central Abitibi subprovince: Significance to the internal subdivision and plutonotectonic evolution of the Abitibi belt: Canadian Journal of Earth Sciences, v. 37, p. 117–133.
Dimroth, E., Imreh, L., Rocheleau, M., and Goulet, N., 1982, Evolution of the south-central part of the Archean Abitibi belt, Quebec. Part 1: Stratigraphy and paleogeographic model: Canadian Journal of Earth Sciences, v. 19, p. 1729–1758.
Dimroth, E., Imreh, L., Goulet, N., and Rocheleau, M., 1983, Evolution of the south-central segment o f the Archean Abitibi belt, Quebec. Part III: Plutonic and metamorphic evolution and geotectonic model: Canadian Journal of Earth Sciences, v. 20, p. 1374–1388.
Dubé, B., Mercier-Langevin, P., Hannington, M., Lafrance, B., Gosselin, G., and Gosselin, P., 2007, The LaRonde Penna world-class Au-rich volcanogenic massive sulfide deposit, Abitibi, Québec: Mineralogy and geochemistry of alteration and implications for genesis and exploration: Economic Geology, v. 102, p. 633–666.
Dufresne, A.-O., 1959, The mining industry of the province of Quebec in 1957: Department of Mines, Quebec, 92 p.
Eakins, P.R., 1972, Canton de Roquemaure, Comté d'Abitibi-Ouest: Ministère des Richesses naturelles du Québec rapport RG 150, 150 p.
Eckstrand, O.R., and Hulbert, L., 2007, Magmatic nickel-copper-platinum group Element deposits: Geological Association of Canada Mineral Deposits Division Special Publication 5, p. 205–222.
Epp, M.S., 1997, Geology, petrography and geochemistry of the Potterdoal Cu-Zn deposit, Kidd-Munro assemblage, Munro Township, Ontario: Unpublished M.Sc. thesis, Hamilton, ON, McMaster University, 143 p.
Faure, S., Jébrak, M., and Bouillon, J.-J., 1990, Géologie et minéralisations en Zn-Cu-Ag-Au des Mines: Canadian Institute of Mining and Metallurgy Special Volume 43, p. 363–372.
Finamore (Hocker), S.M., Gibson, H.L., and Thurston, P.C., 2008, Archean synvolcanic intrusions and volcanogenic massive sulfide at the Genex mine, Kamiskotia area, Timmins, Ontario: Economic Geology, v. 103, p. 1203–1218.
Franklin, J.M., Gibson, H.L., Jonasson, I.R., and Galley, A.G., 2005, Volcanogenic massive sulfide Deposits: Economic Geology 100th Anniversary Volume, p. 523–560.
Gaboury, D., and Daigneault, R., 1999, Evolution from sea floor-related to sulfide-rich quartz vein-type gold mineralization during deep submarine volcanic construction: the Géant Dormant gold mine, Archean Abitibi belt, Canada: Economic Geology, v. 94, p. 3–22.
Galley, A.G., Hannington, M.D., and Jonasson, I.R., 2007, Volcanogenic massive sulphide deposits, *in* Goodfellow, W., ed., Mineral deposits of Canada: A synthesis of major deposit types, district metallogeny, and the evolution of geological provinces, and exploration methods, 5: St. Johns, Geological Association of Canada, Mineral Deposits Division, Special Publication 5, p. 141–162.
Gibson, H.L., and Gamble, A.P.D., 2000, A reconstruction of the volcanic environment hosting Archean seafloor and subseafloor VMS mineralization at the Potter mine, Munro Township, Ontario, Canada: Hobart, Tasmania, Centre for Ore Deposit Research, University of Tasmania Special Publication 3, p. 65–66.
Gibson, H.L., and Watkinson, D.H., 1990, Volcanogenic massive sulfide deposits of the Noranda cauldron and shield volcano, Quebec: Canadian Institute of Mining and Metallurgy Special Volume 43, p. 119–132.
Giovenazzo, D., 2000, Section 3B—Minéralisation nickelifères dans le secteur La Motte-Vassan: La mine Marbridge: Ministère des Ressources naturelles du Québec rapport MB 2000-09, p. 73–75.
Girard, P., Tremblay, Y.L., and Girard, R., 2000, Rapport d'évaluation des ressources géologiques, recommandation d'un programme d'exploration, projet Gemini: Ministère des Ressources naturelles et de la Faune du Québec rapport statutaire GM 58239, 130 p.
Gleason, J.D., Moore, T.C., Johnson, T.M., Rea, D.K., Owen, R.M., Blum, J.D., Pares, J., and Hovan, S.A., 2004, Age calibration of piston core EW9709-07 (equatorial central Pacific) using fish teeth Sr isotope stratigraphy: Palaeogeography, Palaeoclimatology, Palaeoecology, v. 212, p. 355–366.
Goodwin, A.M., 1965, Mineralized volcanic complexes in the Porcupine-Kirkland Lake-Noranda region, Canada: Economic Geology, v. 60, p. 955–971.
——1979, Archean volcanic studies in the Timmins-Kirkland Lake-Noranda region of Ontario and Quebec: Geological Survey of Canada Bulletin 278, 51 p.
Goutier, J., 1997, Géologie de la région de Destor: Ministère des Ressources naturelles du Québec rapport RG 96-13, 37 p.
——2000, Roquemaure—32D11–200–0101: Ministère des Ressources naturelles du Québec carte SIGÉOM 32D11a-C4G-00G.
——2006, Géologie de la région du lac au Goéland (32F/15): Ministère des Ressources naturelles et de la Faune du Québec rapport RG 2005-05, 39 p.
Goutier, J., and Lacroix, S., 1992, Géologie du secteur de la faille de Porcupine-Destor dans les cantons de Destor et Duparquet: Ministère des Ressources naturelles du Québec rapport MB 92-06, 62 p.
Goutier, J., and Melançon, M., 2007, Compilation géologique de la Sous-province de l'Abitibi (version préliminaire): Ministère des Ressources naturelles et de la Faune du Québec.
Goutier, J., Rhéaume, P., and Davis, D.W., 2004, Géologie de la région du lac Olga (32F/14): Ministère des Ressources naturelles et de la Faune du Québec rapport RG 2003-09, 40 p.

Gunning, H.C., and Ambrose, J.W., 1939, The Timiskaming-Keewatin problem in the Rouyn-Harricanaw region, northwestern Quebec: Transactions of the Royal Society of Canada, v. 33, Ser. 3, Sec.4, p. 19–49.

Hall, L.A.F., and Houlé, M., 2003, Geology and mineral potential of Shaw, Eldorado, and Adams Townships, Shaw dome area: Summary of Field Work and other Activities 2003: Ontario Geological Survey Open File Report 6120, p. 6-1–6-14.

Hall, L.A.F., and Smith, M.D., 2002, Precambrian geology of Denton and Carscallen Townships, Timmins West Area: Ontario Geological Survey Open File Report 6093, 75 p.

Hargraves, R.B., 1976, Precambrian geologic history: Science, v. 193, p. 363–371.

Hart, T.R., 1984, The geochemistry and petrogenesis of a metavolcanic and intrusive sequence in the Kamiskotia area, Timmins, Ontario: Unpublished M.Sc. thesis, Toronto, ON, University of Toronto, 174 p.

Hathway, B., Hudak, G.J., and Hamilton, M.A., 2005, Geologic setting of volcanogenic massive sulphide mineralization in the Kamiskotia area: Discover Abitibi Initiative: Ontario Geological Survey Open File 6155, 81 p.

——2008, Geologic setting of volcanic-associated massive sulfide deposits in the Kamiskotia area, Abitibi subprovince, Canada: Economic Geology, v. 103, p. 1185–1202.

Heather, K.B., 2001, The geological evolution of the Archean Swayze greenstone belt, Superior province, Canada: Unpublished Ph.D. thesis, Staffordshire, UK, Keele University, 370 p.

Heather, K.B., Shore, G.T., and van Breemen O., 1995, The convoluted "layer-cake" an old recipe with new ingredients for the Swayze greenstone belt, southern Superior province: Geological Survey of Canada Current Research 1995-C, p. 1–10.

Henry, R.L., and Allard, G.O., 1979, Metallogenic significance of the Lac Sauvage volcanogenic iron formation near Chibougamau, Quebec [abs]: Geological Association of Canada Annual Meeting, Program with Abstracts, v. 4, p. 57.

Hickman, A.H., and Van Kranendonk, M.J., 2004: Diapiric processes in the formation of Archaean continental crust, East Pilbara granite-greenstone terrane, Australia: Amsterdam, Elsevier, Developments in Precambrian Geology 12, p. 54–75.

Higgins, M.W., 1971, Cataclastic rocks: U.S. Geological Survey Professional Paper 687, 97 p.

Hofmann, H.J., and Masson, M., 1994, Archean stromatolites from Abitibi greenstone belt, Quebec, Canada: Geological Society of America Bulletin, v. 106, p. 424–429.

Hofmann, H.J., Sage, R.P., and Berdusco, E.N., 1991, Archean stromatolites in Michipicoten Group siderite ore at Wawa, Ontario: Economic Geology, v. 86, p. 1023–1030.

Houlé, M.G., 2006, Geological and mineral potential of McArthur Township in the Bartlett dome: Ontario Geological Survey Open File Report 6192, p. 6-1–6-14.

Houlé, M., and Guilmette, C., 2004, Geology and mineral potential of Carman and Langmuir Townships, Shaw dome area: Ontario Geological Survey Open File Report 6145, p. 7-1–7-16.

Houlé, M.G., and Solgadi, F., 2007, Geological and mineral potential of Bartlett and Geikie Townships in the Bartlett dome, Abitibi greenstone belt: Ontario Geological Survey Open File Report 6213, p. 7-1–7-15.

Houlé, M., Lesher, C.M., Gibson, H.L., Fowler, A.D., and Sproule, R.A., 2001, Physical volcanology of komatiites in the Abitibi greenstone belt: Ontario Geological Survey Open File Report 6070, p. 13-1–13-17.

Houlé, M.G., Gibson, H.L., Lesher, C.M., Davis, P.C., Cas, R.A.F., Beresford, S.W., and Arndt, N.T., 2008, Komatiitic sills and multigenerational peperite at Dundonald Beach, Abitibi greenstone belt, Ontario: Volcanic architecture and nickel sulfide distribution: Economic Geology, v. 103, p. 1269–1284.

Ispolatov, V., Lafrance, B., Dubé, B. Creaser, R., and Hamilton, M., 2008, Geologic and structural setting of gold mineralization in the Kirkland Lake-Larder Lake gold belt, Ontario: Economic Geology, v. 103, p. 1309–1340.

Jackson, S.L., and Fyon, J.A., 1991, The western Abitibi subprovince in Ontario: Ontario Geological Survey Special Volume 4, Pt. 1, p. 405–482.

Jackson, S.L., and Harrap, R.M., 1989, Geology of parts of Pacaud, Catharine and southernmost Boston and McElroy Townships: Ontario Geological Survey, Miscellaneous Paper 146, p. 125–131.

Jackson, S.L., Fyon, J.A., and Corfu, F., 1994, Review of Archean supracrustal assemblages of the southern Abitibi greenstone belt in Ontario, Canada: Products of micro-plate interactions within a large-scale plate-tectonic setting: Precambrian Research, v. 65, p. 183–205.

Jaffey, A.H., Flynn, K F., Glendenin, L.E., Bentley, W.C., and Essling, A.M., 1971, Precision measurement of half-lives and specific activities of ^{235}U and ^{238}U: Physical Review, v. 4, p. 1889–1906.

Jensen, L.S., 1985, Stratigraphy and petrogenesis of Archean metavolcanic sequences, southwestern Abitibi subprovince, Ontario: Geological Association of Canada Special Publication 28, p. 65–87.

Jensen, L.S., and Langford, F.F., 1985, Geology and petrogenesis of the Archean Abitibi belt in the Kirkland Lake area, Ontario: Ontario Geological Survey Miscellaneous Paper 123, 130 p.

Joanisse, A, 1994, Datation de la carbonatite du lac Shortt: Université du Québec à Montréal unpublished rapport d'activité de synthèse STM 5000–6000, 16 p.

Johns, G.W., and Amelin, Y., 1998, Reappraisal of the geology of the Shining Tree area (east part), Districts of Sudbury and Timiskaming: Ontario Geological Survey Miscellaneous Paper 169, p. 43–50.

Kalogeropoulos, S.I., and Scott, S.D., 1983, Mineralogy and geochemistry of an Archean tuffaceous exhalite: the main contact tuff, Millenbach mine area, Noranda, Quebec: Canadian Journal of Earth Sciences, v. 26, p. 88–105.

Kerr, D.J., and Gibson, H.L., 1993, A comparison of the Horne volcanogenic massive sulfide deposit and intracauldron deposits of the Main Sequence, Noranda, Quebec: Economic Geology, v. 88, p. 1419–1442.

Ketchum, J.W.F., Ayer, J.A., van Breemen, O., Pearson, N.J., and Becker, J.K., 2008, Pericontinental crustal growth of the southwestern Abitibi subprovince, Canada—U-Pb, Hf, and Nd isotope evidence: Economic Geology, v. 103, p. 1151–1184.

Kimberly, M.M., 1978, Paleoenvironmental classification of iron formations: Economic Geology, v. 73, p. 215–229.

Krapez, B., Barley, M.E., and Pickard, A.L., 2003, Hydrothermal and resedimented origins of the precursor sediments to banded iron formation: Sedimentological evidence from the Early Palaeoproterozoic Brockman supersequence of Western Australia: Sedimentology, v. 50, p. 979–1011.

Labbé, J.-Y., 1999, Évolution stratigraphique et structurale dans la région d'Amos-Barraute, Études géologiques dans la région d'Amos: Ministère des Ressources naturelles du Québec rapport ET 98-04, p. 5–36.

Lafrance, B., 2003, Reconstruction d'un environnement du sulfures massifs volcanogènes deformé: Exemple Archéen de Normétal, Abitibi: Unpublished Ph.D. thesis, Université du Québec à Chicoutimi, 471 p.

Lafrance, B., Mueller, W.U., Daigneault, R., and Dupras, N., 2000, Evolution of a submerged composite arc volcano: Volcanology and geochemistry of the Normétal: Precambrian Research, v. 101, p. 277–311.

Lafrance, B., Moorhead, J., and Davis, D.W., 2003, Cadre géologique du camp minier de Doyon-Bousquet-Laronde: Ministère des Ressources naturelles, de la Faune et des Parcs du Québec rapport ET 2002-07, 43 p.

Lafrance, B., Davis, D.W., Goutier, J., Moorhead, J., Pilote, P., Mercier-Langevin, P., Dubé, B., Galley, A.G., and Mueller, W.U., 2005, Nouvelles datations isotopiques dans la portion québécoise du Groupe de Blake River et des unités adjacentes: Ministère des Ressources naturelles et de la Faune du Québec rapport RP 2005-01, 9 p.

Langford, F.F., and Jensen, L., 1976, The development of the Superior province of Northwestern Ontario by merging island arcs: American Journal of Science, v. 276, p. 1023–1034.

Leblanc, G., Johns, G.W., and Fowler, A.D., 2000, Geology, volcanology, lithogeochemistry and alteration associated with volcanogenic base metal mineralization in the Big Four Lake area, Shining Tree, Abitibi greenstone belt: Ontario Geological Survey Open File Report 6032, p. 8-1–8-9.

Legault, M., Gauthier, M., Jébrak, M., Davis, D.W., and Baillargeon, F., 2002, Evolution of the subaqueous to near-emergent Joutel volcanic complex, northern Volcanic zone, Abitibi subprovince, Quebec, Canada: Precambrian Research, v. 115, p. 187–221.

Lesher, C.M., 1989, Komatiite-associated nickel sulfide deposits: Reviews in Economic Geology, v. 4, p. 44–101.

Lesher, C.M., and Keays, R.R., 2002, Komatiite-associated Ni-Cu-(PGE) deposits; geology, mineralogy, geochemistry and genesis: Canadian Institute of Mining and Metallurgy Special Volume 54, p. 579–617.

Lesher, C.M., Goodwin, A.M., Campbell I.H., and Gorton, M.P., 1986, Trace-element geochemistry of ore-associated and barren, felsic metavolcanic rocks in the Superior province, Canada: Canadian Journal of Earth Sciences, v. 23, p. 222–237.

Loutit, T.S., Hardenbol, J., Vail, P.R., and Baum, G.R., 1988, Condensed sections: the key to age determination and correlation of continental margin sequences: Society of Economic Paleontologists and Mineralogists Special Publication 42, p. 183–213.

Lowe, D.R., Byerly, G.R., and Heubeck, C., 1999, Structural divisions and development of the west-central part of the Barberton greenstone belt: Geological Society of America Special Paper 329, p. 37–82.

Ludden, J., Hubert, C., and Gariépy, C., 1986, The tectonic evolution of the Abitibi greenstone belt of Canada: Geological Magazine, v. 123, p. 153–166.

Marmont, S., and Corfu, F., 1989, Timing of gold introduction in the Late Archean tectonic framework of the Canadian Shield: Evidence from U-Pb zircon geochronology of the Abitibi subprovince: Economic Geology Monograph 6, p. 101–111.

McPhie, J., Doyle, M., and Allen, R.L., 1993, Volcanic textures: A guide to the interpretation of textures in volcanic rocks: Hobart, Tasmania, Centre for Ore Deposit and Exploration Studies, University of Tasmania, 197 p.

Mercier-Langevin, P., Dubé, B., Hannington, M.D., Davis, D.W., Lafrance, B., and Gosselin, G., 2007a, The LaRonde Penna Au-rich volcanogenic massive sulfide deposit, Abitibi greenstone belt, Quebec: Part I. Geology and geochronology: Economic Geology, v. 102, p. 585–609.

Mercier-Langevin, P., Dubé, B., Hannington, M.D., Richer-Laflèche, M., and Gosselin, G., 2007b, The LaRonde Penna Au-rich volcanogenic massive sulfide deposit, Abitibi greenstone belt, Quebec: Part II. Lithogeochemistry and paleotectonic setting: Economic Geology, v. 102, p. 611–631.

MER-OGS, 1984, Lithostratigraphic map of the Abitibi subprovince: Ontario Geological Survey and Ministère de l'Énergie et des Ressources, Québec, Map 2484 and DV 83–16.

Miall, A.D., 1990, Principles of sedimentary basin analysis: New York, Springer Verlag, 668 p.

——1994, Sequence stratigraphy and chronostratigraphy: problems of definition and precision in correlation, and their implications for global eustasy: Geoscience Canada, v. 21, p. 1–26.

Milne, V.G., 1972, Geology of the Kukatush-Sewell Lake area, District of Sudbury: Ontario Division of Mines Geoscience Report 097, 116 p.

Mitchum, R.M., 1977, Seismic stratigraphy and global changes of sea level. Part 11: Glossary of terms used in seismic stratigraphy: American Association of Petroleum Geologists Memoir 26, p. 205–212.

Moorhead, J., Tremblay, A., Pelz, P., and Beaudoin, G., 2000a, Section 2—Géologie de la mine Louvicourt: Ministère des Ressources naturelles du Québec rapport MB 2000-09, p. 47–72.

Moorhead, J., Vorobiev, L., and Tremblay, A., 2000b, Caractéristiques lithogéochimiques et corrélations lithostratigraphiques des roches volcaniques du secteur du canton Vauquelin, Sous-province de l'Abitibi, Québec: Ministère des Ressources naturelles du Québec rapport MB 2000-16, 59 p.

Morey, G.B., and Meints, J., 2000, Geologic map of Minnesota, bedrock geology, 3rd ed.: University of Minnesota, Minnesota Geological Survey State Map series S-10.

Mortensen, J. K., 1993a, U-Pb geochronology of the eastern Abitibi subprovince: Part 2: Noranda-Kirkland Lake area: Canadian Journal of Earth Sciences, v. 30, p. 29–41.

——1993b, U-Pb geochronology of the eastern Abitibi subprovince. Part 1: Chibougamau-Matagami-Joutel region: Canadian Journal of Earth Sciences, v. 30, p. 11–28.

Mueller, W., 1991, Volcanism and related slope to shallow marine volcaniclastic sedimentation: An Archean example, Chibougamau, Quebec, Canada: Precambrian Research, v. 49, p. 1–22.

Mueller, W., and Donaldson, J.A., 1992a, A felsic dike swarm formed under the sea: the Archean Hunter Mine Group, south-central Abitibi belt, Quebec, Canada: Bulletin of Volcanology, v. 54, p. 602–610.

——1992b, Development of sedimentary basins in the Archean Abitibi belt, Canada: An overview: Canadian Journal of Earth Sciences, v. 29, p. 2249–2265.

Mueller, W.U., and Mortensen, J.K., 2002, Age constraints and characteristics of subaqueous volcanic construction, the Archean Hunter Mine Group, Abitibi greenstone belt: Precambrian Research, v. 115, p. 119–152.

Nunes, P.D., and Jensen, L.S. 1980, Geochronology of the Abitibi metavolcanic belt, Kirkland Lake area—progress report: Ontario Geological Survey Miscellaneous Paper 92, p. 32–39.

O'Dowd, P., 1989, Estrades deposit main zone, 1989 definition drilling program and mineral inventory, Estrades property: Travaux statutaires déposé au Ministère des Ressources naturelles et de la Faune du Québec rapport GM 53422, 97 p.

Pearson, V., 2005, The Blake River Group: An imbricated caldera complex: Ministère des Ressources naturelles et de la Faune du Québec, résumés des conférences et des photoprésentations, Québec Exploration 2005, rapport DV 2005-03, 105 p.

Péloquin, A.S., Houlé, M., and Gibson, H.L., 2005, Geology of the Kidd-Munro assemblage in Munro Township, and the Tisdale and lower Blake River assemblages in Currie Township: Ontario Geological Survey Open File Report 6157, 94 p.

Percival, J.A., 2007, Geology and metallogeny of the Superior province, Canada: Geological Association of Canada, Mineral Deposits Division, Special Publication 5, p. 903–928.

Percival, J.A., and Williams, H., 1989, The Late Archean Quetico accretionary complex, Superior province, Canada: Geology, v. 17, p. 23–25.

Peschler, A.P., Benn, K., and Roest, W.R., 2004, Insights on Archean continental geodynamics from gravity modelling of granite-greenstone terranes: Journal of Geodynamics, v. 38, p. 185–207.

Piché, M., Guha, J., and Daigneault, R., 1993, Stratigraphic and structural aspects of the volcanic rocks of the Matagami mining camp, Quebec: Implications for the Norita ore deposit: Economic Geology, v. 88, p. 1542–1558.

Piché, M., Guha, J., Daigneault, R., Sullivan, J.R., and Bouchard, G., 1990, Les gisements volcanogènes du camp minier de Matagami: Structure, stratigraphie et implications métallogéniques: Institut Canadien des Mines et de la Métallurgie Volume Spécial 43, p. 327–335.

Pickard, A.L., Barley, M.E., and Krapez, B., 2003, Deep-marine depositional setting of banded iron formation: Sedimentological evidence from interbedded clastic sedimentary rocks in the early Palaeoproterozoic Dales Gorge Member of Western Australia: Sedimentary Geology, v. 170, p. 37–62.

Pilote, P., 2006, Métallogenie de l'extrémité est de la sous-province de l'Abitibi, *in* Pilote, P., ed., Le camp minier de Chibougamau et le parautochtone Grenvillien: métallogénie, métamorphisme et aspects structuraux: Geological Association of Canada, livret-guide d'excursion B1, 138 p.

Pilote, P., Brisson, H., Demers, M., and Gilbert, M., 1999, Géologie de la région entourant les gisements aurifères Casa-Berardi Est et Ouest, Explorer au Québec: Le défi de la connaissance. Séminaire d'information sur la recherche géologique: Ministère des Ressources naturelles du Québec rapport DV 1999-03, 53 p.

Pilote, P., Moorhead, J., and Mueller, W., 2000, Partie A—Développement d'un arc volcanique, la région de Val-d'Or, ceinture de l'Abitibi: Volcanologie physique et évolution métallogénique: Ministère des Ressources naturelles du Québec rapport MB 2000-09, p. 1–20.

Pyke, D.R., 1978, Geology of the Redstone River area, District of Timiskaming: Ontario Geological Survey Report 161, 75 p.

Pyke, D.R., Naldrett, A.J., and Eckstrand, O.R., 1973, Archean ultramafic flows in Munro Township, Ontario: Geological Society of America Bulletin, v. 84, p. 955–978.

Robert, F., 2003, Giant gold deposits of the Abitibi greenstone belt, Western Australia gold giants and global gold giants: University of Western Australia Short Course for M.Sc. students, Perth, Western Australia, February 6–7, 2003, p. 81–90.

Roberts, R.G., and Morris, J H., 1982, The geologic setting of the Upper Beaver mine, Kirkland Lake district, Ontario: A copper-gold deposit in mafic volcanic rocks: Canadian Institute of Mining and Metallurgy Special Volume 24, p. 73–82.

Rogers, N., 2002, Geology: Confederation Lake, Ontario: Geological Survey of Canada Open File Map 4265.

Rogers, N., McNicoll, V., van Staal, C.R., and Tomlinson, K.Y., 2000, Lithogeochemical studies in the Uchi-Confederation greenstone belt, northwestern Ontario: Implications for Archean tectonics: Current Research Part C, Geological Survey of Canada, p. 1–11.

Sanborn-Barrie, M., Skulski, T., and Parker, J., 2001, Three hundred million years of tectonic history recorded by the Red Lake greenstone belt, Ontario: Geological Survey of Canada Current Research Part C19, p. 1–19.

Scholl, D.W., and von Hueme, R., 2004, Recycling of continental crust at modern subduction zones: Implications for Precambrian crustal growth, supercontinent constructions, and littering the mantle with continental debris [abs]: Geological Society of America Abstracts with Programs, v. 36, p. 205–206.

Scott, C.R., Mueller, W.U., and Pilote, P., 2002, Physical volcanology, stratigraphy and lithogeochemistry of an Archean volcanic arc: Evolution from plume-related volcanism to arc rifting of SE Abitibi greenstone belt, Val-d'Or, Canada: Precambrian Research, v. 115, p. 223–260.

Shanmugam, G., 1988, Origin, recognition, and importance of erosional unconformities in sedimentary basins, *in* Kleinspehn, K.L., and Paola, C., eds., New perspectives in basin analysis: New York, Springer Verlag, p. 83–108.

Sharpe, J.I., 1968, Géologie et gisements de sulfures de la région de Matagami: Ministère des Richesses naturelles du Québec rapport RG 137, 130 p.

Shaw, H. R., 1985, Links between magma-tectonic rate balances, plutonism and volcanism: Journal of Geophysical Research, v. 90, p. 11,275–11,288.

Siever, R., 1992, The silica cycle in the Precambrian: Geochimica et Cosmochimica Acta, v. 56, p. 3265–3272.

Simonson, B.M., and Hassler, S. W., 1996, Was the deposition of large Precambrian iron formations linked to major marine transgressions?: Journal of Geology, v. 104, p. 665–676.

Snyder, D.B., Bleeker, W., Reed, L.E., Ayer, J.A., Houlé, M.G., and Bateman, R., 2008, Tectonic and metallogenic implications of regional seismic profiles in the Timmins mining camp: Economic Geology, v. 103, p. 1135–1150.

Snyder, D.L., and Reed, L.E., 2005, Seismic surveys in the Timmins/Kirkland Lake region as part of the Discover Abitibi project: Canadian Institute of Mining Conference, Toronto, 2005, Paper 2041.

Sproule, R.A., Lesher, C.M., Ayer, J.A., Thurston, P.C., and Herzberg, C.T., 2002, Secular variation in the geochemistry of komatiitic rocks from the Abitibi greenstone belt, Canada: Precambrian research: Precambrian Research, v. 115, p. 153–186.

Sproule, R.A., Lesher, C.M., Houlé, M., Keays, R.R., Ayer, J., and Thurston, P.C., 2005, Chalcophile element geochemistry and metallogenesis of komatiitic rocks in the Abitibi greenstone belt, Canada: Economic Geology, v. 100, p. 1169–1190.

Stone, M.S., and Stone, W.E., 2000, A crustally contaminated komatiitic dike-sill-lava complex, Abitibi greenstone belt, Ontario: Precambrian Research, v. 102, p. 21–46.

Stott, G.M., Corkery, T., Leclair, A., Boily, M., and Percival, J., 2007, A revised terrane map for the Superior province as interpreted from aeromagnetic data [abs.]: Institute on Lake Superior Geology Annual Meeting, 53rd, Lutsen, Minnesota, Proceedings, v. 53, pt.1, p. 74–75.

Sylvester, P.J., Attoh, K., and Schulz, K.J., 1987, Late Archean bimodal volcanism in the Michipicoten (Wawa) greenstone belt, Ontario: Canadian Journal of Earth Sciences, v. 24, p. 1120–1134.

Théberge, L., Daigneault, R., Labbé, J.-Y., and Brisson, T., 1999, Reconnaissance de l'héritage volcanogène d'une minéralisation de sulfures massifs en zone de forte déformation: le cas type de gisement de la mine Langlois, Lebel-sur-Quévillon, Abitibi: Ministère des Ressources naturelles du Québec rapport MB 99-38, 53 p.

Thériault, R., 2002, Geological map of Quebec—edition 2002: Ministère des Ressources naturelles, Québec Map DV 2002-07.

Thurston, P.C., 1991, Archean geology of Ontario: Introduction: Ontario Geological Survey Special Volume 4, Part 1, p. 73–80.

——2002, Autochthonous development of Superior province greenstone belts?: Precambrian Research, v. 115, p. 11–36.

Thurston, P.C., and Chivers, K.M., 1990, Secular variation in greenstone sequence development emphasizing Superior province, Canada: Precambrian Research, v. 46, p. 21–58.

Tourigny, G., Doucet, D., and Bourget, A., 1993, Geology of the Bousquet 2 mine: An example of a deformed, gold-bearing polymetallic sulfide deposit: Economic Geology, v. 88, p. 1578–1597.

Trowell, N.F., 1986, Geology of the Savant Lake area, Districts of Kenora and Thunder Bay: Ontario Geological Survey Open File Report 5606, 181 p.

Vail, P.R., Mitchum R.M., J., Todd, R.G., Widmier, J.M., Thompson, S., III, Sangree, J. B., Bubb, J.N., and Hatlelid, W.G., 1977, Seismic stratigraphy and global changes of sea-level I: American Association of Petroleum Geologists Memoir 36, p. 49–212.

Vail, P.R., Hardenbol, J., and Todd, R.G., 1984, Jurassic unconformities, chronostratigraphy and sea level changes from seismic stratigraphy and biostratigraphy: American Association of Petroleum Geologists Memoir 36, p. 129–144.

van Breemen, O., Heather, K.B., and Ayer, J., 2006, U-Pb geochronology of the Neoarchean Swayze sector of the southern Abitibi greenstone belt: Geological Survey of Canada Current Research 2006-F1, p. 1–32.

van den Boorn, S.H.J.M., van Bergen, M.J., Nijman, W., and Vroon, P.Z., 2007, Dual role of seawater and hydrothermal fluids in Early Archean chert formation: Evidence from silicon isotopes: Geology, v. 35, p. 939–942.

Van Kranendonk, M.J., 2006, Volcanic degassing, hydrothermal circulation and the flourishing of early life on Earth: A review of the evidence from ca. 3490–3240 Ma rocks of the Pilbara Supergroup, Pilbara craton, Western Australia: Earth-Science Reviews, v. 74, p. 197–240.

Van_Kranendonk, M.J., Hickman, A.H., Smithies, R.H., Nelson, D.N., and Pike, G. 2002, Geology and tectonic evolution of the Archaean North Pilbara terrain, Pilbara craton, Western Australia. Economic Geology, v. 97, p. 695–732.

Van Kranendonk, M.J., Collins, W.J., Hickman, A.H., and Pawley, M.J., 2004, Critical tests of vertical vs. horizontal tectonic models for the Archaean East Pilbara granite-greenstone terrane, Pilbara craton, Western Australia: Precambrian Research, v. 131, p. 173–211.

Van Kranendonk, M.J., Smithies, R.H., Hickman, A.H., and Champion, D.C. 2007, Secular tectonic evolution of Archaean continental crust: Interplay between horizontal and vertical processes in the formation of the Pilbara craton, Australia: Terra Nova, v. 19, p. 1–38.

Van Wagoner, J.C., Posamentier, H.W., Mitchum, R.M., Vail, P.R., Sarg, J.F., Loutit, T.S., and Hardenbol, J., 1988, An overview of the fundamentals of sequence stratigraphy and key definitions: Society of Economic Paleontologists and Mineralogists Special Publication 42, p. 39–42.

Van Wagoner, J.C., Mitchum, R.M., Campion, K.M., and Rahmanian, V.D., 1990, Siliciclastic sequence stratigraphy in well logs, cores, and outcrops: Tulsa, Oklahoma, American Association of Petroleum Geologists Methods in Exploration Series 7, 55 p.

Vearncombe, S., Vearncombe, J., and Barley, M.E., 1998, Fault and stratigraphic controls on volcanogenic massive sulfide deposits in the Strelley belt, Pilbara craton, Western Australia: Precambrian Research, v. 88, p. 67–82.

Wilks, M.E., and Nisbet, E.G., 1988, Stratigraphy of the Steep Rock Group, northwest Ontario: A major Archaean unconformity and Archaean stromatolites: Canadian Journal of Earth Sciences, v. 25, p. 370–391.

Williams, H.R., Stott, G.M., and Thurston, P.C., 1992, Tectonic evolution of Ontario: Summary and synthesis. Part 1: Revolution in the Superior province: Geological Survey of Ontario Special Volume 4, Part 2, p. 1255–1294.

Wilson, M.E., 1941, Noranda district, Quebec: Geological Survey of Canada Memoir 229, 162 p.

Wong, L., Davis, D.W., Krogh, T.E., and Robert, F., 1991, U-Pb zircon and rutile chronology of Archean greenstone formation and gold mineralization in the Val d'Or region, Quebec: Earth and Planetary Science Letters, v. 104, p. 325–336.

Wyman, D., Kerrich, R., and Polat, A., 2002, Assembly of Archean cratonic mantle lithosphere and crust: Plume-arc interaction in the Abitibi-Wawa subduction-accretion complex: Precambrian Research, v. 115, p. 37–62.

Zhang, Q.-Z., Machado, N., Ludden, J.N., and Moore, D.M., 1993, Geotectonic constraints from U-Pb ages for the Blake River Group, the Kinojévis Group and the Normétal mine area, Abitibi, Québec [abs]: Geological Association of Canada Abstracts, v. 18, p. A114.

APPENDIX 1

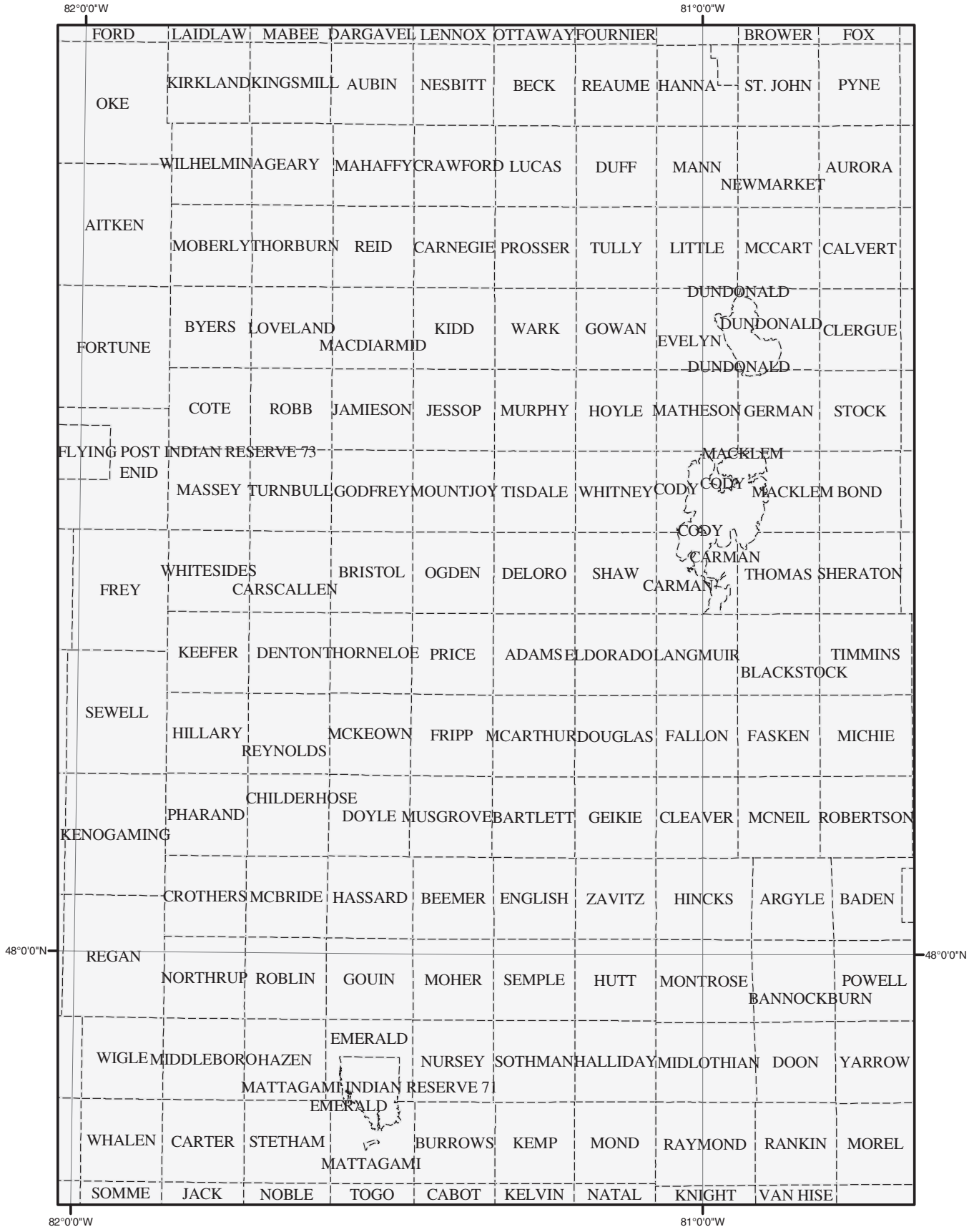
82°0'0"W
81°0'0"W
48°0'0"N
FORD
LAIDLAW
MABEE
DARGAVEL
LENNOX
OTTAWAY
FOURNIER
BROWER
FOX
OKE
KIRKLAND
KINGSMILL
AUBIN
NESBITT
BECK
REAUME
HANNA
ST. JOHN
PYNE
WILHELMINA
GEARY
MAHAFFY
CRAWFORD
LUCAS
DUFF
MANN
NEWMARKET
AURORA
AITKEN
MOBERLY
THORBURN
REID
CARNEGIE
PROSSER
TULLY
LITTLE
MCCART
CALVERT
DUNDONALD
BYERS
LOVELAND
MACDIARMID
KIDD
WARK
GOWAN
EVELYN
DUNDONALD
DUNDONALD
CLERGUE
FORTUNE
COTE
ROBB
JAMIESON
JESSOP
MURPHY
HOYLE
MATHESON
GERMAN
STOCK
FLYING POST INDIAN RESERVE 73
ENID
MACKLEM
MASSEY
TURNBULL
GODFREY
MOUNTJOY
TISDALE
WHITNEY
CODY
CODY
MACKLEM
BOND
CODY
CARMAN
FREY
WHITESIDES
CARSCALLEN
BRISTOL
OGDEN
DELORO
SHAW
CARMAN
THOMAS
SHERATON
KEEFER
DENTON
THORNELOE
PRICE
ADAMS
ELDORADO
LANGMUIR
TIMMINS
BLACKSTOCK
SEWELL
HILLARY
REYNOLDS
MCKEOWN
FRIPP
MCARTHUR
DOUGLAS
FALLON
FASKEN
MICHIE
CHILDERHOSE
PHARAND
DOYLE
MUSGROVE
BARTLETT
GEIKIE
CLEAVER
MCNEIL
ROBERTSON
KENOGAMING
CROTHERS
MCBRIDE
HASSARD
BEEMER
ENGLISH
ZAVITZ
HINCKS
ARGYLE
BADEN
REGAN
NORTHRUP
ROBLIN
GOUIN
MOHER
SEMPLE
HUTT
MONTROSE
POWELL
BANNOCKBURN
EMERALD
WIGLE
MIDDLEBORO
HAZEN
NURSEY
SOTHMAN
HALLIDAY
MIDLOTHIAN
DOON
YARROW
MATTAGAMI INDIAN RESERVE 71
EMERALD
WHALEN
CARTER
STETHAM
BURROWS
KEMP
MOND
RAYMOND
RANKIN
MOREL
MATTAGAMI
SOMME
JACK
NOBLE
TOGO
CABOT
KELVIN
NATAL
KNIGHT
VAN HISE

APPENDIX 2
Geochronology Results and Discussion

04PCT-0064 Quartz-phyric gabbro dike, Bartlett Township
(NAD83, Zone 17 UTM 482078E, 5331967N; A) in Fig. 7)

A sample of quartz-phyric gabbro was collected from a dike cutting Deloro assemblage rocks in Bartlett Township. This dike is representative of numerous similar east- to west-striking dikes, which emanate from the underlying Muskasenda gabbro body and have been interpreted to feed overlying Tisdale assemblage mafic volcanic rocks occurring farther to the east (Ayer et al., 2004b).

Heavy mineral concentrates from this gabbro yielded very little zircon, except for extremely tiny, clouded, and stained grains of relatively low quality. Minor, small blade fragments of very pale brown baddeleyite were also present, and a selection of these fragments was chosen for U/Pb analysis. A dull luster on all grains suggests the possible presence of fine zircon coatings. Results for four fractions, each comprising three small, thin blades of baddeleyite are presented in Table 8 and Figure 10A. All of the data are highly collinear and regress to yield an upper intercept age of 2705.7 $^{+4.4}_{-3.8}$ Ma (86% probability of fit; MSWD = 0.15) and a lower intercept age of 810 Ma. The Th/U ratios for the analyzed grain fractions range from 0.07 to 0.25. This is relatively high for baddeleyite but is appropriate for a mixture of baddeleyite and zircon, the latter of which may be present as (late magmatic?) coatings on early igneous baddeleyite grains. This is also supported by the observation that the variation in Pb/U (i.e., Pb loss) appears to be broadly correlated with Th/U, suggesting that the grains with the greater proportion of zircon rim development or growth also show the highest degree of discordance. Direct dating of the large, sill-like Muskasenda gabbro has not been carried out previously, but the intrusion is known to enclose an enclave of Deloro assemblage felsic metavolcanic rocks, which have been dated at 2727.9 ± 2.2 Ma (Ayer et al., 2003), thereby providing a maximum age for the younger host gabbro. A primary igneous age of 2705.7 $^{+4.4}_{-3.8}$ Ma for the east-west gabbro dike presented here establishes with reasonable confidence that the dikes (and by inference the Muskasenda gabbro sill) intruded Deloro assemblage stratigraphy during a period contemporaneous with Tisdale assemblage volcanism.

C89-7 Pegmatitic gabbro sill, Ghost Range complex, Lamplugh Township
(NAD83, Zone 17 UTM 585970E, 5376800N)

Uranium-lead (U/Pb) isotope data for this differentiated gabbroic sill were originally presented by Corfu (1993), and the data are reproduced here (shaded ellipses: Fig. 10B). The dated phases comprised mostly single grains of fragmented, euhedral, and partly turbid zircon, and brown, translucent to opaque baddeleyite. All analyses were variably discordant, but a fit through the most discordant zircon analysis (3z) and a subgroup of the cluster near concordia (1z, 4bd) yielded an upper intercept age of 2713 $^{+7}_{-5}$ Ma (Corfu, 1993) and a lower intercept age of ca. 1250 Ma. Analysis of additional fractions from this sample was warranted by the desire to improve the precision of the original age determination in the context of the surrounding stratigraphy, as well as to assess correlation with the newly dated 2706.8 ± 1.2 Ma Centre Hill mafic to ultramafic complex in Munro Township (see 04JAA-0002 above). Two fractions of tiny baddeleyite fragments were picked from the residues of the original Corfu study, enough to comprise roughly 1 μg each. Because the grains showed a very dull luster, each fraction was given a brief wash in concentrated HF to remove any possible overgrowths of zircon (late magmatic or metamorphic), which might be carrying a Pb-loss signature resulting from a 1250 Ma or even younger isotopic disturbance. The resulting two analyses (Bd-1, Bd-2: Fig. 10B; Table 8) are more concordant (~99.1–98.9%) than the previous three baddeleyite analyses from this sample, but, like two of those baddeleyite (and one of the zircon) analyses, these new data fall to the right of the aforementioned regression of Corfu (1993). Assuming only a recent Pb-loss event to have affected the most concordant baddeleyites, then regression of analyses Bd-1, Bd-2, and 5bd through the origin yields an upper intercept age of 2712.4 ± 1.1 Ma (see Fig. 10C, inset), which is almost identical to the original Corfu (1993) age, only more precise. Regression of the more discordant, turbid, and cracked zircon analyses (2z, 3z) together with those for the older four baddeleyites (5bd, 6bd, Bd-1, and Bd-2) results in an unrealistically old upper intercept age (2724 Ma), which is greater than the accepted age of the host Kidd-Munro assemblage volcanic rocks (ca. 2719–2711 Ma: Nunes and Jensen, 1980; Corfu et al., 1989; Barrie and Davis, 1990; Corfu and Noble, 1992; Corfu, 1993; Ayer et al., 2002). This fact, combined with the agreement to the earlier Corfu (1993) result, suggests that the 2712.4 ± 1.1 Ma age represents an accurate and precise estimate of the timing of emplacement of the Ghost Range sill. The age for the Ghost Range gabbroic complex is now considered distinct and separate from the age of other mafic to ultramafic complexes found elsewhere in the Kidd-Munro assemblage, including the 2706.8 ± 1.2 Ma Centre Hill complex (see 04JAA-0002 above), the Munro-Warden sill (2704.9 ± 1.9 Ma: Barrie and Corfu, 1999), the Dundonald mafic to ultramafic sill (2707 $^{+3}_{-2}$ Ma: Barrie and Corfu, 1999), as well as the 2707 to 2705 Ma Kamiskotia Gabbroic Complex (2707 ± 2 Ma gabbro: Barrie and Davis, 1990; Corfu and Noble, 1992; 2704.8 ± 1.5 Ma granophyre: Ayer et al., 2005). Regional mafic to ultramafic intrusions elsewhere in the Timmins-Kidd Creek area also include the Mann mafic to ultramafic intrusion in Mann Township (2704.0 ± 4.9 Ma; Barrie, 1999) and a dunite differentiate from Deloro Township (2707 $^{+3}_{-2}$ Ma; Corfu and Noble, 1992; Corfu, 1993), both of which are distinctly younger than the Ghost Range sill age refined here.

04JAA-0002 Leucogabbro, Centre Hill complex, north-central Munro Township
(NAD83, Zone 17 UTM 558199E, 5383067N)

A coarse-grained variety of leucogabbro exists in the upper fractionated portions of the Centre Hill mafic to ultramafic

complex. A sample of this unit was collected for dating purposes to test the hypothesis that the Centre Hill complex might represent a synvolcanic intrusion related to the VMS mineralization in the overlying Potter mine. The Centre Hill leucogabbro contained a moderately abundant population of both zircon and baddeleyite. Zircon occurs as large, colorless, sometimes cloudy, subhedral to anhedral grains with square cross sections or as skeletal grains with flat, flangelike or partly hollow crystals. Some crystals are fragments of larger euhedra and many grains are cracked. Discrete, smaller and rounded, xenocrystic zircons are also present and were excluded from analysis. Baddeleyite grains in this sample occur as fine- to medium-grained, brown, striated blocky and blade varieties. Most baddeleyite grains show a dull luster, suggestive of a fine-grained partial overgrowth or replacement by fine-grained zircon, an observation confirmed by secondary electron imaging. Isotope dilution results for two zircon single-grain analyses are shown in Table 8 and Figure 10C. The data are only slightly discordant (0.4–0.5%) and have identical $^{207}Pb/^{206}Pb$ ages at 2706.6 and 2706.9 Ma. Results for two analyzed single grains of baddeleyite (unabraded) are slightly more discordant (1.0–1.4%) but yield similar $^{207}Pb/^{206}Pb$ ages as the zircon analyses. Regression of all four analyses results in an upper intercept age of 2706.8 ± 1.2 Ma with a very high probability of fit (94%; MSWD = 0.13). The regression is anchored through the origin and the goodness of fit for this discordia suggests that the Pb-loss behavior observed in the baddeleyites is a result of modern (zero-age) disturbances and not an older secondary Pb-loss event. Thus, the partial zircon frosting present on the baddeleyites likely reflects local, late saturation of the magma in silica rather than a younger metamorphic reaction. A primary magmatic crystallization age of 2706.8 ± 1.2 Ma for leucogabbro from the Centre Hill mafic to ultramafic complex is similar in age to the nearby Munro-Warden sill at 2704.9 ± 1.9 Ma (Barrie, 1999), the Middle zone gabbro of the Kamiskotia Gabbroic Complex (2707 ± 2 Ma: Barrie and Davis, 1990), and the mafic Dundonald sill (2707 Ma: Barrie and Corfu, 1999), all of which were emplaced into slightly older rocks of the Kidd-Munro assemblage.

APPENDIX 3

U-Pb Isotope Data for Zircon and Baddeleyite from Sample Localities in the Southern Abitibi Greenstone Belt, Ontario

Sample Fraction	Analysis no.	Description	Weight (mg)	U (ppm)	Th/U	Pb* (pg)	Pb_C (pg)	$^{206}Pb/^{204}Pb$	$^{206}Pb/^{238}U$	±2σ	$^{207}Pb/^{235}U$	±2σ	$^{207}Pb/^{206}Pb$	±2σ	$^{207}Pb/^{206}Pb$ Age (Ma)	±2σ	Disc. (%)	Corr. Coeff.
04PCT-0064		Quartz-phyric gabbro dike, Bartlett Township																
Bd-1	MAH4100	Three small, thin, pbr blade frags, frosted?	0.0001	267	0.11	14.3	0.8	1072	0.51202	0.00273	13.0622	0.0817	0.18502	0.00053	2698.4	4.7	1.5	0.8889
Bd-2	MAH4101a	Three small, thin, pbr blade frags, frosted?	0.0001	726	0.07	34.6	1.0	2198	0.51227	0.00168	13.0775	0.0496	0.18515	0.00032	2699.6	2.8	1.5	0.8937
Bd-3	MAH5005	Three small, thin, pbr blade frags, frosted?	0.0002	303	0.25	32.5	1.2	1704	0.49792	0.00135	12.6228	0.0451	0.18386	0.00035	2688.0	3.1	3.8	0.8533
Bd-4	MAH5006a	Three small, thin, pbr blade frags, frosted?	0.0001	287	0.12	21.7	1.2	1131	0.51613	0.00184	13.1874	0.0625	0.18531	0.00051	2701.0	4.5	0.8	0.8186
C89-7		Pegmatitic gabbro, Ghost Range sill, Lamplugh Township (Corfu, 1993)																
Bd-1	MAH5025	Three small, thin, br blade frags, frosted; HF etched	0.0010	313	0.07	168.2	5.1	2057	0.51761	0.00157	13.3232	0.0492	0.18668	0.00030	2713.1	2.6	1.1	0.9053
Bd-2	MAH5026	Three small, thin, br blade frags, frosted; HF etched	0.0010	209	0.06	112.2	0.8	8777	0.51825	0.00101	13.3358	0.0318	0.18663	0.00016	2712.7	1.4	0.9	0.9391
04JAA-0002		Leucogabbro, Centre Hill complex, north-central Munro Township																
Z2	MAH4068	One clr, cls square skeletal flange	0.0004	119	1.73	33.7	0.5	3365	0.51971	0.00180	13.3245	0.0505	0.18595	0.00024	2706.6	2.1	0.4	0.9418
Z3	MAH5001a	One clr, cls euh, skeletal	0.0008	287	1.26	149.6	5.9	1246	0.51897	0.00134	13.3073	0.0595	0.18597	0.00056	2706.9	5.0	0.5	0.7613
Bd-1	MAH4069a	One unabr, frosted?	0.0001	135	0.14	10.2	0.9	688	0.51421	0.00306	13.1697	0.1035	0.18575	0.00075	2704.9	6.7	1.4	0.8626
Bd-3	MAH5002	One unabr, large blade frag	0.0009	288	0.18	148.3	2.0	4409	0.51648	0.00116	13.2446	0.0358	0.18599	0.00020	2707.0	1.8	1.0	0.9221

Notes: All analyzed fractions represent least magnetic, air-abraded single zircon grains, free of inclusions, cores or cracks, unless otherwise noted; abbreviations: clr = clear, cls = colorless, pyell = pale yellow, brn = brown, pbr = pale brown, eq = equan, subeq = subequant, elong = elongate, euh = euhedral, prism = prismatic, frag =fragment, frac.= fracture(s), subrnd = subrounded, incl = inclusion; Pb* is total amount (in pg) of radiogenic Pb; Pb_C is total measured common Pb (in pg) assuming the isotopic composition of laboratory blank: 206/204 = 18.221, 207/204 = 15.612, 208/204 = 39.360 (errors of 2%); Pb/U atomic ratios are corrected for spike, fractionation, blank, and, where necessary, initial common Pb, $^{206}Pb/^{204}Pb$ is corrected for spike and fractionation; Th/U is model value calculated from radiogenic $^{208}Pb/^{206}Pb$ ratio and $^{207}Pb/^{206}Pb$ age assuming concordance; Disc. (%) = percent discordance for the given $^{207}Pb/^{206}Pb$ age; uranium decay constants are from Jaffey et al. (1971)